Analytical Treatment of Some Quantum Transitions in Molecular Dynamic Processes

Lukáš Pichl

2000

Department of Functional Molecular Science

School of Mathematical and Physical Science

Graduate University of Advanced Studies Japan

Authors of the Work and their current affiliations

[1]Lukáš Pichl,

[2]Vladimir I. Osherov, [3]Hiroshi Deguchi, [4]Jiří Horáček and

[1]Hiroki Nakamura[5]

[1]Department of Functional Molecular Science, Graduate University of Advanced Studies, Japan

[2]Institute of Chemical Physics, Russian Academy of Sciences, Chernogolovka, Moscow 142432, Russia

[3]Graduate School of Economics, Kyoto University, Yoshida-Honmachi, Sakyo-ku 606-8501, Japan

[4]Institute of Theoretical Physics, Charles University, V Holešovičkách 2, 180 00 Praha 8, Czech Republic

[5]Department of Theoretical Studies, Institute for Molecular Science, Myodaiji, Okazaki 444, Japan

Author of the Thesis

Lukáš Pichl

Preface

It was the year 1997, end of August, when I returned from my vacation in Latin America. A letter of invitation from the Japanese Ministry of Education, Science, Sports and Culture awaited me at home. Only one month left for the preparations and I arrived to this wonderful country as a Japanese Government Fellow. I am grateful and indebted for the three years I spent here in which I learnt a lot not only about the Japanese but also about the Czech. I do sincerely believe that this is just a beginning. The common features between the Czech and the Japanese as well as the ever-lasting mutual learning about ourselves will certainly contribute to the common wealth of our two countries. If I was allowed to do just a small step forward, I am glad.

We would like to express our sincere gratitude to the Ministry of Education, Science, Sports and Culture of Japan for the Research Grant No. 10441079.

Enormous help, guidance and patience of Profs. Hiroki Nakamura, Hiroshi Deguchi, Vladimir I. Osherov and Jiří Horáček is acknowledged as well as the support of my family.

I am grateful to His Excellency, Mr. Josef Havlas, ambassador of the Czech Republic in Japan, for his promotion of my economic studies in the Prague School of Economics.

Last but not least, Mr. Motohiro Nakajima, my karate teacher, Mrs. Yoko Okawara, my Japanese mother, Mrs. Hikosaka, my calligraphy teacher, and Mr. and Mrs. Tunehiko and Fusako Nakanishi, my best friends, and not only them, made these three years in Japan an unforgettable experience. My work was inspired by Toshie of Daijuji, Nobue, the Dream, and Hiromi, the Caster.

Lukáš Pichl

Okazaki 17. 7. L. P. 2000

Contents

I Introduction

Any introduction is limited by the time, space and circumstances, reflects the author's philosophy and can never be comprehensive. Taking this kindly into consideration, the reader may find it useful to consult my Glossary at the end of thesis providing some clue to my understanding of the subject. A specialist in the field, an experimentalist, an official, a friend of mine, everybody is hoped to understand this introduction.

As follows from the title, we have been concerned with analysis of quantum transitions in the field of molecular dynamics. We worked on physical processes such as dissociative recombination, complete reflection and transmission, or scattering.

Let us commence[1] with the description of the system. For simplicity of explanation we first restrict ourselves to a two-state system in quantum physics. Any molecule can be chosen as an example, if we select just two states. However, such a choice must be well-defined (for example, the rest of the states does not know about the selected pair, or, more realistically, it is known how to incorporate the interaction for the later purposes). The wave function, that is a projection of the state on a continuum, describes the system in full. In the context of the thesis the continuum is called an adiabatic parameter, and is mostly represented by the internuclear distance in a molecule. Time development of a state is described by the evolution operator while the eigenstates of the whole system are given by the hamiltonian. This operator is further projected on the subspace of our two states and its matrix elements in continuum are called diabatic potentials (for the diagonal elements) and coupling (for the off-diagonal elements). Eigenvalues of the potential matrix are the so called adiabatic potentials. Here we see how the two-state system can be embedded in the field of molecular physics.

First part of the thesis is related to nonadiabatic transitions, a dynamical process in which the adiabatic state of the system changes. In order to keep the explanation clear let us restrict ourselves to the two-state system. The numbering of the states can correspond to the electronic valence states of a molecule. Choosing the initial conditions so that the system is in a state A we change the adiabatic parameter. The system can either stay in its initial state A or can be switched to the other state, B. In quantum physics we can not say when this switching happens. One could follow Zhu and Nakamura, who chose the value of adiabatic parameter at which the difference of adiabatic potentials reaches a minimum, made it a criterion for the so called avoided crossing, and assigned this value to the change of adiabatic states, that is to the nonadiabatic transition.

In this picture the process can be described as follows below. The system starts in the initial state A, moves along the adiabatic potential by changing the adiabatic parameter, arrives to the avoided crossing, and is switched to the state

[1] confer with Jan Amos Komenský, the Teacher of Nations

B with the so called nonadiabatic transition probability, the so called small p. Since we stay in quantum physics, small p can not describe the nonadiabatic transition in full. While moving along each adiabatic potential, some phase is accumulated. The same rule for the phase applies to the quantum transition, even if the transition is assigned to a point. Thus the full description of the nonadiabatic transition must include also two, so called dynamical, phases ϕ and ψ. Obviously, the system is given by the diabatic potentials and the coupling between them (input), while the nonadiabatic transition is described by the three quantities p, ϕ and ψ (output). This relation between the input and output quantities is the subject of our interest and can be studied using various models. In this framework we completed the description of nonadiabatic transitions in the exponential potential model, introduced an exactly solvable diabatically avoided crossing model and treated semiclassically some potential systems common in molecular physics.

The reason for which we have been concerned with the exponential potential model follows. The linear model, solved for all ranges of coupling strength and energy by Zhu and Nakamura, and the quantum Rozen-Zener-Demkov model, solved exactly by Osherov and Voronin, can be covered by the exponential model within the semiclassical framework. This fact was recognized by Nikitin, although he restricted himself to the nonadiabatic transition probability. We can prove this coverage also for the dynamical phases. Moreover, we clarified and greatly improved the accuracy of the parameters which Nikitin used for his solution. However, since our improvement is based on potentials in the complex coordinate plane, experimentalists will find the improved parameters of small use at the moment.

The reason for which we solved the first diabatically avoided crossing model follows. In the diabatically avoided crossing model the diabatic potentials do not cross and that is why the linear model of the crossing by Zhu and Nakamura is not applicable. Moreover, within the class of quantum models exactly solvable in terms of Meijer G functions, which properties are known, this was a model which nobody considered. Osherov might have omitted the model because the diabatic potentials are sharp at one point which is not esthetical.

The reason for which we derived the conditions for the complete reflection and for the complete transmission in some two-state systems, common in molecular physics, follows. Since these systems are common, they are interesting for both theorists and experimentalists. Reflection and transmission are basic processes across all physics and their completness is theoretically interesting. The complicated semiclassical conditions for complete reflection and transmission were easily achieved by the simple technique of sewing up the wave function.

The dissociative recombination in the last part of the thesis is a rearrangment problem. We considered a collision of a positively charged hydrogen molecule with an electron. The charge recombines while the molecule disintegrates into two neutral hydrogen atoms. Within the framework of Multi-channel Quantum

Defect Theory, developed by Seaton, we contributed to the methods of solving integral equations with a singular kernel.

The thesis itself consists of two parts. The first of them is devoted to physics, (cf. Papers 1-4), while in the second one we are concerned with economics (cf. Papers 5-6). The physical problems, main part of the thesis, can be divided to two groups. The first of them are nonadiabatic transitions (sections II-IV), the second one is the dissociative recombination (section V). See the List of Papers at the end of thesis.

The theses themselves are divided into the following. In section II we complete the description of nonadiabatic transitions in the exponential potential model. In section III we give the exact quantum mechanical solution for a model of diabatically avoided crossing and analyze this model semiclassically. In section IV we derive the semiclassical conditions for the complete reflection and the complete transmission in some potential systems common in molecular physics. In section V we develop a numerical technique for solving integral equations involved in the dissociative recombination process and derive the exact solution of Lippman-Schwinger equation for the case of separable electronic coupling.

Opening and closing remarks to each section are borrowed from our papers in respective journals. Only small changes were made in order to preserve the general structure of the thesis. Amendments contain useful mathematical identities. In Illustrations, there are all the figures referred upon from the text. Tables and Glossary follow afterwards. Appendix comprises one of our ideas of applying the formalism used in physics to economics.

II Exponential Potential Model

Here we review to a certain extent our achievements in the exponential potential model. The full account is given in the Papers 2 and 4.

II.1 Opening remarks

It is well known that nonadiabatic transitions play an important role in various fields of physics, chemistry and biology [1-3]. The most fundamental models are classified in to the Landau-Zener-Stueckelberg (LZS) type curve crossing and the Rozen-Zener-Demkov (RZD) type noncrossing problem.

In the last several years, the LZS problems have been solved completely [8-9], and the efficient and accurate theory has been successfully developed even for multi-channel curve crossing problems [10,11]. On the other hand, the exact analytical solution of the RZD model was obtained recently by Osherov and Voronin [12]. In addition, some special exponential potential models have also been solved quantum mechanically exactly [13,14]. This remarkable progress encourages our efforts to formulate a unified theory that covers the above mentioned cases and gives a general formula for the nonadiabatic transition matrix in terms of integrals along the adiabatic potentials.

Here we are concerned with such an exponential model that the diabatic potentials and coupling are given by the same exponential function (see Eq. (II.2) below). The easier attractive case was examined in detail previously [15], and thus in this section the main attention is paid to the semiclassical treatment of the repulsive case. The purpose is to give a derivation of precise formulae of basic parameters which should be used in Nikitin's model [1] and which has not been known so far. Furthermore it is confirmed that the nonadiabatic transition matrix in the exponential model covers both the Landau-Zener (LZ) and the Rozen-Zener (RZ) type matrices as limiting cases. Based on these results the unification of LZ and RZ can be made and will be reported.

The section II is organized as follows. First we define the exponential model and review the treatment of the attractive case. Then the total wave function for repulsive model is obtained by the WKB (Wentzel-Kramer-Brillouin) type semiclassical methods using the high energy approximation. Next the scattering and nonadiabatic transition matrices are given and the validity of the double passage formula is demonstrated. The final formulae are expressed in terms of the model-independent parameters, and are applicable to general potentials. Their accuracy is demonstrated by using various numerical examples. We conclude with remarks for the future research. Amendment II contains the most mathematical parts which are not necessary to be shown in the main text.

II.2 Solving the model

We solve the coupled Schrődinger equations

$$\left[-\frac{\hbar^2}{2M}\frac{d^2}{dx^2}+\hat{V}(x)\right]\hat{\psi}(x)=E\hat{\psi}(x) \tag{II.1}$$

with

$$\hat{\psi}=\begin{pmatrix}\psi_1(x)\\ \psi_2(x)\end{pmatrix}$$

and

$$\hat{V}(x)=\begin{pmatrix}U_1-V_1\exp(-\alpha x) & V\exp(-\alpha x)\\ V\exp(-\alpha x) & U_2-V_2\exp(-\alpha x)\end{pmatrix}. \tag{II.2}$$

In dimensionless units $[E]=\hbar^2\alpha^2/(2M)$ and $[x]=1/\alpha$, the above equations have the form

$$-\psi_1''(x)+(U_1-V_1\exp(-x)-E)\,\psi_1(x)+V\exp(-x)\psi_2(x)=0 \tag{II.3}$$

and

$$-\psi_2''(x)+(U_2-V_2\exp(-x)-E)\,\psi_2(x)+V\exp(-x)\psi_1(x)=0.$$

Without loss of generality we choose $U_1>U_2$. In both attractive ($V_i>0$) and repulsive ($V_i<0$) cases we assume that $V_1V_2>V^2$ in order to avoid the case of three asymptotically open channels. In the adiabatic representation the coupling is localized and the diagonal adiabatic potentials are given by

$$u_{1,2}^{(a)}(x)=\frac{V_{11}+V_{22}}{2}\pm\left[\left(\frac{V_{11}-V_{22}}{2}\right)^2+V_{12}^2\right]^{1/2}, \tag{II.4}$$

where $V_{ij}(x)$ are the elements of the matrix $\hat{V}(x)$ in Eq. (II.2). The adiabatic wave functions $\phi_i(x)$ $(i=1,2)$ obey the transformation,

$$\begin{pmatrix}\phi_1(x)\\ \phi_2(x)\end{pmatrix}=\hat{R}(\theta(x))\begin{pmatrix}\psi_1(x)\\ \psi_2(x)\end{pmatrix}, \tag{II.5}$$

where

$$\hat{R}(\theta)=\begin{pmatrix}\cos\theta & -\sin\theta\\ \sin\theta & \cos\theta\end{pmatrix}\ \text{with}\ \theta(x)=\frac{1}{2}\arctan\left(\frac{2V_{12}(x)}{V_{22}(x)-V_{11}(x)}\right), \tag{II.6}$$

and $\theta\in[0,\,\pi/2]$. A new variable ρ defined by

$$\rho=2\sqrt{|V|}\exp\left(-\frac{x}{2}\right), \tag{II.7}$$

and the parameters

$$\mu \equiv 2\sqrt{E-U_2}, \quad \nu \equiv 2\sqrt{E-U_1}, \text{ and } \beta_i \equiv \frac{V_i}{|V|} \tag{II.8}$$

reduce the coupled differential equations (II.3) into the following form:

$$\left[\rho^2\frac{d^2}{d\rho^2}+\rho\frac{d}{d\rho}+\nu^2+\beta_1\rho^2\right]\psi_1=\rho^2\psi_2 \tag{II.9}$$

and

$$\left[\rho^2\frac{d^2}{d\rho^2}+\rho\frac{d}{d\rho}+\mu^2+\beta_2\rho^2\right]\psi_2=\rho^2\psi_1.$$

In order to decouple Eq. (II.9) we perform the modified Bessel transformation

$$\psi_i(\rho)=\int_C dpp\,F_i(p)\,Z_a(\rho p), \tag{II.10}$$

where C is a certain contour in the complex p-plane. Z_a stands for any appropriate kind of the Bessel function ($H^{(1,2)}_{\pm i\nu}$ here) [16], which satisfies

$$\left[z^2\frac{d^2}{dz^2}+z\frac{d}{dz}\right]Z_a(z)=-\left(z^2+\nu^2\right)Z_a(z). \tag{II.11}$$

We note that it is necessary to choose appropriate combinations of the Bessel function Z and the corresponding contour C in Eq. (II.10) in order (1) to satisfy the boundary conditions and (2) to fulfill the conditions imposed on the asymptotic behavior of $F_j(p)$ by Bessel transformation [15]. It suffices to use an appropriate kind of Bessel function for each independent solution.

Having substituted Eq. (II.10) into Eq. (II.9), we can decouple $F_2(p)$ from $F_1(p)$ as,

$$F_2(p)=\mathrm{sgn}(V)\left(\beta_1-p^2\right)F_1(p). \tag{II.12}$$

In the obtained exact differential equation for $F_1(p)$ we first cancel $F_1'(p)$ by substituting

$$f_1(p)\equiv\sqrt{p}\left(p^2-a_1\right)\left(p^2-a_2\right)F_1(p), \tag{II.13}$$

where

$$a_{1,2}=\frac{1}{2}\left(\beta_1+\beta_2\right)\mp\sqrt{\left(\frac{\beta_1-\beta_2}{2}\right)^2+1}. \tag{II.14}$$

The meaning of $|a_iV|$ in Eq. (II.14) is nothing but a preexponential constant of the i-th adiabatic potential in the classically forbidden region (see Eqs. (II.4) and (II.8)). The resulting differential equation is further reduced in the quasiclassical limit $\alpha\to 0$ (that is μ^2, ν^2, $\mu^2-\nu^2\sim\alpha^{-2}\gg 1$) to the following form

$$\left[\frac{d^2}{dp^2}+P_0(p)\right]f_1(p)=0, \tag{II.15}$$

where

$$P_0(p) \equiv \frac{\mu^2}{p^2}\frac{(p^2-c_1)(p^2-c_2)}{(p^2-a_1)(p^2-a_2)}, \tag{II.16}$$

and the coefficients c_1, c_2 are defined as

$$c_{1,2} = \frac{1}{2}\left(\beta_1 + \beta_2\frac{\nu^2}{\mu^2}\right) \mp \sqrt{\left(\beta_1 - \beta_2\frac{\nu^2}{\mu^2}\right)^2 + \frac{\nu^2}{\mu^2}}. \tag{II.17}$$

In the high energy limit

$$c_i \overset{E\to\infty}{\to} a_i. \tag{II.18}$$

We simplify the formal WKB solution of Eq. (II.15)

$$f_1^{(n)} = \frac{1}{\sqrt[4]{P_0}}\exp\left(\mp i\int^p \sqrt{P_0}\,dp\right), \quad n = 1,2, \tag{II.19}$$

by means of the high energy approximation $\nu^2 \gg 1$:

$$\sqrt{P_0} \simeq \frac{\nu}{p} + \delta_1\frac{2p}{p^2-a_1} + \delta_2\frac{2p}{p^2-a_2} + O(\delta^2), \quad \sqrt[4]{P_0} \simeq \sqrt{\frac{\mu}{p}}. \tag{II.20}$$

The energy dependent parameters δ's in Eq. (II.20) are defined in terms of the mixing angle in the limit of asymptotically forbidden region,

$$\delta_i \simeq \mu\frac{a_i - c_i}{4a_i} = \frac{\mu-\nu}{4}\left(1 \pm \cos\left(2\theta(-\infty)\right)\right), \tag{II.21}$$

$$\delta = \delta_1 + \delta_2.$$

In addition to the WKB approximation in Eq. (II.19), we expand also the Hankel function in Eq. (II.10) using Eq. (II.85) of the Amendment. Then the contour integral of Eq. (II.10) contains the phase integral given by

$$S(\rho, p) = \int^p \sqrt{P_0(p)}\;dp - \int^{\rho p}\sqrt{1+\frac{\nu^2}{\xi^2}}\;d\xi. \tag{II.22}$$

The main contribution comes from the saddle points $p_j\dagger(\rho)$ defined by

$$\frac{\partial}{\partial p}S(\rho, p)\Big|_{p=p_j\dagger} = 0, \tag{II.23}$$

and given explicitly by

$$(p_j\dagger(\rho))^2 = \frac{\beta_1+\beta_2}{2} - \frac{\nu^2-\mu^2}{2\rho^2} \pm \sqrt{\left(\frac{\beta_1-\beta_2}{2} - \frac{\mu^2-\nu^2}{2\rho^2}\right)^2 + 1} \quad j = 1,2. \tag{II.24}$$

Because of this ρ - p correspondence the above action simply becomes

$$S\left(\rho,\, p_j\dagger(\rho)\right) = \int^x \sqrt{E - u_j^{(a)}(x)}\; dx \equiv S_j(\rho). \tag{II.25}$$

The procedure in this section defines the semiclassical approximation used to solve the present exponential model. We cut the complex p-plane along the four branch cuts of $(P_0)^{1/2}$ chosen on the imaginary axis

$$\left(i\sqrt{|c_j|},\, i\sqrt{|a_j|}\right), \quad \left(-i\sqrt{|a_j|},\, -i\sqrt{|c_j|}\right) \quad j = 1, 2. \tag{II.26}$$

II.2.1 Repulsive case

Since we deal with two coupled differential equations of the second order, we first represent the total wave function as a linear combination of four fundamental solutions given by some, yet uknown, contour integrals. Then we evaluate these integrals in the limits $x \to \mp\infty$ and determine the four constants of this linear combination. When x lies in the classically inaccesible region, we obtain two restrictions on these constants because of the decay of wave function in each adiabatic channel. Evaluating the contour integrals for $x \to \infty$, we get the asymptotic form of the wave function. In order to obtain the S-matrix we set one more condition that the total wave function is of such a form that the incident wave propagates only in one channel. Then the last constant is just a multiplicative factor of the total wave function. Thus we can finally obtain the S-matrix.

Independent solutions At $x \to \infty$, the independent solutions in the adiabatic representation should behave like

$$\phi_1(\rho) \sim \rho^{\pm i\nu} \sim e^{\mp ik_1 x} \text{ and } \phi_2(\rho) \sim \rho^{\pm i\mu} \sim e^{\mp ik_2 x} \quad (\rho \to 0). \tag{II.27}$$

In the classically inaccessible region they correspond to exponentially growing functions, in general,

$$\phi_1(\rho) \sim \exp\left(|\sqrt{a_1}|\rho\right), \quad \phi_2(\rho) \sim \exp\left(|\sqrt{a_2}|\rho\right) \quad (\rho \to \infty). \tag{II.28}$$

Eq. (II.27) follows from the fact that the diabatic potentials are asymptotically flat and the coupling vanishes, while Eq. (II.28) can be obtained by solving the Schrődinger equation with the diagonal adiabatic potential matrix (we note that the rotation angle in Eq. (II.6) tends to a constant). If only the leading order term is retained, then we have

$$\left[\rho^2 \frac{d^2}{d\rho^2} + a_i\right] \phi_i(\rho) \simeq 0. \tag{II.29}$$

In Eq. (II.28) the exponentially decreasing terms have been omitted, since they are only subdominant in the region. Taking into account Eqs. (II.27) and (II.28), we can represent the wave function in Eq. (II.10) as

$$\psi_j(\rho) = \sum_{m,n=1}^{2} \gamma_{mn} I_{mn}^{(j)}(\rho), \tag{II.30}$$

where

$$I_{mn}^{(j)}(\rho) \equiv \int_{C_{mn}} dp\, p F_j^{(n)}(p) Z^{(n)}(\rho p). \tag{II.31}$$

Here $F_j^{(n)}$ are derived from Eq. (II.19), using Eqs. (II.12) and (II.13). The first index m indicates which couple of symmetric branch cuts is winded around by the contour, while the index n specifies in which complex half-plane the branch is located:

$$\begin{aligned} &n = 1, \quad Z^{(n)} = H_{-i\nu}^{(1)}, \quad \text{lower branch cut} \\ &n = 2, \quad Z^{(n)} = H_{i\nu}^{(2)}, \quad \text{upper branch cut.} \end{aligned} \tag{II.32}$$

The case $n = 1$ ($n = 2$) corresponds to the contour tips at $p = +i\infty$ ($p = -i\infty$) as shown in Fig. 1. From this figure and Eqs. (II.10), (II.19) and (II.85) it follows that

$$I_{mn}^{(j)} = \left(I_{m,3-n}^{(j)}\right)^{*}. \tag{II.33}$$

This condition ensures the unitarity of the S-matrix. The saddle point analysis, carried out in the high energy limit [15], proves that the main contribution to the integrals in Eq. (II.30) comes from regions in the complex p-plane such that

$$z = \rho p \sim 0 \text{ for } \rho \to 0 \tag{II.34}$$

and

$$|z| = |\rho p| \sim \infty \text{ for } \rho \to \infty.$$

This allows us to expand the Bessel function $H_{\pm i\nu}(z)$ in Eq. (II.10) (cf. Eqs. (II.81) and (II.82) in the Amendment). Eq. (II.27) follows from the transformation based on $H_{\pm i\nu}(z)$ (or alternatively on $H_{\pm i\mu}(z)$). In the limit $\rho \to \infty$ the saddle points tend to $\sqrt{a_i}$ (cf. Eqs. (II.14) and (II.24)), which gives Eq. (II.28). Thus the conditions in Eqs. (II.27) and (II.28) can be satisfied by our choice of contours and wave functions.

Wave function at $x \to -\infty$ In order to derive the wave function in the forbidden region, we perform the standard procedures, i.e. analyzing the singularities, solving the comparison equation and final asymptotic matching [1,6,7].

The total wave function

$$\Phi(\rho) = \begin{pmatrix} \phi_1 \\ \phi_2 \end{pmatrix} \tag{II.35}$$

should not contain exponentially growing terms at $\rho \to \infty$. In order to satisfy this physical condition we first evaluate the integrals $I^{(j)}_{nm}(\rho)$ of Eq. (II.30) for $\rho \to \infty$. To do this, we first have to match the local solution of Eq. (II.15) at $p \sim \sqrt{a_i}$ to the WKB solution Eq. (II.19). The procedure is explained in the Appendices B and C, and the final expressions of $I^{(j)}_{nm}(\rho)$ are given in Eqs. (II.D.3) and (II.D.4) in the Amendment. Then we rotate the diabatic wave functions $\psi_j(x)$ given by Eq. (II.30) into the adiabatic ones $\phi_j(x)$ using the matrix in Eq. (II.6) (cf. Eq. (II.D.5) in the Amendment). To cancell the contribution of exponentially diverging terms in adiabatic wave functions in Eq. (II.28), the following condition should be satisfied (cf. Eq. (II.D.7) in the Amendment)

$$\frac{\gamma_{12}}{\gamma_{11}} = \exp(i\alpha_1), \quad \frac{\gamma_{22}}{\gamma_{21}} = \exp(i\alpha_2), \tag{II.36}$$

where

$$\alpha_i = -2\left(\arg(\Gamma(i\delta_i)) + \delta_{3-i}\ln(a_2 - a_1) + \frac{\nu}{2}\ln(-a_i) + \delta_i \ln\left(\frac{-a_i}{\mu}\right)\right). \tag{II.37}$$

Wave function at $x \to \infty$ Evaluating integrals in Eq. (II.31) at $\rho \to 0$, we get the total wave function

$$\psi_1(\rho) = \pi\frac{\rho^{i\nu}}{\sqrt{\nu}}e^{i(\phi_0+\pi/4)}\frac{\Gamma(1+i\delta)(a_2-a_1)^{-i\delta-1}}{\Gamma(1+i\delta_1)\Gamma(1+i\delta_2)}\left(-e^{\pi\delta_2}\gamma_{11} + e^{-\pi\delta_2}\gamma_{21}\right) + \tag{II.38}$$

$$+\pi\frac{\rho^{-i\nu}}{\sqrt{\nu}}e^{-i(\phi_0+\pi/4)}\frac{\Gamma(1-i\delta)(a_2-a_1)^{i\delta-1}}{\Gamma(1-i\delta_1)\Gamma(1-i\delta_2)}\left(-e^{\pi\delta_2}\gamma_{12} + e^{-\pi\delta_2}\gamma_{22}\right),$$

and

$$\psi_2(\rho) = -i\frac{\rho^{i\mu}}{\sqrt{\mu}}e^{i(\phi_0-\delta\ln(4\nu)-\pi/4)}\Gamma(-i\delta)e^{\pi\delta/2} \tag{II.39}$$

$$\left(e^{-\pi\delta_1}\mathrm{sh}(\pi\delta_1)\gamma_{11} + e^{-\pi\delta_2}\mathrm{sh}(\pi\delta_2)\gamma_{21}\right) +$$

$$+i\frac{\rho^{-i\mu}}{\sqrt{\mu}}e^{-i(\phi_0-\delta\ln(4\nu)-\pi/4)}\Gamma(i\delta)e^{\pi\delta/2}\left(e^{-\pi\delta_1}\mathrm{sh}(\pi\delta_1)\gamma_{12} + e^{-\pi\delta_2}\mathrm{sh}(\pi\delta_2)\gamma_{22}\right),$$

where Γ is the Gamma function [16] and the phase factor

$$\phi_0 \equiv \nu\ln\left(\frac{e}{2\nu}\right) \tag{II.40}$$

comes from the expansion of Hankel and Gamma functions (cf. Eqs. (II.82) and (II.84) in the Amendment).

The details how to evaluate $\psi_j(\infty)$ are given in Amendment E (cf. Eqs. (II.E.4) and (II.E.6)).

Scattering Matrix and Nonadiabatic Transition Matrix In this section we first derive the scattering matrix containing parameters of the present exponential potential model. Then we evaluate the adiabatic scattering phase-shifts in order to subtract the nonadiabatic transition probability and dynamical phases, using the idea of double passage. Finally the total S-matrix can be put in a form which is free from the particular parameters of our model.

Scattering matrix Let us first denote the adiabatic momenta,

$$k_i(x) = \sqrt{E - u_i^{(a)}(x)} \text{ and } k_i \equiv \lim_{x\to\infty} k_i(x). \tag{II.41}$$

Then the scattering matrix in the present case is defined as

$$\begin{array}{l|l} \text{channel } \psi_i & \text{channel } \psi_j \\ \leftarrow 1 & \leftarrow 0 \\ \rightarrow -S_{ii} & \rightarrow -S_{ij} \end{array}, \tag{II.42}$$

where the arrows mean

$$\left.\begin{array}{l} \overleftarrow{\text{incoming}} \text{ wave} \\ \overrightarrow{\text{outgoing}} \text{ wave} \end{array}\right\} \frac{\exp(\mp i k_j x)}{\sqrt{k_j}} \text{ or } \frac{\exp(\mp i \int_{x_j'}^{x} k_j(x)dx)}{\sqrt{k_j}}; \tag{II.43}$$

and x_j' represents the turning point. While the plane waves in Eq. (II.43) are connected by the scattering matrix, $S(E)$, the latter adiabatic waves define the reduced scattering matrix, $S^R(E)$.

The matrix $S(E)$ can be deduced from $\Psi(x)|_{x\to\infty}$ as explained below. In Eqs. (II.38) and (II.39) the four parameters γ_{ij} are restricted by the two conditions from Eqs. (II.36). We impose one more restriction on γ_{ij} in order to specify the boundary condition of only outgoing wave in the first channel (to obtain S_{2j} elements) or in the second channel (to obtain S_{1j} elements). Thus all γ_{ij} can be found up to a multiplicative constant and the S-matrix elements are evaluated using Eqs. (II.36), (II.38) and (II.39) as follows:

$$\begin{aligned} S_{11}(E) = i\exp\left(2i\left[\delta\ln(a_2-a_1) + \arg\left(\Gamma(i\delta_1)\right) + \arg\left(\Gamma(i\delta_2)\right) - \arg\left(\Gamma(i\delta)\right)\right]\right) \\ \times \exp\left(2i\left[-\phi_0 - \nu\ln(2\sqrt{V})\right]\right)\left(pe^{i\alpha_2} + (1-p)e^{i\alpha_1}\right), \end{aligned} \tag{II.44a}$$

$$\begin{aligned} S_{12}(E) = -i\frac{\sqrt{\delta_1\delta_2}}{\pi}\frac{\sinh(\pi\delta_1)\sinh(\pi\delta_2)\,\Gamma(i\delta_1)\,\Gamma(i\delta_2)}{\sinh(\pi\delta)}e^{\pi(\delta_1-\delta_2)/2} \\ \times \exp\left(i\left[\delta\ln\left(4\nu(a_2-a_1)\right) - 2\phi_0 - (\nu+\mu)\ln(2\sqrt{V})\right]\right)\left(e^{i\alpha_2} - e^{i\alpha_1}\right), \end{aligned} \tag{II.44b}$$

$$S_{21}(E) = -i\frac{\pi}{\sqrt{\delta_1\delta_2}}\frac{\exp\left(i\left[\delta\ln\left(4\nu(a_2-a_1)\right) - 2\phi_0 - (\nu+\mu)\ln(2\sqrt{V})\right]\right)}{\sinh(\pi\delta)\,\Gamma(-i\delta_1)\,\Gamma(-i\delta_2)}e^{\pi(\delta_1-\delta_2)/2} \tag{II.44c}$$

$$\times \left(e^{i\alpha_2} - e^{i\alpha_1}\right),$$

and

$$S_{22}(E) = i\exp\left(2i\left[-\phi_0 + \delta\ln(4\nu) + \arg\left(\Gamma(i\delta)\right) - \mu\ln(2\sqrt{V})\right]\right) \qquad \text{(II.44d)}$$

$$\times \left(pe^{i\alpha_1} + (1-p)e^{i\alpha_2}\right),$$

where

$$p = \exp(-\pi\delta_2)\frac{\sinh(\pi\delta_1)}{\sinh(\pi\delta)}. \qquad \text{(II.45)}$$

The S-matrix given above satisfies symmetry and unitarity (cf. Eqs. (II.F.1)-(II.F.7) in the Amendment). The total transition probability $|S_{12}|^2$ is given by

$$|S_{12}(E)|^2 = 4\frac{\exp(\pi\delta)\sinh(\pi\delta_1)\sinh(\pi\delta_2)}{\left[\exp(\pi\delta)\sinh(\pi\delta_2) + \sinh(\pi\delta_1)\right]^2}\sin^2\left(\frac{\alpha_2 - \alpha_1}{2}\right). \qquad \text{(II.46)}$$

II.2.2 Double passage

With use of the idea of the double passage, the S-matrix can be expressed as a product of the nonadiabatic transition matrix and the adiabatic propagation matrix [3,7,10,11]. The nonadiabatic transition matrix connects the WKB wave functions

$$\frac{1}{\sqrt{k_i(x)}}\exp(i\int_{x_s}^{x} k_i(y)dy) \qquad \text{(II.47)}$$

from left to the right, both far from the reference point x_s. It generally has the form

$$I(x_s) = \begin{pmatrix} \sqrt{1-p}\exp(-i\phi) & -\sqrt{p}\exp(-i\psi) \\ \sqrt{p}\exp(i\psi) & \sqrt{1-p}\exp(i\phi) \end{pmatrix}, \qquad \text{(II.48)}$$

where p is the nonadiabatic transition probability for one passage through the transition region, and ψ and ϕ are the dynamical phases. If the turning points are well separated from the transition region and the WKB approximation does not break, then the S-matrix is decomposed to have the following double passage form

$$S_{11} = i\exp(i(2(d_1 - \phi) - \Phi_{12}))\left((1-p)e^{i\Phi_{12}} + pe^{-i\Phi_{12}}\right), \qquad \text{(II.49)}$$

$$S_{22} = i\exp(i(2(d_2 + \phi) + \Phi_{12}))\left((1-p)e^{-i\Phi_{12}} + pe^{i\Phi_{12}}\right),$$

and

$$S_{12} = S_{21} = -2\exp(i(d_1 + d_2))\sqrt{p(1-p)}\sin(\Phi_{12}),$$

where

$$\Phi_{12} = \Delta_1 - \Delta_2 + \psi - \phi. \qquad \text{(II.50)}$$

The quantities d_i are the adiabatic elastic scattering phase shifts and Δ_i are the adiabatic scattering phases from the turning points to the reference point $x_s = \Re x_*$, where x_* is the complex crossing point (see Eq. (II.54) below). Our goal now is to subtract the parameters p, ϕ and ψ from Eqs. (II.44a)-(II.44d) using this double passage formula. It is easy to see that p of Eq. (II.45) is the nonadiabatic transition probability in Eq. (II.49), which has the same form as in the attractive case. Indeed, in the case of asymptotically high energies the transition probability should not depend on the sign of potential slopes. Comparing Eqs. (II.44a)-(II.44d) and (II.49) we can also identify Φ_{12} of Eq. (II.50) as

$$2\Phi_{12} = \alpha_2 - \alpha_1. \tag{II.51}$$

To obtain explicit expressions of ϕ and ψ it is necessary to evaluate the phase shift integrals on the adiabatic potentials, d_i and Δ_i. The exact results can not be obtained analytically but we can obtain analytical results within the high energy expansion. For this purpose we make use of Eq. (II.22).

The adiabatic elastic scattering phase shifts are defined by

$$d_i \equiv \left(\lim_{X\to\infty} \int_{x_i'}^{X} \sqrt{E - u_i^{(a)}(x)}\, dx - X\sqrt{E - U_i} \right). \tag{II.52}$$

The phase shifts between the reference point and the turning points are given as

$$\Delta_i \equiv \int_{x_i'}^{x_s} \sqrt{E - u_i^{(a)}(x)}\, dx. \tag{II.53}$$

In order to represent the scattering matrix in the double passage form we choose the reference point as a real part of the complex crossing point of adiabatic potentials,

$$x_s \equiv \Re x_* = -\ln \left(\frac{(U_1 - U_2)/(2|V|)}{\sqrt{1 + \left(\frac{\beta_1 - \beta_2}{2}\right)^2}} \right). \tag{II.54}$$

In addition to this we modify Eq. (II.22) to the following form

$$\int_{x_j'}^{x} \sqrt{E - u_j^{(a)}(y)}\, dy = \int_{\sqrt{c_j}}^{p_j\dagger(\rho)} \sqrt{P_0(p)}\; dp - \int_{i\nu}^{\rho p_j\dagger(\rho)} \sqrt{1 + \frac{\nu^2}{\xi^2}}\; d\xi, \tag{II.55}$$

and note that

$$p_1\dagger(\rho) \overset{\rho\to 0}{\to} \sqrt{\beta_1},$$
$$p_2\dagger(\rho) \overset{\rho\to 0}{\to} \sqrt{\mu^2 - \nu^2}/\rho.$$

Equations (II.54) and (II.55) enable us to evaluate the phases in Eqs. (II.52) and (II.53). The results follow (cf. Eqs. (II.G.1)-(II.G.7) in the Amendment)

$$d_1 = \nu\ln\nu - \nu - \frac{\nu}{2}\ln|V| - \frac{\nu}{2}\ln|a_1| - \delta_1 \ln\left|\frac{a_1}{\mu}\right| + \delta_1 - \delta_1 \ln\sqrt{\delta_1\delta_2} + \delta_2 \ln\frac{\delta_2}{\delta}, \tag{II.56}$$

$$d_2 = \mu \ln \mu - \mu - \frac{\mu}{2} \ln |V| - \frac{\mu}{2} \ln |a_2| + \delta_1 \ln \left| \frac{a_2}{\mu} \right| - \delta_1 + \delta_1 \ln \sqrt{\delta_1 \delta_2} - \delta_2 \ln \frac{\delta_2}{\delta}, \quad \text{(II.57)}$$

and

$$\Delta_1 - \Delta_2 = \frac{\nu}{2} \ln \left(\frac{a_2}{a_1} \right) + \delta \ln \frac{a_2}{a_1} + \delta_1 - \delta_1 \ln \frac{\delta_1}{\mu} + \delta_2 \ln |a_1| + (\delta_1 - \delta_2) \ln \frac{\delta}{\sqrt{\delta_1 \delta_2}} \quad \text{(II.58)}$$

$$-\delta_2 + \delta_2 \ln \frac{\delta_2}{\mu} - \delta_1 \ln |a_2| - \Re \left\{ \int_{\Re x_c}^{x_c} (k_1(x) - k_2(x)) dx \right\}.$$

The general $S-$matrix Identifying p of the S-matrix formula with that of the I-matrix we can find the dynamical phases. First we substitute Eqs. (II.56), (II.57) and (II.58) into the double pasage formula in Eq. (II.49). The dynamical phases follow when comparing the result with the S-matrix in Eqs. (II.44a)-(II.44d). We remind the notation

$$\gamma(X) = X \ln(X) - X - \arg\left(\Gamma(iX)\right), \quad \text{(II.59)}$$

in terms of which the dynamical phases result in

$$\phi = \gamma(\delta_2) - \gamma(\delta) \quad \text{(II.60)}$$

and

$$\psi = \gamma(\delta_1) - \gamma(\delta) - 2 \left[\sqrt{\delta \delta_2} + \frac{\delta_1}{2} \ln \frac{\sqrt{\delta} - \sqrt{\delta_2}}{\sqrt{\delta} + \sqrt{\delta_2}} \right]. \quad \text{(II.61)}$$

The phases ψ and ϕ, unlike from the previous S-matrix in Eqs. (II.44a)-(II.44d), depend only on the parameters δ_i. Furthermore we show that δ_i can be considered as being free from the particular parameters of the exponential model.

We have proven above that the total S-matrix can be put to a general form

$$S_{ij}(E) = \lim_{x \to \infty} \exp\left(-\imath(k_i(\infty) + k_j(\infty))x\right) \quad \text{(II.62)}$$

$$\left[P(x, x_s) I(x_s; E) P(x_s, x^t) \imath P^*(x^t, x_s) I^t(x_s; E) P^*(x_s, x) \right]_{ij},$$

where the diagonal matrix P represents the uncoupled adiabatic propagation,

$$P_{ij}(b, a) = \delta_{ij} \exp\left(i \int_{a_j}^{b_j} k_j(y)\, dy \right). \quad \text{(II.63)}$$

Finally, the nonadiabatic transition matrix I is given by Eq. (II.48), with the parameters p, ϕ and ψ defined in Eqs. (II.45), (II.60) and (II.61). I^t in Eq. (II.62) is a transpose of I and P^* is a complex conjugate of the matrix in Eq. (II.63). The energy dependent parameters $\delta_i(E)$ are nothing but the contour integrals of

adiabatic momenta in the complex coordinate plane. In the attractive case they have the following form [15],

$$\delta_1 = \frac{1}{\pi}\Im\left\{\int_{x_2'}^{x_*} k_2(x)\,dx - \int_{x_1'}^{x_*} k_1(x)\,dx\right\} \tag{II.64}$$

and

$$\delta_2 = \frac{1}{\pi}\Im\left\{\int_{\Re(x_*)}^{x_*} [k_2(x) - k_1(x)]\,dx\right\}, \tag{II.65}$$

where x_i' are the turning points (complex in the attractive case) and x_* is the crossing point of adiabatic potentials in the complex plane. For the proof of Eqs. (II.64) and (II.65) confer with Eqs. (II.H.1)-(II.H.5) in the Amendment and Figs. 2-4.

In the repulsive case (cf. Eqs. (II.H.6)-(II.H.13) in the Amendment) that

$$\delta_1 = \delta - \delta_{LZ} \tag{II.66}$$

and

$$\frac{1}{\pi}\Im\left\{\int_{\Re(x_*)}^{x_*} [k_2(x) - k_1(x)]\,dx\right\} \equiv \delta_{LZ}, \tag{II.67}$$

where

$$\delta = \frac{\mu - \nu}{2} \equiv \delta_{RZ}. \tag{II.68}$$

The Rozen-Zener parameter in the above equation can be expressed as follows

$$\delta_{RZ} = \frac{1}{2\pi\imath}\oint_{\infty} [k_2(x) - k_1(x)]\,dx, \tag{II.69}$$

as it can be seen when introducing a new variable, $z = e^{-x}$. Finally, based on the symmetries between the attractive and repulsive case (cf. Eq. (II.H.7) in the Amendment), the formulae in Eqs. (II.66) and (II.67) are equivalent to

$$\delta_1 = \frac{1}{\pi}\Im\left\{\int_{\Re(x_*)}^{x_*} [k_2(x + i\pi) - k_1(x + i\pi)]\,dx\right\}, \tag{II.70}$$

and

$$\delta_2 = \frac{1}{\pi}\Im\left\{\int_{x_2'}^{x_*} k_2(x + i\pi)\,dx - \int_{x_1'}^{x_*} k_1(x + i\pi)\,dx\right\}. \tag{II.71}$$

These formulae have a very illustrative meaning. In Fig. 4 (attractive case) we can see that the parameter δ=$\delta_1 + \delta_2$ is given by the two contour integrals of adiabatic momenta between the adjacent complex turning points. In the repulsive case, however, the pairs of turning points degenerate on the real axis (regardless of the exponential model) and the only independent contour integral is that one for δ_{LZ}. The parameter δ_{RZ} (also δ_{LZ}) can be obtained by inverting the potential,

$$V_{ij}(x)|_{attr.} = V_{ij}^{(a)}(\infty) - (V_{ij}(x) - V_{ij}(\infty))\,, \tag{II.72}$$

and substituting the corresponding adiabatic momenta $k_i(x)|_{attr}$ into Eqs. (II.70) and (II.71) instead of $k_i(x+i\pi)$. It is well known in semiclassical analysis that the results for the attractive and repulsive cases do not differ in the high energy limit. The advantage of the above formulae, however, is that their validity does not require energy much bigger than the asymptotic separation of adiabatic potential energy levels. Such an achievement is quite substantial as we demonstrate in the next section. This is due to the contour integral definition of the substantial parameters δ_1 and δ_2 which enables us to apply the above formulae for energies even quite below the diabatic crossing point.

II.3 Numerical examples

We could expect that the high energy approximation is the critical factor which limits the accuracy of the present semiclassical treatment (see Eq. (II.20)). This approximation means in terms of energy

$$E \geq \frac{(\Delta U)^2}{\delta^2}, \quad \delta \to 0, \tag{II.73}$$

when we neglect quantities $\sim \delta^2$. However, we found that the results in Eqs. (II.44a)-(II.44d) are far more accurate than it could follow from Eq. (II.73). It is surprising that the theory works even when the energy is below the crossing point of diabatic potentials. Moreover, using the general formulae in Eqs. (II.64) and (II.65) we can extend the validity region of our results to a larger range of energy. Particular examples are given in Figs. 6 and 7. The following three quantities are shown in these figures:

$$P(E) = \left|S_{12}^R(E)\right|^2, \tag{II.74}$$

$$\Phi(E) = \frac{1}{\pi}\arg\left\{\frac{S_{11}^R(E)}{S_{22}^R(E)}\right\}, \tag{II.75}$$

and

$$\Psi(E) = \frac{1}{\pi}\arg\left\{S_{11}^R(E)S_{22}^R(E)\right\}. \tag{II.76}$$

The exact numerical solution (full line) is compared with our analytical solution (circles) from Eq. (II.62). We note that

$$S^R(E)_{ij} = \exp\left(-\imath(d_i + d_j)\right) S(E)_{ij}. \tag{II.77}$$

The phases of the reduced scattering matrix vary slowly with energy compared to those of $S(E)$. As it follows from Eq. (II.49) Ψ is equal to ± 1 as long as the double passage formula is justified. Φ includes the quantum phases ϕ and ψ as

well as the adiabatic phases Δ_1 and Δ_2. In Figs. 6-7 it can also be seen that the transition probability for asymptotically high energy has a simple form,

$$|S_{12}|^2 \sim \sin^2(2\theta(-\infty)) \sin^2\left(\frac{\sqrt{E}}{2} \ln \frac{a_1}{a_2}\right), \tag{II.78}$$

as follows from Eq. (II.46) in the limit $\delta \to 0$. In Fig. 6 the Stueckelberg oscillations can be seen not only in the overall transition probability, $P(E)$, but also in the S-matrix phase, $\Phi(E)$. In Fig. 7 these oscillations are very slow since the adiabatic potentials are almost parallel and $U_1 - U_2$ is small.

The above comparison of exact and analytical values can not be done, strictly speaking, for the nonadiabatic transition matrix. This is because the reduced scattering matrix in the form of double passage has only two independent parameters, P and Φ,

$$S^R(E) = \begin{pmatrix} i\sqrt{1-P(E)}\exp(i\pi\Phi(E)/2) & -\sqrt{P(E)} \\ -\sqrt{P(E)} & i\sqrt{1-P(E)}\exp(-i\pi\Phi(E)/2) \end{pmatrix}, \tag{II.79}$$

which can not provide enough equations for the three parameters of nonadiabatic transition matrix, p, ϕ and ψ. In other words, for any nonadiabatic transition matrix I we can find a group of matrices $IU(\omega; E)$,

$$U(\omega; E) \equiv \begin{pmatrix} \pm\sqrt{1-\omega} & \mp\sqrt{\omega}\exp(-\imath(\Delta_2 - \Delta_1)) \\ \pm\sqrt{\omega}\exp(\imath(\Delta_2 - \Delta_1)) & \pm\sqrt{1-\omega} \end{pmatrix}, \tag{II.80}$$

$0 < \omega < 1$, resulting in the same matrix $S^R(E)$. There is only one phase factor in the above matrix, $\Delta_2(E) - \Delta_1(E)$, which compensates the difference of adiabatic phase shifts between the turning points and the reference point. If used in Eq. (II.62) instead of I, U yields the same scattering matrix as $I = 1$.

II.4 Closing remarks

We have semiclassically solved the exponential potential model. The final expressions of the nonadiabatic transition matrix are given in terms of two parameters δ_1 and δ_2 which are defined by the general contour integrals of adiabatic momenta and are free from particular parameters of the exponential model. The expressions for nonadiabatic transition probability as well as the dynamical phases in terms of δ_1 and δ_2 are confirmed to be the same as found by Nikitin. The theory works well even at low energies far beyond the high energy approximation used in the beginning of our analysis. Interesting oscillation of the total transition probability was found at energies lower than the diabatic crossing point. This can be explained by the fact that the adiabatic avoided crossing point is much lower than the diabatic one. Our semiclassical treatment can reproduce even this

oscillation. The present theory is expected to be applicable to a broader class of potential models which have similar structures of the singularities in the complex plane.

Amendment

This amendment provides useful mathematical descriptions to such an extent that is sufficient for understanding the previous results in section II.

II.A. Hankel functions

First let us clarify what kind of Bessel functions we use for the four contour integrals. On the contours asymptotically bound to the upper half of the complex p plane $H^{(1)}_{-i\nu}(\rho p)$ function is used, while on those leading to the lower half plane $H^{(2)}_{i\nu}(\rho p)$ stands for the transformation kernel. Then the asymptotic form of the wave functions follows from the following expansions: for $\rho \to \infty$ $(z \to \infty)$ (corresponding to the closed channel region)

$$H^{(1)}_{-i\nu}(z) = \sqrt{\frac{2}{\pi z}} e^{-\pi\nu/2} \exp\left(i\left(z - \pi/4\right)\right) + O\left(z^{-3/2}\right) \tag{II.81}$$

and

$$H^{(2)}_{i\nu}(z) = \sqrt{\frac{2}{\pi z}} e^{-\pi\nu/2} \exp\left(-i\left(z - \pi/4\right)\right) \quad + O\left(z^{-3/2}\right) \quad (z \to \infty),$$

and for $\rho \to 0$ $(z \to 0)$ (corresponding to the open channel region)

$$H^{(1)}_{-i\nu}(z) = -\frac{1}{\sinh(\pi\nu)} \left(\frac{z}{2}\right)^{i\nu} \frac{1}{\Gamma(1+i\nu)} \left(1 - \frac{\left(\frac{z}{2}\right)^2}{1+i\nu}\right) \left[1 + O\left(z^2\right) + O\left(\exp(-\pi\nu)\right)\right] \tag{II.82}$$

and

$$H^{(2)}_{i\nu}(z) = -\frac{1}{\sinh(\pi\nu)} \left(\frac{z}{2}\right)^{-i\nu} \frac{1}{\Gamma(1-i\nu)} \left(1 - \frac{\left(\frac{z}{2}\right)^2}{1-i\nu}\right) \left[1 + O\left(z^2\right) + O\left(\exp(-\pi\nu)\right)\right].$$

In Eq. (II.82) it is convenient to take

$$\left(1 - \frac{\left(\frac{z}{2}\right)^2}{1 \pm i\nu}\right) \simeq \exp\left(\frac{\mp z^2}{4\nu}\right), \tag{II.83}$$

and also to apply the high energy limit,

$$\arg\left(\Gamma(1+i\nu)\right) = \frac{\pi}{4} + \nu \ln \nu - \nu + O(\nu^{-1}). \tag{II.84}$$

Finally we give the semiclassical Hankel functions. Substituting $Z(z) = y(z)/\sqrt{z}$ in Eq. (II.11) we obtain the WKB form of $y(z)$. In the limit $\nu^2 \gg 1$ the two independent solutions read

$$H^{(1,2)}_{\mp i\nu}(z) \sim \frac{1}{\sqrt{\nu^2 + z^2}} \exp\left(\pm i \int^z \sqrt{1 + \frac{\nu^2}{\xi^2}} d\xi\right). \tag{II.85}$$

II.B. Local solutions of Eq. (II.15)

Here we give the mathematical preliminaries of evaluating wave functions at $\rho \to \infty$, that means the solution in the classically inaccessible region. We expand Eq. (II.15) at each singular point of its solution (cf. Eq. (II.13)), because all smoothly varying terms are effectively canceled by the highly oscillating transforming Hankel functions in Eq. (II.10). After finding the local solutions we match them to the asymptotic WKB form.

Let us start with the Whittaker's standard form of confluent hypergeometric equation, i.e. in our case

$$\frac{d^2}{dz^2} f(z) + \left(-\frac{1}{4} + i\frac{\Delta}{z}\right) f(z) = 0, \quad \Im\Delta = 0. \tag{II.B.1}$$

The independent solutions of (II.B.1) are given in terms of confluent hypergeometric functions Φ and Ψ as

$$f_1(z) = z \exp(-z/2)\Phi(1 - i\Delta, 2, z) \tag{II.B.2}$$

and

$$f_2(z) = z \exp(-z/2)\Psi(1 - i\Delta, 2, z).$$

Taylor series to the order $O(1/|z|)$ yield

$$f_1(z) \simeq z^{i\Delta} \frac{\exp(-z/2)\exp(i\pi\epsilon)^{1-i\Delta}}{\Gamma(1 + i\Delta)} - z^{-i\Delta} \frac{\exp(z/2)}{\Gamma(1 - i\Delta)} \tag{II.B.3}$$

and

$$f_2(z) \simeq z^{i\Delta} \exp(-z/2), \quad \epsilon \equiv \operatorname{sgn}(\Im z), \quad \exp(z) \simeq 1,$$

the last relation indicating that p is still sufficiently close to the point of expansion. To match directly (II.B.3) to the WKB solutions of nonexpanded Schrődinger equation we need to introduce

$$f_+(z) \equiv f_2(z) \simeq z^{i\Delta} \tag{II.B.4}$$

and

$$f_-(z) \equiv Q f_1(z) + R f_2(z) \simeq z^{-i\Delta},$$

where

$$R = \frac{\Gamma(-i\Delta)}{i\Delta} \exp(i\pi\epsilon)^{1-i\Delta}. \tag{II.B.5}$$

Close to the origin it holds

$$\Phi(1-i\Delta,2,z) \simeq 1+o(z) \text{ and } \Psi(1-i\Delta,2,z) = \frac{1}{\Gamma(1-i\Delta)}\frac{1}{z} + o(\ln(z)). \tag{II.B.6}$$

Thus only the z^{-1} singular term arising from Ψ contributes $2\pi\imath$ (and the respective multiplicative constants) to the integral of the type

$$\int \frac{dz}{z} f_{\pm}(z) H(\kappa z), \quad \kappa \to \infty. \tag{II.B.7}$$

II.C. Confluent hypergeometric integral formulae

The confluent hypergeometric function Ψ which appears in Eq. (II.B.1) is defined as,

$$\Psi(a,c,\xi) = \frac{1}{2\pi i} \exp(-a\pi i)\Gamma(1-a) \int_{\infty e^{i\phi}}^{0^+} e^{-\xi t} t^{a-1}(1+t)^{c-a-1}. \tag{II.C.1}$$

Φ is related to Ψ by the Kummer relation

$$\Psi(a,c,\xi) = \frac{\Gamma(c-1)}{\Gamma(a-c+1)}\Phi(a,c,\xi) + \frac{\Gamma(c-1)}{\Gamma(a)}\xi^{1-c}\Phi(a-c+1,2-c,\xi), \tag{II.C.2}$$

and we have

$$\Phi(a,c,\xi) = 1 + o(\xi). \tag{II.C.3}$$

II.D. Bessel-Fourier contour integrals at $x \to -\infty$

Eq. (II.15) can not be solved in the WKB form when $x \to -\infty$, since the saddle points approach the singularities $p = \pm\sqrt{|a_i|}$. That is why we expand Eq. (II.15) to series, solve it locally for $p \sim \sqrt{a_i}$ and match to the asymptotic WKB form. From now on we assume that the definition of $\sqrt{a_i}$ or $\sqrt{c_i}$ is chosen for each contour in accordance with the respective branch cut (see Fig. 1). Substituting

$$z_i = -\frac{2i\mu}{\sqrt{a_i}}(p - \sqrt{a_i}) \tag{II.D.1}$$

we get (with the accuracy up to $O(\delta_i)$, $O(z_i)$)

$$\frac{d^2 f_1}{dz_i^2} + \left(-\frac{1}{4} + i\frac{\delta_i}{z_i}\right) f_1 = 0. \tag{II.D.2}$$

The asymptotic form of solutions of local Eq. (II.D.2) (see Eq. (II.B.4)) corresponds to that of the WKB solutions in Eq. (II.19). Thus they can be matched. Making use of Eqs. (II.12), (II.81) and (II.B.1-II.B.7) we finally get

$$I^{(1)}_{mn}(\rho) = \frac{\pi}{\sqrt{\mu}} \frac{s_n}{\delta_m \Gamma(\imath s_n \delta_m)} (a_m - a_{3-m})^{\imath s_n \delta_m} |a_m|^{i\nu/2} \left|\frac{a_m}{\mu}\right|^{\imath s_n \delta_m} \tag{II.D.3}$$

$$\times e^{\left(\frac{\pi}{2}(-\nu+\delta_m)\right)} \frac{\exp\left(|\sqrt{a_m}|\rho - \pi\nu/2\right)\sqrt{2}}{\left(\pi|\sqrt{a_m}|\rho\right)^{1/2}}; \quad c_m \equiv (-1)^{m-1}, \ \rho \to \infty.$$

Since only the singularity contributes to the integral, from Eq. (II.12) it follows that

$$I^{(2)}_{mn}(\rho) = (\beta_1 - a_m)\, I^{(1)}_{mn}(\rho), \ \rho \to \infty. \tag{II.D.4}$$

Thus the adiabatic wave functions are obtained by rotating the diabatic ones

$$\phi_1(\rho \to \infty) = (\gamma_{11} I^{(1)}_{11} + \gamma_{12} I^{(1)}_{12})(\cos\theta_0 - (\beta_1 - a_1)\sin\theta_0) \tag{II.D.5}$$

$$+(\gamma_{21} I^{(1)}_{21} + \gamma_{22} I^{(1)}_{22})(\cos\theta_0 - (\beta_1 - a_2)\sin\theta_0),$$

and

$$\phi_2(\rho \to \infty) = (\gamma_{11} I^{(1)}_{11} + \gamma_{12} I^{(1)}_{12})(\sin\theta_0 + (\beta_1 - a_1)\cos\theta_0)$$

$$+(\gamma_{21} I^{(1)}_{21} + \gamma_{22} I^{(1)}_{22})(\sin\theta_0 + (\beta_1 - a_2)\cos\theta_0),$$

where

$$\theta_0 \equiv \lim_{x \to -\infty} \theta(x).$$

It can be seen easily that

$$\cos\theta_0 - (\beta_1 - a_1)\sin\theta_0 \equiv 0 \equiv \sin\theta_0 + (\beta_1 - a_2)\cos\theta_0, \tag{II.D.6}$$

while the other terms in Eq. (II.D.5) are nonvanishing and growing exponentially with ρ. Since the adiabatic wave functions should vanish when $x \to -\infty$, we get the two conditions

$$\gamma_{21} I^{(1)}_{21} + \gamma_{22} I^{(1)}_{22} = 0 \text{ and } \gamma_{11} I^{(1)}_{11} + \gamma_{12} I^{(1)}_{12} = 0. \tag{II.D.7}$$

II.E. Bessel-Fourier contour integrals at $x \to \infty$

The WKB solution (II.19) of the Schrödinger equation (II.15) in the approximation (II.20) has the form (cf. Eqs. (II.13) and (II.19))

$$F^{(n)}_1(p) = \frac{1}{\sqrt{\mu}} \left(p^2 - a_1\right)^{\mp i\delta_1 - 1} \left(p^2 - a_2\right)^{\mp i\delta_2 - 1}, \quad n = 1, 2. \tag{II.E.1}$$

Making use of the Bessel function expansions (cf. Eqs. (II.82) and (II.84)) we get

$$I^{(1)}_{mn}(\rho \to 0) = \frac{\rho^{\imath c_n \nu}}{\sqrt{\mu}} e^{\imath c_n(\pi/4-\phi_0)} \int_{C_{mn}} (p^2-a_1)^{\mp i\delta_1 - 1}(p^2-a_2)^{\mp i\delta_2 - 1} p\, dp. \quad \text{(II.E.2)}$$

This integral can be reduced to the confluent hypergeometric function integral of Eq. (II.C.1) by means of the substitution

$$t_m = \frac{p^2 - a_m}{a_{3-m} - a_m}. \quad \text{(II.E.3)}$$

Evaluating the confluent hypergeometric functions at zero argument (see Eqs. (II.C.2) and (II.C.3)) we obtain

$$I^{(1)}_{mn}(\rho \to 0) = -\pi c_m \frac{\rho^{\imath c_n \nu}}{\sqrt{\mu}} e^{\imath c_n(\phi_0+\pi/4)} \frac{\Gamma(1+\imath c_n\delta)(a_2-a_1)^{-\imath c_n\delta - 1}}{\Gamma(1+\imath c_n\delta_1)\Gamma(1+\imath c_n\delta_2)}. \quad \text{(II.E.4)}$$

When evaluating $I^{(2)}_{mn}$, the integrand in Eq. (II.E.2) differs only by

$$\beta_1 - p^2 = c_m(a_2-a_1)(t_m + \delta_m/\delta). \quad \text{(II.E.5)}$$

Thus in the case of ψ_2 the leading order terms coming from Eq. (II.C.2) cancel. This is the reason why the ρ^2 term of Eq. (II.83) must be retained here. It comes from Eqs. (II.82), (II.83), (II.C.1), (II.C.2), and gives the difference between $\rho^{i\nu}$ and $\rho^{i\mu}$. The final result is

$$I^{(2)}_{mn}(\rho \to 0) = -c_n \frac{\rho^{\imath c_n \mu}}{\sqrt{\mu}} e^{\imath c_n(\phi_0 - \delta\ln(4\nu) - \pi/4)} e^{\pi\delta/2}\Gamma(-\imath c_n\delta) e^{-\pi\delta_m} \mathrm{sh}(\pi\delta_m). \quad \text{(II.E.6)}$$

II.F. Proof of the unitarity of S-matrix

Using the following identities

$$\Gamma(1-i\delta) = -i\delta\Gamma(-i\delta), \quad \text{(II.F.1)}$$

$$|\Gamma(i\delta)|^2 = \frac{\pi}{\delta \mathrm{sh}(\pi\delta)}, \quad \text{(II.F.2)}$$

and

$$(a_2 - a_1) = \frac{\delta}{\sqrt{\delta_1\delta_2}}, \quad \text{(II.F.3)}$$

we can find that the S-matrix in Eqs. (II.44a)-(II.44d) satisfies

$$S_{12} = S_{21}, \quad |S_{11}|^2 = |S_{22}|^2 \text{ and } |S_{11}|^2 + |S_{12}|^2 = 1. \quad \text{(II.F.4)}$$

The last unitarity condition to be proven is

$$S_{11}S^*_{12} + S_{12}S^*_{22} = 0, \quad \text{(II.F.5)}$$

or in other words

$$\arg(S_{11}) + \arg(S_{22}) - 2\arg(S_{12}) = (2k+1)\pi, \quad k \in Z. \tag{II.F.6}$$

Taking into account the extracted prefactors in the S-matrix of Eqs. (II.44a)-(II.44d) it is sufficient to prove that

$$\arg\left[\mathrm{sh}(\pi\delta_1)e^{i\alpha_1} + \mathrm{sh}(\pi\delta_2)e^{\pi\delta}e^{i\alpha_2}\right] + \arg\left[\mathrm{sh}(\pi\delta_1)e^{i\alpha_2} + \mathrm{sh}(\pi\delta_2)e^{\pi\delta}e^{i\alpha_1}\right] = \tag{II.F.7}$$

$$= 2\arg\left[e^{i\alpha_2} - e^{i\alpha_1}\right] + (2k+1)\pi,$$

which is just an algebra.

II.G. Adiabatic scattering phase shifts

First we give an account of real definite integrals

$$\int_\epsilon^x \frac{dx}{x-d}\sqrt{\frac{x-\epsilon}{x}} = \ln|x-d| - \ln|d| + \tag{II.G.1}$$

$$\frac{\epsilon}{2d}(1 - \ln|\epsilon| - \ln|x-d| + \ln|d| + \ln|x| + 2\ln 2) + O(\epsilon^2),$$

$$\int_\epsilon^x \frac{dx}{(x-d)(x-e)}\sqrt{\frac{x-\epsilon}{x}} = \frac{1}{e-d}(\ln|d| - \ln|x-d| - \ln|e| + \ln|x-e|) + O(\epsilon), \tag{II.G.2}$$

and

$$\int_{i\nu}^x \sqrt{1 + \frac{\nu^2}{\xi^2}}\, d\xi = \nu + \frac{\nu}{2}\ln\frac{x}{\nu} + \frac{x^2}{4\nu} + O(\nu^{-3/2}). \tag{II.G.3}$$

Manipulating the second term in Eq. (II.55) yields (note that $c_i < 0$)

$$\int_{\sqrt{c_i}}^p \sqrt{\frac{(p^2-c_1)(p^2-c_2)}{(p^2-a_1)(p^2-a_2)}}\frac{dp}{p} = \tag{II.G.4}$$

$$\frac{1}{2}\int_{c_i-a_i}^{p^2-a_i} \frac{dx}{x+a_i}\sqrt{\frac{x-(c_i-a_i)}{x}}\sqrt{1 - \frac{c_{3-i}-a_{3-i}}{x-(a_{3-i}-a_i)}}.$$

Evaluating the phase shifts d_i and Δ_i we can expand the second square root in Eq. (II.G.4) with respect to $a_i - c_i$, which is proportional to the inverse of energy. Using identities in Eqs. (II.G.1) - (II.G.3), we can evaluate all the phaseshifts. The results are given in Eqs. (II.56), (II.57) and (II.58). The last term in Eq. (II.58) originates from the following

$$\Delta_1 - \Delta_2 = \Re\left\{\int_{x_1'}^{x_c} k_1(x)dx - \int_{x_2'}^{x_c} k_2(x)dx + \int_{x_c}^{\Re x_c}(k_1(x) - k_2(x))dx\right\}. \tag{II.G.5}$$

The first two integrals in Eq. (II.G.5) follow from Eqs. (II.G.1) - (II.G.3), while the last one can be evaluated by Taylor expansion,

$$k_j(x) = \sqrt{E - u_j^a(x)} \simeq \sqrt{E} - \frac{u_j^a(x)}{2\sqrt{E}}, \tag{II.G.6}$$

since the last integration path is separated from the turning point. Then the exact result is the same as in the attractive case [15], i.e.,

$$\frac{1}{2\sqrt{E}} \Re \left\{ \int_{\Re x_c}^{x_c} (u_1^a(x) - u_2^a(x))\, dx \right\} = 2\sqrt{\delta_1 \delta_2} + \delta_1 \ln \frac{\sqrt{\delta} - \sqrt{\delta_2}}{\sqrt{\delta} + \sqrt{\delta_2}}. \tag{II.G.7}$$

II.H. Contour integrals to define δ_j

The parameters δ_1 and δ_2 introduced in Eq. (II.21) are defined as [15]

$$\delta_i = \frac{1}{2\pi i} \oint_{L_j} \sqrt{P_0}\, dp, \tag{II.H.1}$$

where L_i-th contour encircles the branch cut between $\sqrt{a_i}$ and $\sqrt{c_i}$ in the positive direction. For details see Fig. 2. Eq. (II.21) is a result of high energy approximation of Eq. (II.H.1), i.e. the high energy expansion of $\sqrt{P_0}$ in powers of $a_i - c_i$. Let us show now that Eq. (II.H.1) can be put to a form of adiabatic momentum contour integral. We start with Eqs. (II.22) and (II.25) and the easier attractive case. Then it suffices to find contours in the ρ^2 plane corresponding to the contours L_i in the p plane (using Eq. (II.24)),

$$\rho^2 = P_0(p_i^\dagger) - \frac{\nu^2}{p_i^{\dagger 2}}. \tag{II.H.2}$$

The transformed contours are shown in Fig. 3. None of these closed contours encircles $\rho^2 = 0$ or ρ_0^2, the solution of

$$p_j^\dagger(\rho_0) = 0, \tag{II.H.3}$$

given by

$$\rho_0^2 = -\frac{4\beta_1(U_1 - U_2)}{\beta_1\beta_2 - 1} \quad (j = 1, (2) \text{ attractive (repulsive) case}), \tag{II.H.4}$$

that is why the last integral in Eq. (II.22) on such a contour must vanish,

$$\oint \sqrt{1 + \frac{\nu^2}{\xi^2}}\, d\xi \equiv 0. \tag{II.H.5}$$

Since the contours L_i in the ρ^2 plane are symmetric with respect to the real axis and the integrand in Eq. (II.H.1) is complex conjugate with respect to this axis,

the real part of the integral must vanish and the contribution of the imaginary part coming from the upper and lower half-plane doubles. Then Eqs. (II.64) and (II.65) follow from Fig. 3 and Eqs. (II.22) and (II.H.5). Note that the integration path in the x plane is just distorted in a way which does not change the result (see Figs. 3 and 4).

Though in the repulsive case the contours for δ_1 and δ_2 in the p-plane (see Fig. 2) are very similar to those in the attractive case, the general expressions in terms of contour integrals in the x-plane are quite different. Let us start with a note on the difference between the two cases,

$$V_i \to -V_i, \quad \beta_i \to -\beta_i, \quad a_i \to -a_{3-i} \text{ and } c_i \to -c_{3-i}. \tag{II.H.6}$$

As a result,

$$\delta_i \to \delta_{3-i}, \tag{II.H.7}$$

both for the approximate expression of δ_i from Eq. (II.21) and the exact one from Eqs. (II.16) and (II.H.1). The change of the sign in Eq. (II.H.6) is equivalent to

$$x \to x \pm i\pi, \tag{II.H.8}$$

leaving the preexponential constants V_i, (i=1,2) unchanged.

The contours for δ_1 and δ_2 in the ρ^2-plane (repulsive case) are shown in Fig. 5. Both of them encircle zero, thus before they can be moved through it, the behaviour of the integrand at this point must be clarified. We have

$$\sqrt{P_0(p_j)}\frac{dp_j}{d(\rho^2)} = (-1)^j \frac{\nu^2-\mu^2}{4p_j^2\rho^4} \frac{p_{3-j}^2 - \beta_2}{\sqrt{1+\left(\frac{\beta_1-\beta_2}{2} - \frac{\mu^2-\nu^2}{2\rho^2}\right)^2}} \sqrt{zp^2+\nu^2}. \tag{II.H.9}$$

From the above equations it follows that

$$\sqrt{P_0(p_1)}\frac{dp_1}{d(\rho^2)} = C + O(\rho^2), \quad C \in Z \tag{II.H.10}$$

and

$$\sqrt{P_0(p_2)}\frac{dp_2}{d(\rho^2)} = -\frac{\mu}{2z} + O(1). \tag{II.H.11}$$

As a result of Eq. (II.H.11) the zero has a contribution to δ_2,

$$\frac{1}{2\pi_1}\oint_0 \sqrt{P_0(p_2)}\frac{dp_2}{d(\rho^2)}d\rho^2 = \frac{\mu}{2}. \tag{II.H.12}$$

While the contour for δ_1 avoids ρ_0^2 (the contour L_1 in the p-plane can go around $\sqrt{\beta_1}$ instead of the turning point $\sqrt{c_1}$), the contour for δ_2 does not (the contour L_2 in the p-plane can go around $p=0$ which corresponds to ρ_0^2). That is why there is one more contribution to δ_2 from the integral in the complex $\rho p(\rho)$-plane,

$$\frac{1}{2\pi_1}\oint_{\rho_0 p_1(\rho_0)} \sqrt{1+\frac{\nu^2}{\xi^2}}d\xi = -\frac{\nu}{2}. \tag{II.H.13}$$

The contributions to δ_2 arising from the zero $\rho^2 = 0$ and from the second term in Eq. (II.22) finally give

$$\delta = \delta_1 + \delta_2 = \frac{\mu - \nu}{2}. \qquad \text{(II.H.14)}$$

The contour integrals encircling the complex crossing points in the ρ^2-plane both for δ_1 and δ_2 have the form of Eq. (II.65), differing just by a sign due to the opposite fixing of branch cuts (in Fig. 5a) the integrand is k_1 while in Fig 5b) the integrand is k_2).

The alternative way to examine the contours is as follows. We start with Eqs. (II.22) and (II.25) which can be modified to the following form

$$\oint_{L_i} P_0(p)dp = \oint \sqrt{E - u_i^{(a)}(\rho^2)}\frac{d(\rho^2)}{\rho^2} - \frac{\nu}{2}\left[\ln\frac{1 + 2\sqrt{E - u_i^{(a)}}}{1 - 2\sqrt{E - u_i^{(a)}}}\right]. \qquad \text{(II.H.15)}$$

The closed contours are always oriented in the positive direction and encircle zero in the ρ^2 plane. Evaluating the second integral in Eq. (II.H.15) by the residue theorem and taking into account that $[\ ] = 2i\pi$ we obtain the same results as above.

III Diabatically Avoided Crossing

Here we review our achievements in the diabatically avoided crossing system. The full account is given in the Paper 3 (sections I, II, IV therein).

III.1 Opening remarks

Needless to say, nonadiabatic transitions among mutually coupled potential energy curves play crucial roles in variety of fields of physics, chemistry, biology [1-19] and, if properly generalized, even in social sciences [20]. There are two most fundamental types of nonadiabatic transitions due to curve crossing, i.e. the Landau-Zener (LZ) type in which two diabatic potentials cross with the same sign of slopes, and the nonadiabatic tunneling (NT) type in which two diabatic potentials cross with opposite signs of slopes [18,19]. The NT type presents a very interesting and important mechanism, because (1) a potential barrier is created by the coupling and it can be a crucial mechanism of phase transition, and (2) furthermore the complete reflection occurs. This phenomenon is utilized to suggest a new type of molecular switching [21-23]

Recently, there has been a significant development in the theoretical studies of controlling atoms and molecules by lasers [24-26] Intense time-dependent electromagnetic fields are used to enhance or suppress processes such as photodissociation branching, autoionization, spontaneous emission and many others [24-38]. Many molecular processes in laser fields can be explained just as a sequence of nonadiabatic transitions [19,33,38] in the dressed state or the Floquet state formalism [39]. In the case when the energy levels cross with each other as a function of time, the semiclassical theory of time-dependent LZ-type nonadiabatic transition can be utilized [40]. On the other hand, if we use the dressed state picture in the spatial coordinate, i.e. when the potential energy curves cross as a function of spatial coordinate among the dressed states, then the NT type of curve crossings also appear. In such cases, the above mentioned phenomenon of complete reflection should play an interesting role and must be useful to control various molecular processes [21-23,35]. To this aim we first examine in section III a diabatically avoided crossing model.

III.2 Exact quantum solution

We start with the following quantum model,

$$-\frac{\hbar^2}{2M}\psi_1'' + (V_{11}(x) - E)\psi_1 + V_{12}(x)\psi_2 = 0, \tag{III.1}$$

$$-\frac{\hbar^2}{2M}\psi_2'' + (V_{22}(x) - E)\psi_2 + V_{12}(x)\psi_1 = 0, \tag{III.2}$$

where the two diabatic potentials behave as

$$\lim_{|x|\to\infty} V_{11}(x) = \infty \text{ and } V_{22}(x) \leq C. \tag{III.3}$$

In the diabatically avoided crossing type it holds

$$\forall x, \quad V_{11}(x) \neq V_{22}(x). \tag{III.4}$$

One example of the diabatically avoided crossing type is a ground state potential with a barrier shifted up by the photon frequency to such an extent that it can not intersect with an excited electronic state which has a well. We introduce a new analytical model based on exponential potential functions. Unlike from the other models of exponential potentials,[12-14] which represent a one turning point case, here we have two turning points on the upper potential curve. The possible applications include inhibition of collision processes by a high frequency laser field. Such a model is important, because (1) it is exactly solvable and (2) enables an interesting comparison with the crossing cases. It should be noted that in the dressed state picture the diabatic states considered here are the ordinary Born-Oppenheimer adiabatic states without laser fields and the diabatic coupling is nothing but the interaction with the field.

We remark that in the time-independent scheme there are only few models which can be solved exactly in terms of wave functions [19,41-44]. In addition to these, the present one is the first diabatically avoided crossing model.

The diabatically avoided crossing (DAC) model is defined by the following potential matrix

$$V = \begin{pmatrix} U + Ve^{\alpha|x|} & C \\ C & U - Ve^{\alpha|x|} \end{pmatrix}. \tag{III.5}$$

Although the model has an exact solution for the two different exponential constants, α_1 for $x < 0$ and α_2 for $x > 0$, here we restrict ourselves to the case $\alpha_1 = \alpha_2$. Let us make a constant rotation by $\pi/4$, then Eq. (III.5) reduces to a half-cut Rosen-Zener-Demkov (RZD) model, [12]

$$R(\pi/4)VR(-\pi/4) = \begin{pmatrix} U_1 & Ve^{\alpha|x|} \\ Ve^{\alpha|x|} & U_2 \end{pmatrix}, \tag{III.6}$$

where $R(\Theta)$ represents the rotation by angle Θ and

$$U_1 = U + C, \quad U_2 = U - C. \tag{III.7}$$

Eigenvalues of the above matrix (which coincide with the RZD adiabatic potentials) are (see Fig. 8a)

$$u_{1,2}^{(a)}(x) = U \pm \sqrt{(Ve^{\alpha|x|})^2 + C^2} \tag{III.8}$$

Introducing a new variable and the dimensionless parameters,

$$z(x) = \frac{M^2V^2}{4(\hbar\alpha)^4}e^{-2\alpha x} \quad q_i = \sqrt{2M(E-U_i)}/\hbar\alpha, \quad i = 1,\ 2, \tag{III.9}$$

it turns out that the model is one of those that can be solved exactly in terms of the Meijer G functions, [47]

$$G^{mn}_{pq}\left(z|\ \begin{matrix}\{a\}\\ \{b\}\end{matrix}\right). \tag{III.10}$$

In Eq. (III.10) a and b are certain energy dependent parameters. For further details about the Meijer G functions, see Amendment A. The four independent solutions of the DAC wave function are given analytically by (see also Eqs. (III.A.5) and (III.A.9) in the Amendment))

$$\Psi_r = \frac{1}{\sqrt{2}}\begin{pmatrix} G^{40}_{04}(e^{2\pi i r}z|\{b\}) - (-1)^{r+1}G^{40}_{04}(e^{2\pi i r}z|\{b'\}) \\ G^{40}_{04}(e^{2\pi i r}z|\{b\}) + (-1)^{r+1}G^{40}_{04}(e^{2\pi i r}z|\{b'\}) \end{pmatrix}, \tag{III.11}$$

$$r = -1, \ldots 2, \quad \{b\} \equiv \{b_1, b_2, b_3, b_4\},$$
$$b_{1,2} = \pm iq_1/2, \quad b_{3,4} = 1/2 \pm iq_2/2, \tag{III.12}$$

z is defined in Eq. (III.9) and

$$\{b'\} = \{b\}|_{q_1 \leftrightarrow q_2}. \tag{III.13}$$

Thus we can expand the total wave function as

$$\begin{pmatrix} \psi_1 \\ \psi_2 \end{pmatrix} = \sum_{r=-1,0,1,2} c_r \Psi_r. \tag{III.14}$$

Taking into account the asymptotic behavior of Meijer G functions at $x \to -\infty$ ($z \to \infty$),

$$\begin{aligned} G^{40}_{04}(e^{-2\pi i}z|\cdot) &\sim \tfrac{e^{i\eta}}{\sqrt{\eta}}, \\ G^{40}_{04}(z|\cdot) &\sim \tfrac{e^{-\eta}}{\sqrt{\eta}}, \\ G^{40}_{04}(e^{2\pi i}z|\cdot) &\sim \tfrac{e^{-i\eta}}{\sqrt{\eta}}, \\ G^{40}_{04}(e^{4\pi i}z|\cdot) &\sim \tfrac{e^{\eta}}{\sqrt{\eta}}, \\ \eta &= 4\sqrt[4]{z}, \end{aligned} \tag{III.15}$$

and the boundary conditions, we have for $x < 0$:

$$\begin{pmatrix} \psi_1 \\ \psi_2 \end{pmatrix} = \alpha\Psi_{-1} + \beta\Psi_0 \tag{III.16}$$

and for $x > 0$:

$$\begin{pmatrix} \psi_1 \\ \psi_2 \end{pmatrix} = \gamma\Psi_{-1} + \delta\Psi_0 + \Psi_1. \tag{III.17}$$

Here $|\alpha|^2$ represents the transmission coefficient and $|\gamma|^2$ the reflection coefficient, $|\alpha|^2 + |\gamma|^2 = 1$. The constants $\{\alpha, \beta, \gamma, \delta\}$ that are to be determined follow from the condition that at $x = 0$ the wave function and its first derivative must be continuous. The constant α should not be confused with α in Eq. (III.5). Transformation of the kinetic energy operator,

$$\frac{d}{dx} = \frac{dz}{dx}\frac{d}{dz} \text{ and } \left.\frac{d}{dx}e^{2|x|}\right|_{x=0} = \pm 2, \tag{III.18}$$

and the routine manipulations lead to the following system of equations,

$$\begin{pmatrix} G^{(-1)}(b) & -G^{(-1)}(b) & G^{(0)}(b) & -G^{(0)}(b) \\ G^{(-1)}(b') & -G^{(-1)}(b') & -G^{(0)}(b') & G^{(0)}(b') \\ G^{(-1)},(b) & G^{(-1)},(b) & G^{(0)},(b) & G^{(0)},(b) \\ G^{(-1)},(b') & G^{(-1)},(b') & -G^{(0)},(b') & -G^{(0)},(b') \end{pmatrix} \begin{pmatrix} \alpha \\ \gamma \\ \beta \\ \delta \end{pmatrix}$$

$$= \begin{pmatrix} G^{(1)}(b) \\ G^{(1)}(b') \\ -G^{(1)},(b) \\ -G^{(1)},(b') \end{pmatrix} \tag{III.19}$$

with

$$G^{(r)}(b) \equiv G^{40}_{04}(e^{2\pi i r} z_0 | b), \quad z_0 \equiv z(x = 0), \tag{III.20}$$

and

$$G^{(r)},(b) \equiv \frac{d}{dz} G^{40}_{04}(e^{2\pi i r} z_0 | b) = \frac{1}{z}(G^{(r)}(b_i + \delta_{1,i}) - b_1 G^{(r)}(b)).$$

Let us note that there is a useful relation,

$$\left(G^{(1)}(b)\right)^* = G^{(-1)}(b) \text{ and } \left(G^{(1)},(b)\right)^* = G^{(-1)},(b). \tag{III.21}$$

We denote the column vectors in Eq. (III.19) by the numbers $I - V$ (from left to right) and define

$$M = \det(I, II, III, IV) \text{ and } \mu = \det(V, II, III, IV) \tag{III.22}$$

together with

$$z_1 = \left(G^{(-1)}(b)G^{(0)}(b') + G^{(-1)}(b')G^{(0)}(b)\right) = r_1 \exp(i\phi_1) \tag{III.23}$$

and

$$z_2 = \left(G^{(-1)},(b)G^{(0)},(b') + G^{(-1)},(b')G^{(0)},(b)\right) = r_2 \exp(i\phi_2). \tag{III.24}$$

Then we obtain

$$M = -4r_1 r_2 \exp(i(\phi_1 - \phi_2)) \text{ and } \mu = 4ir_1 r_2 \Im\left\{\exp\left(i(\phi_2 - \phi_1)\right)\right\}. \tag{III.25}$$

Consequently,

$$\alpha = -i \sin(\phi_1 + \phi_2) \exp(i(\phi_2 - \phi_1)) \tag{III.26}$$

and

$$\gamma = -\cos(\phi_1 + \phi_2) \exp(i(\phi_2 - \phi_1)). \tag{III.27}$$

If the coupling vanishes, i.e. $U_1 - U_2 = 0$ and $b' = b$, we have a simple barrier penetration problem, which is solved with

$$\phi_1 = \arg G^{(-1)}_{\cdot}(b), \quad \phi_2 = \arg G^{(1)}(b) \text{ and } \beta = 0 = \delta. \tag{III.28}$$

III.3 Semiclassical solution

Here we give the semiclassical solution in two ways: (1) starting from the exact solution, i.e. ex post, and (2) starting from the Wentzel-Krammers-Brillouine approximation, i.e. ex ante.

III.3.1 Ex post

First, let us try to analyze the behavior of the above expressions at high energies,

$$q_1 \gg 1, \quad q_2 \gg 1 \text{ and } |q_1 - q_2| \gg 1. \tag{III.29}$$

We keep only the leading order term in Eqs. (III.23) and (III.24), use the expansion formula in Eq. (II.3), and define the new phase,

$$\psi = \frac{q_1}{2} \ln|z| - \arg \Gamma(iq_1) + \arg \Gamma\left(\frac{1}{2} + i\frac{q_2 - q_1}{2}\right) + \tag{III.30}$$

$$+\arg \Gamma\left(\frac{1}{2} - i\frac{q_1 + q_2}{2}\right)$$

together with $\psi' = \psi(q_1 \leftrightarrow q_2)$. Then we have

$$\phi_1 \simeq \arctan\left(\frac{\sin(\psi + \psi') + \eta \sin(\psi - \psi')}{2 \cos\psi \cos\psi'}\right) \tag{III.31}$$

and

$$\phi_2 \simeq \arctan\left(\frac{\sin(\psi + \psi') - \eta \sin(\psi - \psi')}{2 \sin\psi \sin\psi'}\right), \tag{III.32}$$

where

$$\eta = \tanh\left(\pi\frac{q_1 - q_2}{4}\right). \tag{III.33}$$

Setting $x_i = \tan\phi_i$, the result for the transmission and reflection coefficients reads

$$|\alpha|^2 \simeq \frac{(x_1 + x_2)^2}{(1 + x_1^2)(1 + x_2^2)} \text{ and } |\gamma|^2 = 1 - |\alpha|^2. \tag{III.34}$$

Hence the complete reflection, $\alpha = 0$, is given by the condition

$$\tan(\psi + \psi') = \eta \tan(\psi - \psi'). \tag{III.35}$$

If we use the simple relations in the high energy approximation,

$$|q_1 - q_2| \sim E^{-1/2} \sim \psi - \psi' \sim \eta, \tag{III.36}$$

we have in the limit of zero-th order,

$$\psi = \psi', \quad \phi_1 = \psi, \quad \phi_2 = \pi/2 - \psi \text{ and } |\alpha|^2 = 1. \tag{III.37}$$

Namely, the transmission coefficient tends to unity at energies asymptotically high. The necessary correction to this oversimplified estimate is to re-express the transmission coefficient near the complete reflection point. Expanding

$$\psi(E) = \frac{\pi}{2} + \omega + \xi(E - E_0) \tag{III.38}$$

$$\psi'(E) = \frac{\pi}{2} - \omega + \xi(E - E_0),$$

and substituting Eq. (III.38) into Eq. (III.34), we obtain

$$|\alpha|^2 = \frac{\epsilon^2}{\epsilon^2 + [\xi(\epsilon - \epsilon_+)(\epsilon - \epsilon_-)]^2}, \quad \epsilon \equiv E - E_0 \quad \epsilon_\pm = \frac{\omega}{\xi}(\eta \pm 1). \tag{III.39}$$

Here

$$\xi = \frac{1}{2}\frac{d}{dE}(\psi + \psi')|_{E=E_0} \text{ and } \omega = \frac{1}{2}(\psi - \psi')|_{E=E_0}. \tag{III.40}$$

The resonance profile in Eq. (III.39) smoothly connects the zero dip in $|\alpha|^2$ to the unity background within the accuracy of the high energy expansion. The resonance position, E_0, follows from Eqs. (III.35) and (III.36), and is given by

$$\psi(E_0) \sim \sqrt{E_0}\left(\frac{1}{2}\ln|z_0| + 2 - \ln(E))\right) = (2n-1)\frac{\pi}{2}. \tag{III.41}$$

This condition coincides with the Bohr-Sommerfeld quantization condition in the upper well,

$$\int_{x_L'}^{x_R'} \sqrt{E - V_{11}(x)}\, dx = \left(n - \frac{1}{2}\right)\pi \quad n = 1, \ldots \tag{III.42}$$

III.3.2 Ex ante

In order to make the physical interpretation of the above equations clear we carry out the semiclassical analysis of the diabatically avoided crossing model. Suppose that the diabatic and adiabatic potentials at $x \to 0$ almost coincide, i.e. $V \ll |U_1 - U_2|$, or in other words the region $x \sim 0$ is far enough from the nonadiabatic transition regions which can be represented by the real parts of the complex crossing points. Then the scattering can be decomposed into adiabatic wave propagation and two nonadiabatic transitions (left and right). Each of them is described by a nonadiabatic transition matrix [1,15]

$$I(x_s) = \begin{pmatrix} \sqrt{1-p_s}\exp(-i\phi_s) & -\sqrt{p_s}\exp(-i\psi_s) \\ \sqrt{p_s}\exp(i\psi_s) & \sqrt{1-p_s}\exp(i\phi_s) \end{pmatrix}, \quad s = L \text{ or } R. \tag{III.43}$$

These matrices connect from left to right the WKB wave functions centered at the transition points, p_s is the nonadiabatic transition probability and ϕ_s and ψ_s are the dynamical phases. The upper (lower) adiabatic channel is indexed by 1 (2) (see Figs. 8a, 9a, 10a). There are three coordinate regions, (x_L^t, x_L), (x_L, x_R), and (x_R, x_R^t) (see Fig. 9a), where x_s^t (x_s) represents the turning point (transition point). The transition points x_L and x_R are the real parts of the corresponding complex crossing points. We denote these regions as i, $i = I, II, III$, $x_i < x < x_{i+1}$ $(x_1 = x_L^t, \ldots, x_4 = x_R^t)$ and introduce the following phase factors,

$$c_i \equiv \exp(id_i) = \exp\left(i\Re \int_{x_i}^{x_{i+1}} \sqrt{E - u_1^{(a)}(x)}\, dx\right), \quad c \equiv c_1 c_2 c_3, \tag{III.44}$$

and

$$d \equiv \exp(i\delta) = \exp\left(i\Re \int_{x_2}^{x_3} \sqrt{E - u_2^{(a)}(x)}\, dx\right) / c_2 \equiv \exp(id_2^2)/c_2. \tag{III.45}$$

The semiclassical diagram [19] corresponding to this problem is shown in Fig. 8 b). The circle, rectangular and arrow indicate turning point, nonadiabatic transition and adiabatic wave propagation, respectively. In order to simplify the following expressions, we introduce the interference terms for a wave propagating from the adiabatic state j (left) to the adiabatic state i (right),

$$z_{ij} \equiv R_{i1}L_{1j} + R_{i2}L_{2j}d, \tag{III.46}$$

where L (R) stands for the left (right) nonadiabatic transition matrix. The matching of corresponding wave functions between the three regions follows. According to Fig. 8b), the waves in region I are determined by the boundary conditions,

$$Ac_1\ \overline{1}\ - iAc_1^*\ \overline{1}\ + B\ \overline{2}\ . \tag{III.47}$$

Then we propagate the total wave function to region II,

$$L_{11}Ac_1c_2\ \overline{1}\ + c_2^*(L_{11}^*c_1^*(-iA) + L_{12}^*B)\ \overline{1}$$

$$+L_{21}c_1c_2dA\ \overrightarrow{2} + c_2^*d^*(L_{21}^*c_1^*(-iA) + L_{22}^*B)\ \overleftarrow{2},$$

and region III,

$$X\ \overrightarrow{1} + Y\ \overleftarrow{1} + z_{21}c_1c_2A\ \overrightarrow{2} + [z_{21}^*c_1^*c_2^*(-iA) + z_{22}^*c_2^*B]\ \overleftarrow{2}\ .$$

The notations c_i, d and z_{ij} are introduced in Eqs. (III.44-III.46); arrows denote the direction of adiabatic wave,

$$X \equiv z_{11}cA,$$

and

$$Y \equiv z_{11}^*c^*(-iA) + c_2^*c_3^*z_{12}^*B.$$

In Eq. (III.47), the so far arbitrary constant A (B) denotes the amplitude of a wave in the upper (lower) channel which satisfies the boundary conditions for scattering from right to left. The right turning point imposes a condition on these constants (see Eq. (III.47)),

$$X(A) = -iY(A, B). \tag{III.48}$$

The reflection coefficient, $|R|^2$, is easily obtained as

$$|R|^2 = \frac{|z_{12}z_{21}|^2}{|z_{12}z_{21}c - (z_{11}c + z_{11}^*c^*)z_{22}|^2}, \quad |T|^2 = 1 - |R|^2. \tag{III.49}$$

There are two special cases that solve Eq. (III.48). Taking $B = 0$, we obtain the complete reflection condition,

$$\int_{x^{(a)}{}_L'}^{x^{(a)}{}_R'} \sqrt{E - u_1^{(a)}(x)}\, dx = (n - \frac{1}{2})\pi + \Delta(E), \tag{III.50}$$

with an additional shift $\Delta(E)$ to the Born-Sommerfeld quantization condition in the upper well,

$$\Delta(E) = \arctan\left(\frac{\zeta \sin(\phi_L + \phi_R) + \sin(\psi_L - \psi_R + \delta)}{\zeta \cos(\phi_L + \phi_R) - \cos(\psi_L - \psi_R + \delta)}\right), \tag{III.51}$$

where

$$\zeta \equiv \sqrt{\frac{(1 - p_L)(1 - p_R)}{p_L p_R}} \tag{III.52}$$

and δ is given in Eq. (III.45). Now, it is clear that Eq. (III.42) is just the high energy limit of Eq. (III.50). If both p_L and p_R are small, the quantization in Eq. (III.50) occurs naturally in the adiabatic well with the imposed shift from diagonal dynamical phases, ϕ_L and ϕ_R (see the above equation). If both p_L and p_R tend to unity, on the other hand, the quantization occurs in the diabatic well

and the imposed phase shift is due to the off-diagonal dynamical phases, ψ_L and ψ_R. Applying the complete transmission condition to Eq. (III.48), which turns out to be equivalent to $A = 0$, we obtain

$$p_L = p_R \equiv p \quad \text{and} \quad \delta + \phi_L + \phi_R + \psi_L - \psi_R = \pi. \tag{III.53}$$

If p tends to zero or unity, the second condition in Eq. (III.53) can be omitted. The above equation has a very simple and interesting physical meaning: the incident wave interferes between the two transition points in such a way that no part of it reaches the turning points in the upper adiabatic channel. This is because in region I (left turning point), $A = 0$, and consequently in region III (right turning point), $X(A) = 0$ and $Y(A, B) = 0$ (see Eqs. (III.47) and (III.48)). The parameters of nonadiabatic transition matrices in Eq. (III.43), in the case of above model, are given in Eq. (III.B.1) in the Amendment. Eqs. (III.49) and (III.B.1) give the semiclassical transmission and reflection coefficients. Let us finally note that Eq. (III.51) is invariant with respect to the following transformation

$$L \leftrightarrow R \text{ and } \psi \leftrightarrow \pi - \psi, \tag{III.54}$$

as it should be due to the symmetry.

III.4 Numerical examples

In order to avoid unnecessary parameters let us use the units

$$[E] = (\hbar\alpha)^2(2M)^{-1}, \quad [x] = \alpha^{-1}. \tag{III.55}$$

Then, as it follows from Eq. (III.5), there are only two substantial parameters, V and C. These parameters affect the general behavior of the transmission coefficient (see Figs. 11), which is: (1) the exponential decrease at energies far below the top of the lower potential, then (2) overall monotonous increase up to the first complete reflection point, and (3) complete reflection dips with an envelope that converges to unity.

In the limit of small coupling, C (see Fig. 11a), the transmission coefficient corresponds to that of a single barrier penetration, except that the complete reflection dips survive with very narrow widths. For large values of C (see Fig. 11b in comparison with Fig. 11a) the first step broadens and the first resonance moves to higher energies because the bottom of the upper adiabatic potential shifts up with growing C. Also the complete reflection dips become wider.

In the limit of small pre-exponential constant, V (see Fig. 11c in comparison with Fig. 11d), the potential curves become flat, the step is sharper and the resonances become more dense because the semiclassical phase in the upper well accumulates easily. The semiclassical theory based on a sequence of two RZ type transitions works well (see Fig. 12). For large values of V (see Fig. 11d), on the

other hand, the dips get narrower again and more separated, and the transmission coefficient decreases slowly at low energies.

In addition to this, there is a nontrivial envelope of the transmission coefficient as clearly seen in Fig. 11c. Such envelope may even have a deep dip before getting converged to unity at large energies.

In the ordinary single unit of NT type of transition,[19,22] the qualitative behavior of the transmission coefficient is quite different. Since the nonadiabatic transition probability tends to unity as energy increases (see Eq. (IV.A.1)), the incoming wave is effectively switched to the upper well at the crossing point, then reflected back at the turning point and returns to the initial channel. Thus the envelope of the transmission coefficient monotonically decreases to zero with increasing energy. In the above DAC model, on the other hand, the evelope behaves in the non-monotonous way (before getting converged to unity). This is basically due to a sequence of two symmetric RZ type nonadiabatic transitions, and is in accordance with the semiclassical analysis made in section II. Another difference between DAC and NT cases is the coupling strength dependence of the transmission coefficient. While in the DAC model the zero coupling limit corresponds to a single barrier penetration problem with nonzero transmission, in a single NT case the transmission is not possible, since each diabatic potential diverges at one side.

III.5 Closing remarks

The phenomena of complete reflection and complete transmission in two coupled potential systems have been discussed and analytical conditions for these phenomena to occur have been formulated. The diabatically avoided crossing case (Fig. 8) was solved quantum mechanically exactly by using the rotated Rosen-Zener model and analyzed semiclassically with the use of exponential model [15]. The complete reflection was found to occur at some discrete energies like in the nonadiabatic tunneling (NT) type of curve crossing, which has been discussed in detail before. Interestingly, the appearance of complete reflection dips is quite different from the NT case.

Amendment

Here we provide some useful equations related to the main text in section III.

III.A. Meijer G functions

In the two state problem the coupled Schrődinger equations can be transformed to a differential equation of the fourth order, i.e. from

$$\psi_1 = \frac{1}{V_{12}(x)} \left(\psi_2'' - (V_{22}(x) - E)\psi_2 \right) , \qquad \text{(III.A.1)}$$

we obtain

$$-\psi_2^{IV}+\psi_2'''\frac{2V_{12}'}{V_{12}}+\psi_2''\left(V_{11}+V_{22}-2E+\frac{V_{12}''}{V_{12}}-2\frac{{V_{12}'}^2}{V_{12}^2}\right) \tag{III.A.2}$$

$$+\psi_2'\left(2V_{22}'+(E-V_{22})\frac{2V_{12}'}{V_{12}}\right)+\psi_2\left(V_{22}''-2V_{22}'\frac{V_{12}'}{V_{12}}+\right.$$

$$\left.(V_{22}-E)\left(\frac{2{V_{12}'}^2}{V_{12}^2}-\frac{V_{12}''}{V_{12}}\right)-(V_{11}-E)(V_{22}-E)+V_{12}^2\right)=0.$$

If we use the variable $z=\exp(\alpha x)$, then the kinetic energy operator transforms as

$$\frac{d}{dx}=\alpha z\frac{d}{dz}. \tag{III.A.3}$$

Furthermore, suppose that the potential terms multiplying the wave function and its derivatives in Eq. (III.A.2) transform to only one arbitrary power of z (or constants otherwise), then Eq. (III.A.2) reduces to

$$\left[(-1)^{p-m-n}z\prod_{j=1}^{p}\left(z\frac{d}{dz}-a_j+1\right)-\prod_{j=1}^{q}\left(z\frac{d}{dz}-b_j\right)\right]G(z)=0, \tag{III.A.4}$$

which can be solved by the Meijer G functions as

$$G_{pq}^{mn}\left(z|\begin{array}{c}\{a\}\\\{b\}\end{array}\right)=\frac{1}{2\pi i}\int_L\frac{\prod_{j=1}^{m}\Gamma(b_j-x)\prod_{j=n}^{m}\Gamma(1-a_j+x)}{\prod_{j=m+1}^{q}\Gamma(1-b_j+x)\prod_{j=n+1}^{p}\Gamma(a_j-x)}z^x dx. \tag{III.A.5}$$

In Eq. (III.A.5) L is a proper contour defined in reference 47. The above reduction can be done for the following cases:

(1) Rosen-Zener-Demkov model, [12]

$$\left(\begin{array}{cc}U_1 & Ve^{-\alpha x}\\ Ve^{-\alpha x} & U_2\end{array}\right). \tag{III.A.6}$$

(2) special case of the exponential potential model, [13]

$$\left(\begin{array}{cc}U_1+V_1e^{-\alpha x} & \sqrt{V_1V_2}e^{-\alpha x}\\ \sqrt{V_1V_2}e^{-\alpha x} & U_2+V_2e^{-\alpha x}\end{array}\right) \text{ and} \tag{III.A.7}$$

(3) special case of the two-exponential-potential model, [14]

$$\left(\begin{array}{cc}U_1+V_1e^{-2\alpha x} & Ve^{-\alpha x}\\ Ve^{-\alpha x} & U_2\end{array}\right). \tag{III.A.8}$$

In the diabatically avoided crossing model ($p=0$ and $q=4$ in Eq. (III.A.4)) we make use of the following expansion of the Meijer G functions: [47]

$$G_{04}^{40}\left(z|\begin{array}{c}\{\ \}\\\{b\}\end{array}\right)=\sum_{h=1}^{4}\left(\prod_{j=1..4}^{j\neq h}\Gamma(b_j-b_h)z^{b_h}\right) \tag{III.A.9}$$

$$\times {}_0F_3[1+b_h-b_1,..*..,1+b_h-b_4,z],$$

with

$${}_0F_3[d_1,d_2,d_3,z]=\sum_{n=0}^{\infty}\frac{z^n}{n!(d_1)_n(d_2)_n(d_3)_n} \qquad \text{(III.A.10)}$$

and $(d)_n = d(d+1)..(d+n-1)$.

III.B. Semiclassical analysis of noncrossing case

The parameters of the left nonadiabatic transition matrix I_L in Eq. (III.43) in the case of DAC coincide with those of the RZD model [1,12,15] and are given as follows

$$p_L=(1+\exp(2\delta))^{-1},\ \ \phi_L=\gamma(\delta)-\gamma(2\delta),\ \text{and}$$

$$\psi_L=\phi_L-2\delta(\sqrt{2}+\ln(\sqrt{2}-1))\ \text{with}\ \gamma(X)=X\ln X-X-\arg\Gamma(iX). \qquad \text{(III.B.1)}$$

The parameter δ is defined as the imaginary part of adiabatic momentum integral. The closed integration contour starts on the real axis and winds around the complex crossing point. Here it yields [15]

$$\delta\simeq\sqrt{E-U_2}-\sqrt{E-U_1}. \qquad \text{(III.B.2)}$$

The nonadiabatic transition matrix I_R is nothing but a transpose of I_L due to the symmetry reasons (see Fig. 8),

$$p_R=p_L,\ \ \phi_R=\phi_L\ \text{and}\ \psi_R=\pi-\psi_L. \qquad \text{(III.B.3)}$$

The transition points for the above matrices are the real parts of the complex crossing points and are given by

$$x_{L,R}=\mp\ln\frac{C}{V}. \qquad \text{(III.B.4)}$$

IV Complete Reflection and Transmission

Here we review our achievements in the analysis of complete reflection in two-state coupled potential systems. The full account is given in the Paper 3 (sections III, IV therein).

IV.1 Opening remarks

Following the opening remarks from section III, in the section IV we give the semiclassical conditions for complete reflection and complete transmission to occur in some crossing and noncrossing two-potential-curve systems.

In particular, here we discuss the conditions for the complete reflection and transmission in the potential systems shown in Fig. 9a and Fig. 10a. We derive the semiclassical conditions for the complete transmission and the complete reflection to occur and also compare these NT-models with the DAC model. Instead of the case in Eq. (III.4) we are concerned with the case

$$\exists x_c, \quad V_{11}(x_c) = V_{22}(x_c). \tag{III.B.5}$$

The most fundamental model in the crossing type is the linear model. Recently, Zhu and Nakamura completely solved the model and developed a comprehensive theory applicable to general curve crossing problems [19,41-43]. This theory has been transformed into the time dependent version [40,43] and used for the control of molecular processes by a laser field [33,38]. Varying the intensity and frequency of the field, $\{I, \omega\}$, and using the idea of dressed state, complete control of some molecular processes can be achieved. Furthermore, the complete reflection phenomenon in the nonadiabatic tunneling type curve crossing, which does not appear in the time-dependent process, has been utilized to control molecular photodissociation [35]. Here, we discuss two types of two crossing potential curves and use the Zhu-Nakamura semiclassical theory in order to analyze the phenomenon.

IV.2 Two-channel case

Let us start with the common case of two diabatic potentials, one barrier and one well, which intersect at two points and are coupled by a diabatic coupling (see Fig. 9a). In the case of dressed states, this coupling is due to the external field.

1. At energies above the top of the barrier, (E_u, ∞) Since the sequence of turning and transition points is the same in both Fig. 8a) and Fig. 9a), Eq. (III.50) with the phase shift in Eq. (III.51) holds. The same applies to Eq. (III.53). However, the nonadiabatic transition matrices are, of course, different.

The expressions for the nonadiabatic transition probability and the dynamical phases are given by the Zhu-Nakamura theory (see Eq. (IV.A.1) in the Amendment). Referring to the results of the previous section we conclude that the complete reflection,

$$\int_{x^{(a)}_L}^{x^{(a)}_R} \sqrt{E - u_1^{(a)}(x)}\, dx = (n - \frac{1}{2})\pi + \Delta(E), \qquad \text{(III.B.6)}$$

(Δ given in Eq. (III.51) with p, ϕ and ψ replaced by Eqs. (IV.A.1)-(IV.A.3), respectively), and the complete transmission,

$$p_L = p_R \equiv p \quad \text{and} \quad \delta + \phi_L + \phi_R + \psi_L - \psi_R = \pi, \qquad \text{(III.B.7)}$$

are possible.

2. At energies between the barrier top and the higher crossing, (E_+, E_u)
In this paragraph we consider energy above the bottom of upper adiabatic potential (which is denoted here as E_+, see Fig. 9a), because the Zhu-Nakamura theory presents different formulas for $E \geq E_+$ and $E \leq E_+$. Since the energy is below the top of higher adiabatic potential (case (b) in Fig. 9a), we use the tunneling matrix M which connects the in/out-going WKB waves from left to right,

$$\begin{pmatrix} \rightarrow \\ \leftarrow \end{pmatrix} = \begin{pmatrix} \sqrt{1+\kappa^2}\exp(-i\Phi) & i\kappa\exp(i\Theta) \\ -i\kappa\exp(-i\Theta) & \sqrt{1+\kappa^2}\exp(i\Phi) \end{pmatrix} \begin{pmatrix} \rightarrow \\ \leftarrow \end{pmatrix}, \qquad \text{(III.B.8)}$$

where $1/\kappa = \exp(-\pi\epsilon)$ represents the Gamov factor with ϵ equal to the tunneling action integral when the energy is lower than the barrier top (for further details see e.g. reference [17]. This situation is schematically shown in the semiclassical diagram, Fig. 9b. Using similar arguments as before, the complete reflection is possible and the condition in Eq. (III.50) still holds with some modifications. In particular, we have

$$I(E) \equiv \Re\left\{\int_{x^{(a)}_L}^{x^{(a)}_R} \sqrt{E - u_1^{(a)}(x)}\, dx\right\} = (n - \frac{1}{2})\pi + \Delta(E), \qquad \text{(III.B.9)}$$

where $\Delta(E)$ reads one of the following forms

$$\Delta_L(E) = -\arg\ \Big\{d\exp(i(\psi_L - \psi_R)) - \zeta\sqrt{1+\kappa^2}\exp(-i(\phi_R + \phi_L + \Phi)) \\ -\zeta\kappa\exp(-i(\Theta + \phi_L - \phi_R))(c_3^* c_2^{R^*})^2\Big\}, \qquad \text{(III.10a)}$$

or

$$\Delta_R(E) = -\arg\ \Big\{d\exp(i(\psi_L - \psi_R)) - \zeta\sqrt{1+\kappa^2}\exp(-i(\phi_R + \phi_L + \Phi))$$

$$-\zeta\kappa\exp(i(\Theta+\phi_L-\phi_R))(c_1^*c_2^{L^*})^2\Big\}. \qquad \text{(III.10b)}$$

That is to say, the complete reflection occurs when $I(E)-\Delta_L(E)=(n-1/2)\pi$ or $I(E)-\Delta_R(E)=(n-1/2)\pi$ is satisfied. The factor $\Delta_L(E)$ ($\Delta_R(E)$) represents the effects of both nonadiabatic coupling and tunneling (and obeys the symmetry relation in Eq. (III.54)). If the tunneling is small, $\Delta_L(E)$ ($\Delta_R(E)$) corresponds to the Bohr-Sommerfeld quantization condition in the left (right) upper adiabatic potential well. If $\kappa=0=\Phi$, namely the matrix in Eq. (III.B.8) turns to unit matrix, then the parameters $\Delta(E)$ in Eqs. (III.10a), (III.10b), and (III.51) are the same (the complete reflection condition naturally agrees with that in the case 1 above). Taking the diabatic limit in Eqs. (III.10a) and (III.10b), i.e. $p_L,\,p_R\to 1$ and thus $\xi\to 0$, yields the Bohr-Sommerfeld quantization condition in the diabatic potential well.

The complete transmission is also possible but its mechanism is quite different from the above-the-barrier case. It occurs when

$$R_{21}L_{12}^*M_{12}(u+u^*)+i\left[ic_2^{R^*}c_3^*(R_{11}^*L_{12}^*M_{22}+R_{12}^*L_{22}^*d^*)+R_{11}L_{12}^*M_{12}c_2^Rc_3\right]$$

$$\times\left[ic_1c_2^L(R_{21}L_{11}M_{11}+R_{22}L_{21}d)+R_{21}L_{11}^*M_{21}^*c_1^*c_2^{L^*}\right]=0 \qquad \text{(III.11)}$$

with

$$u\equiv R_{11}\left(L_{11}M_{11}c_1c_2-iL_{11}^*M_{12}c_1^*c_2^{L^*}c_2^R\right)c_3+R_{12}L_{21}cd.$$

If the tunneling matrix M is replaced by a unity matrix, we obtain Eq. (III.B.7). The constants from Eq. (III.47), A (amplitude of the wave reflected from the left turning point) and B (amplitude of the transmitted wave), must be both nonzero. Physically it means that the complete transmission occurs only when the half-standing waves both left and right from the central barrier interfere destructively with the reflected part of the incident wave. Because of this, Eq. (III.11) is quite complicated and difficult to solve analytically. Thus we restrict ourselves to the exact numerical demonstrations in section IV. Let us also note that depending on the potential parameters, the complete reflection and transmission can occur at energies close to each other, in which case we have the Fano type resonance [45]. A numerical example will be given in section IV-B.

When the maximum of the upper adiabatic potential is so high that the tunneling can be neglected ($\kappa\to\infty$), the formalism simplifies considerably. As also follows from Eqs. (III.10a) and (III.10b) in this limit, the complete reflection occours if

$$\cos(d_1+d_2^L-\phi_L)=0 \text{ or } \cos(d_3+d_2^R-\phi_R)=0, \qquad \text{(III.12)}$$

i.e. its energy is given by the Bohr-Sommerfeld quantization rule with the additional phase correction, ϕ_L or ϕ_R. This is simply equivalent to the case discussed before [19,21-23,35]. The complete transmission condition follows

$$p_R(1-p_L)\cos(d_1+d_2^L-\phi_L)\exp(-i(\phi_L+\psi_L-\psi_R+d_3+d_2^R-d_2^L))$$

$$+p_L(1-p_R)\cos(d_3+d_2^R-\phi_R)\exp(i(\phi_R+\psi_L-\psi_R+d_1+d_2^2-d_2^R))$$
$$+p_Lp_R\cos(d_1+d_2^L+d_2^R+d_3+\delta+\psi_L-\psi_R)=0, \qquad \text{(III.13)}$$

(confer with Eq. (III.54)). The three cosine functions in Eq. (III.13) turn to zero when the scattering energy coincides with a (shifted) bound state in the left, right or the global diabatic well (see Fig. 9). Let us also note that Eq. (III.13) is a limiting case of Eq. (III.11). When we set $\Theta = 0 = \Phi$ and expand Eq. (III.11) in powers of κ, the leading term κ^2 vanishes identically, while the term proportional to κ yields Eq. (III.13).

3. At energies in between the two crossing regions, (E_-, E_+) We can use the above formalism also when the energy is in between E_+ and E_-, where E_- is the bottom of the upper adiabatic potential in the lower crossing region (see Fig. 9a)). In this case, the lower crossing can still be treated by the $I-$matrix (see Eq. (III.43)) as previously, but the upper crossing should be described by the nonadiabatic tunneling matrix (transfer matrix) N,[19,41-43] which connects the waves on both sides of the crossing in the lower adiabatic channel (see also Eq. (III.B.8)). Furthermore, we have to assume that the barrier on the upper adiabatic channel (see Fig. 9a) is high enough so that the tunneling through it can be neglected. Then, the above formalism can still be used with the replacements of the tunneling matrix M and the $I-$matrix for the higher crossing by the $N-$matrix and unit matrix, respectively. Finally we derive the following results:

The complete reflection occurs if the Bohr-Sommerfeld condition in the open adiabatic well is satisfied, i.e. it is also given by Eq. (III.12). The condition for the complete transmission reads

$$2R_{22}N_{12}dc_2\cos(d_2^R+d_3)=R_{21}c_2^R\,(R_{12}N_{12}dc_2c_3+iR_{12}^*N_{22}^*d^*c_2^*c_3^*) \qquad \text{(III.14)}$$

(here we suppose for simplicity that the crossing point energy is higher on the left than on the right).

4. At energies below the crossing points, $(-\infty, E_-)$ Using similar assumptions as in the case 3 above, the semiclassical wave propagation for $E < E_-$ should be described by the two nonadiabatic tunneling matrices (transfer matrices), N (left crossing) and N' (right crossing). These are parametrized with κ, Φ and Θ, similarily as in Eq. (III.B.8). Then we find that the semiclassical complete reflection is not possible. Yet the complete transmission can still occur, provided (1) that energy is above the bottom of the lower adiabatic potential, $E_d < E < E_-$, and (2) the following equation is satisfied,

$$\kappa=\kappa' \text{ and } (dc_2)^2=-\exp(\Phi+\Phi'+\Theta-\Theta'). \qquad \text{(III.15)}$$

Since it is possible to control κ and κ' e.g. by changing the intensity of the laser field, the complete transmission condition above could be useful for enhancing

chemical reactions, especially those which are otherwise unlikely due to the tunneling [46]. At energies below the bottom of the lower adiabatic potential, E_d, the whole scattering can be described by semiclassical analysis only as a single barrier penetration. The complete reflection and the complete transmission are not possible.

IV.3 Three-channel case

Let us consider a barrier coupled with a monotonous potential, such as in Figs. 10a and 10b. With the use of previous notation the propagation of semiclassical wave function yields: (1) the complete reflection is *not* possible in any of the three channels. However, (2) the complete transmission is possible, although only through the barrier in the first channel. In order to have such a situation the following two conditions must be satisfied simultaneously,

$$\frac{\kappa}{\sqrt{1+\kappa^2}} = 1 - p \text{ and } \exp(2i(d_1 + d_2)) = -\exp(i(2\phi + \Phi - \Theta)). \qquad \text{(III.16)}$$

Let us take a limit of a high barrier, $\kappa \to \infty$. Then p must tend to zero from the above equation, and the second equation defines a bound state. On the other hand, for $\kappa \to 0$ the complete transmission occurs only when the incident wave is switched with unit probability just before it reaches the turning point on the right. Generally, if Eq. (III.16) is satisfied, then the transmitted wave is distributed between the left and right lower channels with the ratio of $\kappa/\sqrt{(1+\kappa^2)(1-p)}$.

IV.4 Numerical examples

Atomic units are used throughout this section. The reduced mass is chosen to be $M = 1000$ a.u., if not stated otherwise. First we illustrate the theoretical results for energies below the top of the barrier. The accurasy of the semiclassical theory (cf. Eq. (III.49) and the Zhu-Nakamura formulas in Amendment B) for energies above the barrier top is also demonstrated. Finally we briefly discuss the Fano typ of resonance [45,46] using our semiclassical analysis.

In Figs. 13, numerical examples of the transmission probability are depicted for an asymmetric double NT-type crossing model. These figures demonstrate the occurence of complete reflection and transmission in the energy regions discussed in the previous section.

Fig. 13a shows the overall behavior of the transmission coefficient in the case of asymmetric potential model defined as

$$V_{11} = 0.2 - 0.01x^2, \; V_{22} = 0.01(x-1)^2 - 0.3 \text{ and } V_{12} = 5.10^{-3}. \qquad \text{(III.17)}$$

There appear as expected complete reflection dips for $E > E_-$ and complete transmission peaks for $E > E_d$. The five energy intervals are divided by $E_u = 0.2$,

$E_+ = 5 \times 10^{-3}$, $E_- = -0.095$, and $E_d = -0.3$. In the energy region below the barrier top, both the complete reflection and transmission occur close to each other (see also Fig. 14 below). At energies above the barrier top, the very flat transmission peaks are separated by the complete reflection dips. This follows from Eq. (III.53), since $p_L \simeq p_R \to 1$ and the phase condition therein is also satisfied at large energies. We note, that the dependance of the resonance width on the diabatic coupling strength is not monotonous. This is because both for the weak coupling, $p \to 1$, and for the strong coupling, $p \to 0$, the two subsequent transitions do not allow the wave to reach the turning points and get reflected back.

Fig. 13b shows a magnification of some portion of Fig. 13a, demonstrating the accuracy of the Zhu-Nakamura semiclassical theory (solid circles) given in Amendment B. Figs. 13c and 13d show the transmission coefficient for different coupling strengths, i.e. $V_{12} = 1 \times 10^{-3}$ (c) and $V_{12} = 8 \times 10^{-2}$ (d). Since also here the semiclassical and exact results practically coincide, only one curve is plotted. The Zhu-Nakamura semiclassical theory works very well (also in the tunneling range which is not shown here). Figures 13b-d demonstrate the non-monotonous character of the dip widths on the coupling strength, too.

Finally, we would like to point out that the Fano type resonance [45] discussed by Vardi and Shapiro under the name of laser catalysis [46] can be reproduced by the present analysis. We take the following two diabatic potentials: [46]

$$V_{11} = U_1 - \frac{B\xi}{(1-\xi)^2} \text{ and } \quad V_{22} = U_2 + \frac{B\xi}{(1-\xi)^2} \tag{III.18}$$

with

$$\xi = -\exp(\pi x/2), \tag{III.19}$$

where

$$B = 6.247 \times 10^{-2}; \ U_1 = 3.15 \times 10^{-2} \text{ and } U_2 = 5.917 \times 10^{-2}. \tag{III.20}$$

The coupling is given by the dipole moment and the laser field intensity,

$$V_{12} = 6.8 \times 10^{-5}, \text{ and } M = 1060.83. \tag{III.21}$$

Although in the above mentioned reference the authors used a laser pulse and propagate wave packets, the constant coupling in Eq. (III.21) is adequate, since the field changes slowly. Fig. 14 shows the transmission coefficient as a function of energy. This figure is very similar to Fig. 8 in the reference 46. This is because an infinitesimal shift of a Floquet state by $d\omega$ is roughly equivalent to a shift in scattering energy, $dE = -d\omega$. As a result of a very small coupling, the wave passes through the crossing points almost diabatically ($p_L, \ p_R \sim 1$). Thus the background in Fig. 14 is just a single barrier penetration. Since the phases d_1 and d_3 are very small, Eq. (III.12) can never be satisfied in this particular

energy range. Consequently, the complete reflection is not the same as that in the single NT case. It can also be seen from Eqs. (III.10a) and (III.10b) that the limit of infintely high barrier ($\zeta\kappa \gg 1$) is not justified. Hence, the tunneling through the central potential barrier is responsible for the complete reflection. Taking $\zeta \sim 0$, $\Delta \sim \delta + \psi_L - \psi_R$ (see Eqs. (III.10b) and (III.10a)), the complete reflection condition (III.B.9) reduces to a quantization in the global diabatic well, $d_1 + d_2^L + d_2^R + d_3 + \delta + \psi_L - \psi_R = \pi/2$. This explains the complete reflection in Fig. 14 since the energy is close to the first bound state supported by the diabatic potential V_{22}. For the complete transmission, on the other hand, the tunneling does not play so important role. This can be checked both analytically and numerically. When we increase artificially the heigth of the barrier, the complete reflection disappears while the complete transmission remains stable (bold line in Fig. 14). Thus we can use Eq. (III.13) instead of Eq. (III.11). The first two terms in this equation, proportional to $1 - p$, are very small and the last term turns to zero when $d_1 + d_2^L + d_2^R + d_3 + \delta + \psi_L - \psi_R = \pi/2$. Thus just a small change in energy suffices to switch between the complete reflection and complete transmission and the Fano type of resonance can be nicely explained by the semiclassical picture, and theory.

Fig. 15 shows the transmission probability in the model potential given by

$$V_{11} = 0.06[1 + \tanh(2(x+2))](1-x) \text{ and } V_{22} = 0.1x \qquad \text{(III.22)}$$

with a constant diabatic coupling. The barrier top of V_{11} is 0.265. There appears an example of complete transmission below the top of the barrier in the case of $V_{12} = 4.59 \times 10^{-2}$. The incident wave must first penetrate through the barrier for energies $0.0 \sim 0.270$ a.u. The complete reflection never takes place, as it was already mentioned in Section III.B. The transmission coefficient shows the Stueckelberg oscillations which diminish as energy grows. At high energies the envelope simply converges to unity, since the wave just proceeds diabatically ($p \to 1$) from left to right. With decreasing diabatic coupling the transmission coefficient converges to that of a single barrier penetration (dotted line).

IV.5 Closing remarks

The two channel case (Fig. 9), in which one barrier type and one well type potentials cross with each other at two points, has also been analyzed semiclassically. Both complete reflection and transmission can appear, as can be analyzed by the semiclassical Zhu-Nakamura theory, although they are quite different from those in the single NT type curve crossing. The semiclassical analysis of the three channel case (Fig. 10) has shown that the complete transmission is possible; while the complete reflection is not. In all these cases, the semiclassical theory presents a very useful tool to understand physics.

As in the single NT type curve crossing, the complete reflection and transmission represent very intriguing phenomena in themselves, and could be utilized in

realistic molecular processes. In the Floquet formalism we can realize the potential schemes discussed here by dressing up and down some molecular curves. This means that we may be able to control various molecular processes with the use of such phenomena (cf. refs. 33 and 38). For instance, reaction process may be switched off by complete reflection or enhanced by complete transmission. Vardi and Shapiro discussed such a possibility in the terminology of laser catalysis by using the Fano-type resonance [46]. Our scheme here is different from theirs and could be more versatile. Not only the nonadiabatic transition probability but also various types of phases can be changed by manipulating lasers, and the complete reflection and transmission could be utilized in various desirable ways to control molecular processes. Applications of the formalism to higher dimensional systems would be interesting and desirable. The existence of complete reflection indicates that the bound states in the continuum should also be possible as in the case of periodic systems of NT type curve crossing units [21,22].

Amendment

Here we provide the nonadiabatic transition matrices used in section IV.

IV.A. Semiclassical analysis of crossing case

In the curve crossing case at energies above the bottom of the upper adiabatic well, the nonadiabatic transition matrices I (see Eq. (III.43)) are given by the Zhu-Nakamura theory [19,41-43] as follows:

$$p = \exp\left[-\frac{\pi}{4ab}\left(\frac{2}{1+\sqrt{1-b^{-4}(0.72-0.62a^{1.43})}}\right)^{1/2}\right], \tag{IV.A.1}$$

$$\phi = \frac{\delta}{\pi} - \frac{\delta}{\pi}\ln(\frac{\delta}{\pi}) + \arg\Gamma(i\frac{\delta}{\pi}) + \frac{\pi}{4}, \tag{IV.A.2}$$

and

$$\psi = \frac{R_b - R_t}{|R_b - R_t|}\frac{2\sqrt{1-\gamma^2}}{3a}\frac{[2b^2+\sqrt{b^4-1}]}{\sqrt{b^2+1}+\sqrt{b^2-1}}, \tag{IV.A.3}$$

where

$$a^2 = \frac{(1-\gamma^2)\hbar^2}{\mu(R_b-R_t)^2(E_b-E_t)}, \quad R_b \neq R_t,$$

or

$$a^2 = \frac{\hbar^2}{4\mu(E_b-E_t)}\left[\frac{\partial^2 E_1}{\partial R^2} - \frac{\partial^2 E_2}{\partial R^2}\right]_{R=R_c}, \quad R_b = R_t = R_c,$$

$$b^2 = \frac{E-(E_b+E_t)/2}{(E_b-E_t)/2},$$

$$\gamma = \frac{E_b - E_t}{E_1\left(\frac{R_b + R_t}{2}\right) - E_2\left(\frac{R_b + R_t}{2}\right)},$$

and

$$\delta = \frac{\pi}{8ab}\frac{1}{2}\frac{\sqrt{6 + 10\sqrt{1 - \frac{1}{b^4}}}}{1 + \sqrt{1 - \frac{1}{b^4}}}. \qquad \text{(IV.A.4)}$$

At the reference point, R_t, the lower adiabatic potential has a local maximum, E_t. R_b and E_b correspond to the local minimum of the upper adiabatic potential (see Fig. 9a). The Zhu-Nakamura theory is also available at the lower energies [19,41-43].

V Dissociative Recombination of H_2^+

Here we review our achievements in the analytical treatment of singular integral equations in dissociative recombination. The full acount is given in the Paper 4.

V.1 Opening remarks

The dissociative recombination (DR) process has been a subject of interest for long time. This is an electron-molecular ion recombination process, and represents an important elementary mechanism in a variety of fields such as plasma physics, interstellar chemistry and astronomy [48–51]. The process also presents a theoretically challenging subject, since this is a kind of rearrangement collision, in which the coupling between electronic and nuclear degrees of freedom plays a crucial role.

The Multichannel Quantum Defect Theory (MQDT) was originally designed to deal with two types of states, the electronic continuum and the Rydberg manifold, in a unified way [52–54]. The quantum defect μ as a function of the relative nuclear coordinate plays the most important role in describing various physical processes among these infinite number of states. In the case of DR, there is a third kind of state, that is a dissociative state which diabatically crosses the Rydberg quasi-continuum and goes into the ionization continuum. It is an electronically doubly excited state or an inner-shell excited state, which is generally called "first kind of superexcited state" [55]. The coupling of this state to the ionization continuum called "electronic coupling" represents the electronic autoionization, i.e. ejection of one electron due to the de-excitation of the other one. The MQDT formalism defines two electron coordinate regions; the first of them is an inner region (the reaction zone), where the transition occurs, and the other one is an asymptotic scattering region. Effects of the dissociative channel, arising in the reaction zone, can be incorporated into the framework of MQDT by using the solution of the K-matrix integral equation associated with the electronic coupling [55–56]. The coupling represents the interaction of the dissociative state not only with the ionization continuum, but also with the Rydberg manifold, a sort of quasi-continuum. This quantity is a function of the internuclear distance R and the continuous electron energy ϵ, and couples vibrational states to the dissociative nuclear state. The intermediate states of the Rydberg manifold give rise to an infinite number of dense resonances in the DR process.

The MQDT treatment presents a powerful tool to reveal characteristics and dynamics of superexcited states of molecules with an effective utilization of quantum chemical technique and spectroscopic experiment [57-58]. The formalism deals with the various phenomena by means of two successive frame transformations [56]. First of them defines the eigen-states of the inner region, diagonalizing the K-matrix, while the other one connects the inner and outer regions, incorporating the quantum defect function. Both transformations together produce the

final scattering matrix. The main difficulty of this general procedure developed in refs. [57] and [58] is the treatment of the Lippmann-Schwinger type of integral equation.

The equation comprises a kernel singular in energy representation, which is not easy to treat, especially when many channels are involved. If the singularity is not treated efficiently, the dimension of resulting matrix equations reaches easily the limits of computing facilities. In the literature several approaches have been used so far: the first order perturbation theory that avoids the singularity problem completely but is not often justified to be applicable, and the grid method which encounters the above mentioned difficulties [48–51]. In addition, the second order perturbation theory has been used to incorporate indirect electronic coupling effects [59]. Other methods rely on the Feshbach projection-operator formalism [60], the eigen channel treatment [61], or the R-matrix theory [62].

It is the purpose of this work to propose a new more efficient way of solving the singularity problem that enables us to present very precise and reliable values of DR cross sections. To treat the singularity we introduce a method based on the use of Chebyshev polynomials which allows an analytical evaluation of all singular integrals entering the Lippmann-Schwinger equation [63]. This method proves to be very useful, compared to the conventional ones. That is crucial, since in realistic problems the numerical K-matrix solution should be quite efficient.

A very useful approximation to the DR process can be obtained by realizing that in many cases the electronic coupling is almost separable with respect to the variables R and ϵ. This fact considerably simplifies the kernel of the K-matrix equation that becomes quasi-separable, the definition of which will be given later, and we can find in fact a simple analytical solution. Our procedure thus very much facilitates the MQDT treatment not only of DR but also of other various kinds of dynamic processes involving superexcited states of a diatomic molecule [55].

The section V is organized as follows. First we define the basic quantities and outline the MQDT formalism. Attention is paid to the Lippmann-Schwinger equation and to analytical treatment of the singular kernel. We discuss the separable approximation to the electronic coupling and the resulting analytical K-matrix solution. A general non-separable case is also investigated. Then we compare our method with the grid method and the perturbation method to demonstrate the numerical efficiency of the present treatment. The calculations are based on the parameters of the $H_2^+ + e$ system and their various modifications. We omit the rotational degree of freedom since that is not necessary for the explanation of our method. In section V we summarize the present treatment and its further applicability. Atomic units are used throughout.

V.2 Theory and formalism

First we briefly summarize definitions of the basic quantities and the MQDT treatment. We use $\mathbf{q}^+$ to denote electron coordinates of the molecular ion, $\mathbf{q}$ for those of the neutral molecule, and r, l, k specify the radial coordinate of the incident electron, its angular momentum and the wave number, respectively. H_{el} represents the total hamiltonian except for the nuclear kinetic energy part, i.e. the electronic hamiltonian at fixed internuclear distance.

The vibrational states of the initial cation described by the potential

$$V_+(R) \equiv \langle \phi_+(\mathbf{q}_+ : R) \, | H_{el}(R) | \, \phi_+(\mathbf{q}_+ : R) \rangle_{\mathbf{q}^+} \qquad \text{(IV.A.5)}$$

are represented in terms of the normalized eigen-functions $\{E_v, \Phi_v\}$ of the Schrödinger equation

$$\left[-\frac{1}{2\mu} \frac{d^2}{dR^2} + V_+(R) \right] \Phi_v(R) = E_v \Phi_v(R), \quad ||\Phi_v|| = 1. \qquad \text{(IV.A.6)}$$

$\phi_+(\mathbf{q}^+ : R)$ in Eq. (IV.A.5) stands for the Born-Oppenheimer electronic wave function of the molecular ion and μ in Eq. (IV.A.6) is the reduced mass of the molecule. The wave function of the incident electron is denoted as $\phi_l(k, r; R)$, which is normalized to a delta function with respect to $k^2/2$.

The asymptotic fragment atoms are assumed to have a total electronic energy E_0 after the scattering process is over. The neutral dissociative state of the molecule under such boundary condition is a solution of the Schrödinger equation

$$\left[-\frac{1}{2\mu} \frac{d^2}{dR^2} + V_{dis}(R) \right] \Psi_{dis}(R; E) = E \, \Psi_{dis}(R; E), \qquad \text{(IV.A.7)}$$

normalized with respect to energy as

$$\langle \Psi_{dis}(R; E) | \Psi_{dis}(R; E') \rangle_R = \delta(E - E'), \qquad \text{(IV.A.8)}$$

where the dissociative potential $V_{dis}(R)$ is given as

$$V_{dis}(R) \equiv \langle \psi(\mathbf{q} : R) \, | H_{el}(R) | \, \psi(\mathbf{q} : R) \rangle_{\mathbf{q}} \overset{R \to \infty}{\to} E_0 \qquad \text{(IV.A.9)}$$

and $\psi(\mathbf{q} : R)$ stands for the electronic wave function of the dissociative superexcited state. The electronic coupling between the dissociative state $\psi(\mathbf{q}; R)$ and the ionization continuum is defined as

$$V_l(R, k^2/2) = \left\langle \psi(\mathbf{q} : R) \, | H_{el}(R) | \, \hat{A} \phi_+(\mathbf{q}^+ : R) \phi_l(k, r; R) \right\rangle_{\mathbf{q}}, \qquad \text{(IV.A.10)}$$

where $\hat{A}$ denotes the anti-symmetrization operator. Having defined the electronic as well as nuclear basis states, it is now necessary to describe the processes in the reaction region that result in the atomic rearrangement. In order to take

into account the effects of the coupling, Eq. (IV.A.10), the K-matrix equation is introduced [56]:

$$\langle E, n\,|K(z)|\,E', m\rangle = \langle E, n\,|V|\,E', m\rangle + \qquad \text{(IV.A.11)}$$
$$\mathrm{P}\int_0^\infty dE'' \sum_{\forall p} \langle E, n\,|V|\,E'', p\rangle \frac{1}{z - E''} \langle E'', p\,|K(z)|\,E', m\rangle\,,$$

where the potential $V(E, E')$ is specified below, n, m, p denote all the channels and P indicates the Cauchy type of integral. Solving Eq. (IV.A.11), we obtain N_c $(= N_{vib} + N_{dis})$ additional phase shifts given as

$$\tan\delta_\alpha(E) = -\pi\,\langle E, \alpha\,|K|\,E, \alpha\rangle\,, \quad \alpha = 1 \ldots N_c, \qquad \text{(IV.A.12)}$$

where the eigen-channel representation α diagonalizes the symmetric real $N_c \times N_c$ K-matrix

$$U(z)^T K(z)\, U(z) = \mathrm{Diag}\left(K^{(\alpha)}(z)\right). \qquad \text{(IV.A.13)}$$

The parameters from Eqs. (IV.A.12) and (IV.A.13) are incorporated into the MQDT framework as described below. In order to obtain the final scattering matrix, the following auxiliary matrices, C and S, defined by

$$\mathsf{C}_{v^+\alpha} = \sum_v \left\langle v^+ \left|\cos\left[\pi\mu(R) + \delta_\alpha\right]\right| v\right\rangle U_{v\alpha}, \quad \mathsf{C}_{d\alpha} = U_{d\alpha}\cos\delta_\alpha \qquad \text{(IV.A.14)}$$

and

$$\mathsf{S}_{v^+\alpha} = \sum_v \left\langle v^+ \left|\sin\left[\pi\mu(R) + \delta_\alpha\right]\right| v\right\rangle U_{v\alpha}, \quad \mathsf{S}_{d\alpha} = U_{d\alpha}\sin\delta_\alpha \qquad \text{(IV.A.15)}$$

must be calculated. Here $\mu(R)$ denotes the quantum defect function. Then the elements of the total reactance matrix $\mathcal{R}$ among the open channels (block index o) result from elimination of the closed channels (block index c). Following Seaton [52], the reactance matrix is expressed as

$$\mathcal{R} = \mathsf{R}_{oo} - \mathsf{R}_{oc}\left[\mathsf{R}_{cc} + \mathrm{Diag}\left(\tan(\pi\nu)\right)\right]^{-1}\mathsf{R}_{co}, \qquad \text{(IV.A.16)}$$

with

$$\mathsf{R} \equiv \mathsf{S}\mathsf{C}^{-1}, \text{ and } E - E_v \equiv -(2\nu^2)^{-1}. \qquad \text{(IV.A.17)}$$

The S-matrix is given as usual by

$$S = \frac{1 + i\mathcal{R}}{1 - i\mathcal{R}}, \qquad \text{(IV.A.18)}$$

and finally the cross section for the vibrationaly resolved dissociation reads

$$\sigma_{vd} = g\frac{\pi}{k^2}\left|S_{vd}\right|^2, \qquad \text{(IV.A.19)}$$

where g is a statistical factor. Before examining the K-matrix equation in more detail, let us simplify some of the notations. We use the indices

$$i = v, d, \text{ where } v = 0..N-1 \text{ denotes the vibrational state,} \qquad \text{(IV.A.20)}$$

and d stands for the dissociative channel.

The K-matrix elements are denoted as

$$K_{nm}(E) \equiv \langle E, n \,|K(\underline{z})|\, \underline{E'}, m \rangle \qquad \text{(IV.A.21)}$$

(E' is in fact a kind of dummy parameter when solving Eq. (IV.A.11)). The underlined variables are fixed and omitted, unless it is necessary to indicate them explicitly as parameters. It is convenient to make use of the following properties of the potential energy function

$$V_{dv}(E, E') = \langle \Psi_{dis}(R; E) \,|V_l\,(R; E' - E_v)|\, \Phi_v(R; E_v) \rangle_R \text{ and} \qquad \text{(IV.A.22)}$$

$$V_{nm}(E, E') = 0 \text{ for the blocks of } (n, m)=(d, d) \text{ or } (v, v'). \qquad \text{(IV.A.23)}$$

The latter one follows from the projection technique that is used to separate the Hilbert space into two subspaces: one of them corresponding to the ion arrangement, and its complement corresponding to dissociation. The electronic hamiltonian with the use of such two projectors is divided into a block-diagonal part H_0 and the block-off-diagonal rest V. Eq (IV.A.22) means nothing but taking V matrix element only within the two complement subspaces, since $|E, n\rangle$ in Eq. (IV.A.11) are the eigenstates of H_0 and here V denotes the coupling. Eq. (IV.A.23) indicates that the block-diagonal V-matrix elements vanish.

In order to solve Eq. (IV.A.11) we have to deal with the Cauchy type singular integral,

$$I = \mathrm{P} \int_0^\infty \frac{f\,(E')}{E - E'} dE'. \qquad \text{(IV.A.24)}$$

This is generally a complicated task and a few more or less satisfactory methods have been proposed in the literature to deal with that [63–64]. Here we briefly explain how we treat this kind of integral analytically. We first transform the infinite integration in Eq. (IV.A.24) to a finite range integral by introducing the following transformation, preserving the linear type of the singularity:

$$E'(x) = C\frac{1+x}{1-x} \text{ with } y \equiv \frac{E-C}{E+C}. \qquad \text{(IV.A.25)}$$

Then we get

$$I = \frac{2C}{E+C}\mathrm{P} \int_{-1}^{1} \frac{f\,(E'(x))}{x-y} \frac{dx}{x-1}. \qquad \text{(IV.A.26)}$$

We note that the convergence of the integral in the limit $x \to 1_-$

$$\lim_{x \to 1_-} \int_x^1 \frac{f\,(E'\,(x'))}{x'-y} \frac{dx'}{x'-1} = 0 \qquad \text{(IV.A.27)}$$

is ensured by the existence of the integral (IV.A.24) defined in the infinite range. For instance, if the function $f(E)$ behaves as

$$f(E \to \infty) \sim E^{-n} \quad (n \geq 2) \tag{IV.A.28}$$

then

$$f(x \to 1_-) \sim (x-1)^n \tag{IV.A.29}$$

and Eq. (IV.A.27) holds. For any kind of analytical treatment it is crucial to know how the integrand function behaves near the integration limits. We assume that the functional behavior of $K(E,.)$ and $V(E,.)$ in the same channels is the same. This is completely true for the quasi-separable case, discussed in the next section, and holds well also in the weak coupling case. The vibrational channel does not introduce any non-analyticity in $V_{v,.}(E,.)$ at low energies, even if the electronic coupling is truncated at a Rydberg energy threshold ($\epsilon_n \equiv -1/(2n^2)$, with $n = 2$ or 3), where it still has some non-zero value [71]. In such a case it suffices just to shift the energy integration range. In the dissociation channel the integrand behaves at the threshold $E \to E_0$ as

$$V_{d,.}(E,.) \sim \frac{1}{\sqrt[4]{E-E_0}}, \text{ and thus } V_{.,d}(.,E')K_{d,.}(E',.) \sim \frac{1}{\sqrt{E'-E_0}}. \tag{IV.A.30}$$

This comes from the energy normalization of the dissociative wave function (IV.A.7) and appears in Eqs. (IV.A.11) and (IV.A.24) as a modified weight (cf. Eq. (IV.A.25))

$$\frac{dx}{\sqrt{1-x^2}}(1-x) \tag{IV.A.31}$$

instead of dx. As a next step we expand the function f in terms of certain basis functions, which allows us to evaluate the Cauchy type integrals analytically. We desire, of course, to keep the number of expansion functions as small as possible. All integrals appearing in our problem can be reduced to the following four basic integrals (the reduction is described in detail in the Amendment):

$$\mathrm{P}\int_{-1}^{1} \frac{f(x)}{x-y}\frac{dx}{\sqrt{1-x^2}} \quad |y|<1, \quad \int_{-1}^{1} \frac{f(x)}{x-y}\frac{dx}{\sqrt{1-x^2}} \quad |y|>1 \tag{IV.A.32}$$

and

$$\mathrm{P}\int_{-1}^{1} \frac{f(x)}{x-y}dx \quad |y|<1, \quad \int_{-1}^{1} \frac{f(x)}{x-y}dx \quad |y|>1, \tag{IV.A.33}$$

where the second one in each line is a regular integral without singularity which arises when the channel is energetically closed. All of these can be expressed analytically in terms of Chebyshev polynomials. A useful analytical expression can be found also when $f(E) \sim K(E)V(E) \sim E^{\alpha}$, where α is a non-half-integer in Eq. (IV.A.24).

Solution of K-matrix Equation Because of the off-diagonal property of the potential energy function, Eq. (IV.A.22), the K-matrix equation decouples into the following two sets of equations:

$$K_{dd'}(E) = \sum_{v'} \mathrm{P} \int \frac{V_{dv'}(E, E')}{z - E'} K_{v'd'}(E')\, dE' \text{ and} \tag{IV.A.34}$$

$$K_{vd}(E) = V_{vd}(E, E') + \sum_{d'} \mathrm{P} \int \frac{V_{vd'}(E, E')}{z - E'} K_{d'd}(E')\, dE' \tag{IV.A.35}$$

and

$$K_{uv}(E) = \sum_{d'} \mathrm{P} \int \frac{V_{ud'}(E, E')}{z - E'} K_{d'v}(E')\, dE' \text{ and} \tag{IV.A.36}$$

$$K_{dv}(E) = V_{dv}(E, E') + \sum_{v'} \mathrm{P} \int \frac{V_{dv'}(E, E')}{z - E'} K_{v'v}(E')\, dE'. \tag{IV.A.37}$$

Now we discuss the way of solving these equations. First we factor out the asymptotic behavior as well as the normalization factors and integration weights $(d\mu)$ as is given in Eqs. (IV.A.30) and (IV.A.31),

$$V_{ij}(E, E') \equiv \alpha_i(E)\alpha_j(E')v_{ij}(E, E') \tag{IV.A.38}$$

and

$$K_{i\underline{j}}(E, z) \equiv \alpha_i(E)k_{i\underline{j}}(E, z), \tag{IV.A.39}$$

where

$$\alpha_i = 1 \text{ if } i = d \text{ and } \alpha_i = (E + C)^{-1} \text{ if } i = v.$$

The well behaved functions v_{ij} and $k_{i\underline{j}}$ are expanded in terms of Chebyshev polynomials as

$$v_{ij}(E(y), E'(y')) = \sum_{m,n} c^{(v)ij}_{mn} \mathrm{T}_m(y)\mathrm{T}_n(y'), \tag{IV.A.40}$$

$$v_{i,\underline{j}}(E(y), \underline{z}) = \sum_{m} c^{(z)i}_{\ m} \mathrm{T}_m(y),$$

and

$$k_{i,\underline{j}}(E(y), \underline{z}) = \sum_{m} c^{(k)i}_{\ m} \mathrm{T}_m(y).$$

Our experience shows that these expansions are usually rapidly convergent and the infinite sum may be truncated at some small number N_{pol} of terms, i.e.

$$c^{(v)ij}_{nm} \overset{n,m\to\infty}{\to} 0. \tag{IV.A.41}$$

After inserting Eqs. (IV.A.38)-(IV.A.40) into the Lippmann- Schwinger equation (IV.A.11) the integral part reduces to

$$\sum_{j,m,m'} c^{(v)i,j}_{nm} c^{(k)j}_{\ m'} \mathrm{T}_n(x) \mathrm{P} \int_{-1}^{1} \mathrm{T}_m(x')\mathrm{T}'_n(x') \frac{d\mu(x')}{x' - y}. \tag{IV.A.42}$$

Chebyshev polynomials in the integral (IV.A.42) can be easily reorganized so that we can use the formulae given in the Amendment (cf. Eqs. (V.A.5), (V.A.6), (V.A.8) and (V.A.11)). Finally, N_c matrix equations for $c^{(k)}$ of the order $N_{pol} \cdot N_c$ are obtained,

$$\sum_{j,m'} M(\underline{z})^{ij}_{nm'} c^{(k)j}_{\ \ m'} = c^{(z)i}_{\ \ n}. \qquad \text{(IV.A.43)}$$

This matrix equation can be inverted directly, if the number of polynomials in the truncated expansion (IV.A.40) is sufficiently small. Iteration techniques are also available to solve Eq. (IV.A.43).

V.3 Separable approximation

The electronic coupling $V_l(R, k^2/2)$ defined in Eq. (IV.A.10) is a general function of internuclear distance R and the electron energy $\epsilon = k^2/2$, and not much is known about its shape mainly at larger values of R. It appears, however, and is actually supported by the calculations of a related problem, the dissociative attachment process [65–67], that in many cases the coupling element is separable or nearly separable in the variables R and ϵ,

$$V_l(R, k^2/2) \simeq V_R(R) V_\epsilon(k^2/2), \qquad \text{(IV.A.44)}$$

where V_R and V_ϵ are certain functions. The numerical data for $H_2^+ + e$, which is actually the only case in DR to give explicit dependencies on both R and ϵ, supports this separability, as explained below. In the case of dissociative attachment, quite a lot of information has been accumulated and supports this approximation [65–69]. Domcke made use of the separability in order to simplify the time-dependent wave packet propagation procedure when the T matrix formula is explicitly given. In the MQDT formalism, on the other hand, the separable coupling allows an explicit solution of the Lippmann-Schwinger equation in energy representation.

The separability may be qualitatively understood as follows. Since the valence orbitals are short ranged, the integration in the coupling (IV.A.10) is limited to a relatively small range of the radial distance r_0. For $r > r_0$ the MQDT formalism assumes that only a spherically symmetric Coulomb attraction for the external electron is non vanishing. Inside the reaction zone, $r < r_0$, on the other hand, the external electron is supposed to feel a strong attractive potential as an integral part of the molecule and thus its asymptotically low collision energy can be neglected in the first approximation. Near the boundary the inner wave function is already separated with respect to R and r as

$$\phi_l(k, r; R) \sim \omega(R) \left(\cos(\pi\mu(R))\, \phi_l^{(1)}(r) - \sin(\pi\mu(R))\, \phi_l^{(2)}(r) \right), \qquad \text{(IV.A.45)}$$

where $\omega(R)$ is a certain function of R, and only the energy normalization of the

outer wave function is left to be determined

$$\phi_l(k,\, r;\, R) \sim \frac{N^{-1}(k)}{\sqrt{k}} \left(f_l(k,r) \cos\left(\pi\mu(R)\right) - g_l(k,r) \sin\left(\pi\mu(R)\right)\right). \quad \text{(IV.A.46)}$$

Thus the k dependence of the coupling arises mainly through matching of the k-independent inner wave function $\phi_l^{(j)}(r)$ $(j = 1, 2)$ to regular and irregular Coulomb functions $f_l(k,r)$ and $g_l(k,r)$ at the boundary $r(k) \sim r_0$. The above argumentation holds for the matrix elements such as the electronic coupling (IV.A.10). This should not be used directly to the wave functions, though.

The most thoroughly studied system is H_2 for which the electronic coupling of H_2 $(^1\Sigma_g(2p\sigma_u)^2)$ has been calculated by Hara and Sato [70] in the static exchange approximation. Their matrix element is not precisely separable, but the non separable part is a rather small correction. This clearly follows from Fig. 16, where the solid line represents a separable approximation whereas the circles show the original data of Hara and Sato. Hence, in this case, the separable approximation should work very well and the remainder may be treated, if necessary, as a small perturbation. The other quantities describing $H_2^+ + e$ system, i.e. the dissociative and ionic potentials, are given in Fig. 17.

It is interesting to examine how the separability of electronic coupling in the sense discussed above appears as a quasi-separability of the Lippmann-Schwinger equation. The conventional separability in Eq. (IV.A.11) means

$$V\left(\{n, E\}, \{m, E'\}\right) = \nu_{nm} v_n(E) v_m(E'), \quad v_n \in R \quad \text{(IV.A.47)}$$

and the K-matrix then takes the form

$$\langle E, n \left| K(z) \right| E', m \rangle = \kappa(z)_{nm} v_n(E) v_m(E'), \quad \text{(IV.A.48)}$$

where

$$\kappa(z) = \left(1 - v\,\pi(z)\right)^{-1} v \quad \text{(IV.A.49)}$$

and

$$\pi_{nm}(z) \equiv \delta_{nm}^{\text{Kron}} \mathrm{P} \int_0^\infty \frac{v_n^2(E)}{z - E} dE. \quad \text{(IV.A.50)}$$

Eq. (IV.A.48) gives the operator solution of Eq. (IV.A.11) for all the energies E, E', if z is fixed.

In the present case the electronic coupling is separable in the sense of Eq. (IV.A.44) and thus the energy kernel of Eq. (IV.A.22) ($E = E_v + k^2/2$ or $E = E_0 + E_{nuc}$) given by

$$V\left(\{d, E\}, \{v, E'\}\right) = V_e\left(k(E'); v\right) \int_0^\infty \Psi_{dis}(R; E) V_R(R) \Phi_{vib}(R; E_v)\, dR \quad \text{(IV.A.51)}$$

appears in the form

$$V(\{d, E\}, \{v, E'\}) \equiv V_d(E' - E_v) V_v(E), \quad \text{(IV.A.52)}$$

where we denoted

$$V_v(E) = \int_0^\infty \Psi_{dis}(R;E) V_R(R) \Phi_{vib}(R;E_v)\, dR$$

and

$$V_d(E' - E_v) = V_\epsilon\,(E' - E_v)\,.$$

Although the arguments in Eq. (IV.A.51) are $\{d, E\}$ and $\{v, E'\}$, in Eq. (IV.A.52) the vibrational state v couples with the dissociative state kinetic energy E (through the function V_v) while the dissociative state d couples with continuous electron energy E' (through the function V_d). The solution of Eq. (IV.A.11) with the kernel in Eq. (IV.A.52), $K_{sep}(E) \equiv \langle E, n\,|K(\underline{z})|\,\underline{E'}, m\rangle$, is given below analytically for fixed $\underline{E'}$ and $\underline{z}$ only as a function of E. For determination of the phase shift, Eq. (IV.A.12), we finally set

$$E = \underline{E'} = \underline{z}. \tag{IV.A.53}$$

Because of this we call $K_{sep}(E)$ the "on-shell quasi-separable" solution. To write it down explicitly we consider for simplicity only one dissociative channel d.

The K matrix elements are found in terms of V functions in Eq. (IV.A.52), when we make use of the two separated groups of indices (see Eqs. (IV.A.34) and (IV.A.36))

$$K_{dd}(E) = \sum_v \alpha_v V_v(E), \quad K_{vd}(E) = \beta_v V_d(E - E_v) \tag{IV.A.54}$$

and

$$K_{v_1 v_2}(E) = \gamma_{v_1 v_2} V_d(E - E_{v_1}), \quad K_{dv}(E) = \sum_{v'} \delta_{vv'} V_{v'}(E). \tag{IV.A.55}$$

If we introduce the principal value integrals

$$\pi_v(E) \equiv \mathrm{P}\int_{E_v+\epsilon_n}^\infty \frac{V_d^2(E' - E_v)}{E - E'}\, dE' \;\text{ and }\; \pi_{vv'}(E) \equiv \mathrm{P}\int_{E_0}^\infty \frac{V_v(E')V_{v'}(E')}{E - E'}\, dE', \tag{IV.A.56}$$

then the coefficients in Eqs. (IV.A.54) and (IV.A.55) are given by the relations

$$\beta_v = V_v(E) + \sum_{v'} \pi_{vv'}\pi_{v'}\beta_{v'}, \quad \alpha_v \equiv \beta_v \pi_v \tag{IV.A.57}$$

and

$$\gamma_{v_1 v_2} = V_d(E - E_{v_2})\pi_{v_1 v_2} + \sum_{v'} \pi_{v_1 v'}\pi_{v'}\gamma_{v' v_2}; \tag{IV.A.58}$$

$$\delta_{vv'} \equiv V_d(E - E_v)\,\delta_{vv'}^{\mathrm{Kron}} + \pi_{v'}\gamma_{v'v}.$$

Since the parameter v_2 is dummy in Eq. (IV.A.58) the LU decomposition is useful; thus to get all the K-matrix elements we only need to solve an $N_{vib} \times N_{vib}$ linear matrix equation, which is repeated $N_{vib} + 1$ times (N_{vib} is the number of vibrational channels).

V.4 Numerical examples

Let us briefly discuss the numerical methods used to solve the K-matrix equation. For that purpose the DR process of $H_2^+ + e$ is used as an example. The rotational degree of freedom is not included in the model calculations. We start with the comparison of our method to the grid method. The first order perturbation theory is not applicable in this case. In order to prove it our calculations are presented for a wide range of the modified electronic coupling strength (see Fig. 18).

To get an insight into the problem, let us review the grid method. Essentially, this method uses a numerical quadrature to convert the integral equation (IV.A.11) to a linear set of equations defining the K-matrix at grid points. Such linear system can be solved by standard methods of linear algebra. The dimensions of underlying matrices and the accuracy of the method is to a large extent determined by the numerical quadrature used to approximate the integrals appearing in Eq. (IV.A.11). A typical integral needed for the evaluation of the K-matrix takes the following form

$$I(E) = \mathrm{P}\int_0^\infty \frac{f(E')}{E-E'}dE', \quad f(E') = \theta(E'+\epsilon_n)\,E'^a \exp\left(-bE'\right), \qquad \text{(IV.A.59)}$$

where E is a real number, negative in the case of closed channels and positive if the corresponding channel is open. Here a and b are certain constant parameters [71].

The Cauchy type integral can be evaluated according to the principal value definition with use of the grid method,

$$I(E) = \lim_{\epsilon\to 0}\left[\int_0^{E-\epsilon}\frac{f(E')}{E-E'}dE' + \int_{E+\epsilon}^\infty \frac{f(E')}{E-E'}dE'\right]. \qquad \text{(IV.A.60)}$$

The mesh points $E' = x_j$ are chosen so that we approximately have

$$I(E) \simeq \sum_j w_j \frac{f(x_j)}{E-x_j}, \qquad \text{(IV.A.61)}$$

where w_j are the quadrature weights. Because both integrals in Eq. (IV.A.60) diverge when $\epsilon \to 0$, it is important to use the mesh-points located symmetrically with respect to E in the vicinity of the singular point $x_j \sim E$. If an equidistant grid is used, obviously many grid points have to be used for the case $E \to 0_+$. In principle, more elaborate methods using variable grid steps may be used. Then, however, additional information on the integrand must be added. In that case more analytical approaches could be also used. The sophisticated numerical methods may not allow direct matrix inversion due to the varying number of mesh points and thus require some iterative procedure and implicit interpolation. Regardless of the modifications, the essence of the grid method consists in an

expansion (we assume an equidistant mesh size Δ),

$$f(x) \simeq \sum_n f_n b_n(x), \quad b_n(x) = \delta(x - x_n)\theta(x_{n_-} \leq x \leq x_{n_+})\Delta, \quad f_n = f(x_n), \tag{IV.A.62}$$

in which the principal value integral of the basis functions is

$$\mathrm{P}\int_0^\infty \frac{b_n(x)}{E - x} dx = \Delta \frac{1}{E - x_n}. \tag{IV.A.63}$$

Such expansion ignores the singularity completely and converges very slowly as $1/N$, N being the number of mesh-points. In fact, the following two conditions are tacitly assumed for the grid method to work:
1. The integrated function must change very slowly in the vicinity of the singularity.
2. A large number of grid points are needed, if the singularity approaches the limits of integration.

Instead, after the substitution (IV.A.25), we use Chebyshev polynomials as the basis set $b_n(x)$. If the integrated function is smooth, we can assume rapidly decreasing coefficients f_n within this basis. Taking the identity from the Amendment as an example (using Eqs. (V.A.3) and (V.A.5)), a new energy dependent quadrature with mesh-points independent from the location of the singularity can be introduced. First, the integrand is expanded into the Chebyshev polynomials numerically by taking the projection on a grid x_j, and then the principal value integral is evaluated analytically. Changing the order of summation, we get the quadrature weight at the point x_i when singularity is located at y as

$$2\sum_{n=1}^{N} \mathrm{T}_n(x_i)\mathrm{U}_{n-1}(y) \overset{N\to\infty}{\to} \frac{1}{x_i - y}. \tag{IV.A.64}$$

The limit in Eq. (IV.A.64) can not be reproduced numerically, and the identity above is to be understood in the generalized sense. In fact, the main advantage of this method is that small number of polynomials N_{pol} enables us to reproduce the Cauchy type singular integral accurately. It is not necessary to recalculate either the singularity or the integrated function at a different grid whenever the energy changes. This is important especially for the scattering calculations.

To manifest the difference between both methods we evaluated the principal value integral (IV.A.59) in the open and close channel regions with the singularity close to the limit of integration which means the low energy limit. Equidistant grid points and the trapezoidal quadrature rule are used for the integration. The grid is centered around the singularity (Cauchy type of integral) and its limits are chosen in such a way that the numerical error arising from neglecting the exponentially small integrand tail does not enter the displayed digits. As a minimum, two mesh-points are always used.

In the following we compare results of the grid method with the Chebyshev type calculation based on Eq. (V.A.8). The number of polynomials is equal to the number of quadrature points, which are used to project the function f into the polynomials. We have chosen the values $a = 1$, $b = 1$, $C = 2.5$ and the results are given in Table 1 for $E = \epsilon_n + 0.05$ (principal value integral) and in Table 2 for $E = \epsilon_n - 0.05$ (regular integral).

From these tables we can make the following conclusions:
1. The Chebyshev method converges quickly for both energies studied in this paper and in general. As low number as $N = 10$ gives results correct to 3-4 significant digits. This is also true for other energies.
2. The grid method yields reasonable, but much more slowly converging results, for middle energies. It almost fails in the low energy case, which is essential for MQDT, when the singularity approaches the limit of the integration. Note the plateau in the Table 1 around the values $N \sim 200 - 300$, where the calculation seemingly converged. A wrong answer might be obtained if the calculation was stopped at this point, since the accuracy of the grid method is basically only $\sim 1/N$.

In the following, we investigate the non-separable coupling case using the full K-matrix numerical solution, whilst the results due to the separable approximation (see Fig. 16) are computed from the on-shell quasi-separable analytical solution (OSQS) and the first order perturbation theory (FOPT). Following Takagi [71] we adopt 10 vibrational channels (see Fig. 17) in all the calculations and choose $n = 3$ for the threshold ϵ_n. The number of closed channels is important when solving K-matrix equation, since they enter the summation in the second term on the right-hand side of Eq. (IV.A.11). The statistical factor g in Eq. (IV.A.19) equals 1/4. Finally, the quantum defect function is taken from [72].

In Fig. 18, the eigen phase shifts $\delta_i(\underline{E})$ are plotted as a function of the relative electronic coupling strength $\lambda \in (0, 1)$ for a fixed value of the total energy using the separable electronic coupling. The FOPT results (crosses) start to differ from the exact ones at $\lambda \sim 0.05$, far bellow the actual electronic coupling strength $\lambda = 1$. Fig. 19 shows the energy dependence of the eigen phase shifts. In both Figs. 18 and 19, the separable approximation can not be practically distinguished from the exact non-separable results (solid lines).

In Figs. 20 the DR cross sections for $v = 0 \rightarrow d$ are shown. Fig. 20a presents the result of the separable approximation (OSQS), which is confirmed to coincide with the exact one as in the case of phase shift. This guarantees that the present separable approximation can very much simplify the analysis of DR processes. It should be noted that the solution of the K-matrix equation can be obtained almost analytically under this approximation. Fig. 20b depicts the result of FOPT which differs noticeably from Fig. 20a. This fact has been pointed out by Takagi in ref. [73] by using the grid method. The difference in resonance shape is due to indirect electronic mechanism omitted in FOPT and has been discussed in detail by Guberman and Giusti-Suzor in ref. [59]. We have also confirmed the

previous FOPT result based on energy-independent constant electronic coupling (Figs. 4 and 6a of ref. [72]). We note, that even in the FOPT case the results differ depending on whether some closed channels are considered or not.

V.5 Closing remarks

In this section we used a new technique for solving principal value integral equations that appear as a substantial part of the MQDT formalism of dissociative recombination. It enables us to treat the equations very efficiently, removing the problems of the conventional methods. Particularly, there is no need to change the grid and thus to recalculate or interpolate the coupling as well as the dissociative wave functions to re-express the kernel whenever the energy is changed. The resulting linear system for the K-matrix was shown to be of much smaller size compared to that of the grid method. The "on-shell quasi-separable" approximation in the Lippmann-Schwinger equation, arising from the separable electronic coupling, was discussed and a formal analytical K-matrix solution was introduced. Summarizing, the present method can make the MQDT treatment of various dynamic processes of super-excited molecular states as well as DR [55] very efficient. It is important especially for detailed calculations, when the rotational degree of freedom has to be taken into account, as well as for the case that more than one dissociative states are considered. We omitted these additional channels in this work since their incorporation can be done in a straightforward manner and they are not necessary for the demonstration of our method. Calculations of the $H_2^+ + e$ dissociative recombination process including also the additional channels has been carried out by Takagi [73] by using the grid method.

It was recognized to be important to consider the electronic coupling as a function of the internuclear distance as well as the continuous electron energy. We have to be careful about the constant coupling approximation. Changes of the K-matrix amplitudes, resulting from different types of approximations, influence the DR cross sections substantially. Separability of the coupling is useful because of the available analytical solution. This was found to be a very reasonable approximation which considerably facilitates the numerical calculation. Roughly speaking, the first order perturbation theory is justified when the electronic coupling is smaller than 5×10^{-3} a.u. Precise estimates for the applicability of FOPT need to take into account also the particular functionality of the electronic coupling. If the magnitude of all dimensionless quantities defined in Eq. (IV.A.56) is small, $|\pi_{\nu\nu'}\pi_v| \ll 1$, FOPT method works well. The grid method is less efficient than the analytical treatment of the principal value integral, as we have pointed out. It can be improved using the iteration type of solution and the variable grid size. The most elaborate way is, however, to use such a numerical technique that adopts the integration weight on a stable grid accurately and treats the singularity within a special class of integrand functions. The present work is an example of such a strategy for a particular expansion prescription. Our new method can

facilitate the DR calculations very much even for general diatomic molecules by incorporating into the general procedure developed in ref. [58].

Amendment

Here we provide the mathematical background for section V.

V.A. Chebyshev polynomials

First, some basic relations of the Chebyshev polynomials are summarized [16].
(1) Recursion relation for the first kind of polynomials:

$$\mathrm{T}_n(x) = 2x\mathrm{T}_{n-1}(x) - \mathrm{T}_{n-2}(x), \quad x \in \langle -1, 1 \rangle, \quad n \in N \cup \{0\} \tag{V.A.1}$$

$$\mathrm{T}_0(x) = 1, \quad \mathrm{T}_1(x) = x.$$

The same recursion relation holds for the second kind of Chebyshev polynomials with

$$\mathrm{U}_{-1}(x) = 0, \quad \mathrm{U}_0(x) = 1. \tag{V.A.2}$$

(2) Orthogonality for both sets of polynomials on $(-1, 1)$ with the weight

$$d\mu(x) = \frac{dx}{\sqrt{1-x^2}}. \tag{V.A.3}$$

The norm is $\pi/2$ for all the polynomials except T_0, norm of which is π.
(3) Numerical quadrature

$$\int_{-1}^{1} f(x)\frac{dx}{\sqrt{1-x^2}} \approx \sum_{i=1}^{N} w_i f(x_i), \tag{V.A.4}$$

where

$$w_i = w = \frac{\pi}{N}, \quad x_i = \cos\left[\left(i - \frac{1}{2}\right)w\right],$$

in which orthogonal relations are valid for indices $n, m \leq N$. Next, let us summarize some principal value integrals.
(1) Chebyshev principal value integral for $|y| < 1$ [63]

$$\mathrm{P}\int_{-1}^{1} \frac{\mathrm{T}_n(x)}{x-y}\frac{dx}{\sqrt{1-x^2}} = \pi \mathrm{U}_{n-1}(y). \tag{V.A.5}$$

(2) Chebyshev integral for $|y| > 1$

$$\int_{-1}^{1} \frac{\mathrm{T}_n(x)}{x-y}\frac{dx}{\sqrt{1-x^2}} = 2\pi\frac{Y^{n+1}}{Y^2-1}, \tag{V.A.6}$$

where

$$Y = \left\{ \begin{array}{ll} \sqrt{y^2-1}-y & y>1 \\ -y-\sqrt{y^2-1} & y<-1 \end{array} \right\} \quad |\,Y\,| < 1 \tag{V.A.7}$$

We have developed the two following quadratures:
(3) Principal value integral with non Chebyshev weight

$$\mathrm{P}\int_{-1}^{1} \frac{\mathrm{T}_n(x)}{x-y}dx = \frac{1}{2}\left(P_{n+1}(y) - P_{n-1}(y)\right), \tag{V.A.8}$$

where

$$P_n(y) \equiv \mathrm{P}\int_0^{\pi} \frac{\sin(n\theta)}{\cos\theta - y}d\theta, \quad y \in (-1,1), \quad P_{-n}(y) \equiv -P_n(y). \tag{V.A.9}$$

$$P_n(y) = -\pi\frac{\mathrm{T}_n(y)}{\sqrt{1-y^2}} + 2\left[\sum_{m=0}^{n-2}\frac{1}{n-m-1}\left(1+(-1)^{n-m}\right)\mathrm{U}_m(y) + \right.$$

$$\left. + \left\{\ln\sqrt{\frac{1-y}{1+y}} + \frac{\pi}{2}\frac{y}{\sqrt{1-y^2}}\right\}\mathrm{U}_{n-1}(y) - \frac{\pi}{2}\frac{1}{\sqrt{1-y^2}}\left(\mathrm{U}_{n-2}(y) - \delta_{n,0}\right)\right].$$

This shows clearly the divergence at $y = \pm 1$, where the operation of principal value stops to be defined. The following formula may be useful for numerical computations:

$$P_{n+1} = \frac{2}{n}\left(1-(-1)^n\right) + 2yP_n - P_{n-1} \quad |y| < 1. \tag{V.A.10}$$

(4) Integral with non-Chebyshev weight

$$\int_{-1}^{1} \frac{\mathrm{T}_n(x)}{x-y}dx = \left(I_{n+1}(y) - I_{n-1}(y)\right), \quad I_{-n}(y) \equiv -I_n(y), \tag{V.A.11}$$

where (cf. Eq. (V.A.7))

$$I_n(y) = \frac{S_n(Y_1) - S_n(Y_2)}{Y_1 - Y_2}, \quad Y_1 < 1, \quad Y_2 > 1$$

with

$$S_n(Y) \equiv 2\sum_{i=0}^{\left[\frac{n-1}{2}\right]}\frac{Y^{n-2i-1}}{2i+1} - Y^n \ln\left(\frac{1+Y}{1-Y}\right) \overset{Y\geq 1}{=} -2\sum_{i=\left[\frac{n+1}{2}\right]}^{\infty}\frac{Y^{n-2i-1}}{2i+1}.$$

(5) Following Domcke [74], we have

$$\mathrm{P}\int_0^{\infty}\frac{E'^{\alpha}}{E-E'}\exp(-E')\,dE' = \exp(-E)\left(\pi\frac{E^{\alpha}}{\tan(\pi\alpha)} - \Gamma(\alpha)\,{}_1F_1(-\alpha, 1-\alpha, E)\right), \tag{V.A.12}$$

$$\alpha > 0, \quad \alpha \neq n.$$

The singular case $\alpha = n$ can be treated by the formulae (V.A.8) and (V.A.11).

VI Conclusion

We have completed the semiclassical theory of nonadiabatic transitions in the exponential potential model. In particular, we solved the repulsive potential case and re-expressed the nonadiabatic transition matrix in terms of contour integrals of adiabatic momenta in the complex coordinate plane. Such formula has the conceptual advantage of being free from the parameters pertinent to the exponential potential model. On the basis of Meijer G functions we derived the first quantum mechanical exact analytical solution of a diabatically avoided crossing model and analyzed this model semiclassically. The semiclassical conditions for the complete transmission and the complete reflection in some two-state quantum systems common in molecular physics were given. We developed a powerful technique for solving integral equations with a singular kernel useful in the framework of Multi-channel Quantum Defect Theory and suggested a separable approximation for the electronic coupling, under which we derived an exact analytical solution of Lippman-Schwinger Equation. We also proposed applications of formalism used in physics to economics, in particular the concept of a potential and the concept of nonadiabatic transition.

Illustrations

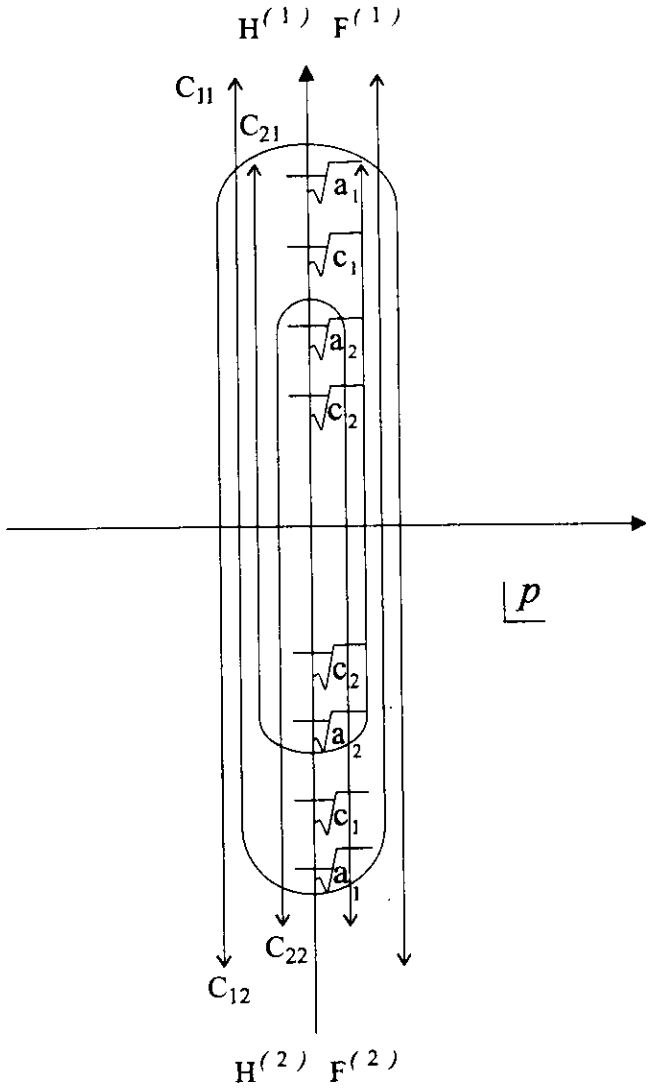

Figure 1 Bessel transformation contours in the complex p-plane.

Two contours (C_{i1}, $i = 1, 2$) wind the branch cuts at the lower complex half-plane of p and go to $+i\infty$, while the two others (C_{i2}, $i = 1, 2$) wind the branch cuts at the upper half-plane and go to $-i\infty$. The numbering of contours, C_{ij}, corresponds to the Hankel functions, $H^{(j)}$, and the WKB wave functions, $F^{(j)}$.

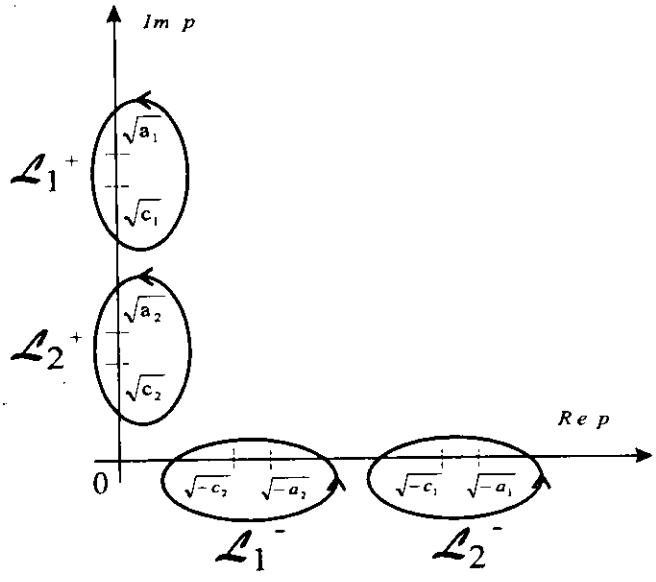

Figure 2 Contours L_i.

The two contours L_1 and L_2 define the parameters δ_i of Eqs. (II.64) and (II.65) in the complex p-plane. These are shown both for the repulsive case, L_i^+ (branch cuts on the imaginary axis), and for the attractive case, L_i^- (branch cuts on the real axis), (see Eq. (II.H.6)).

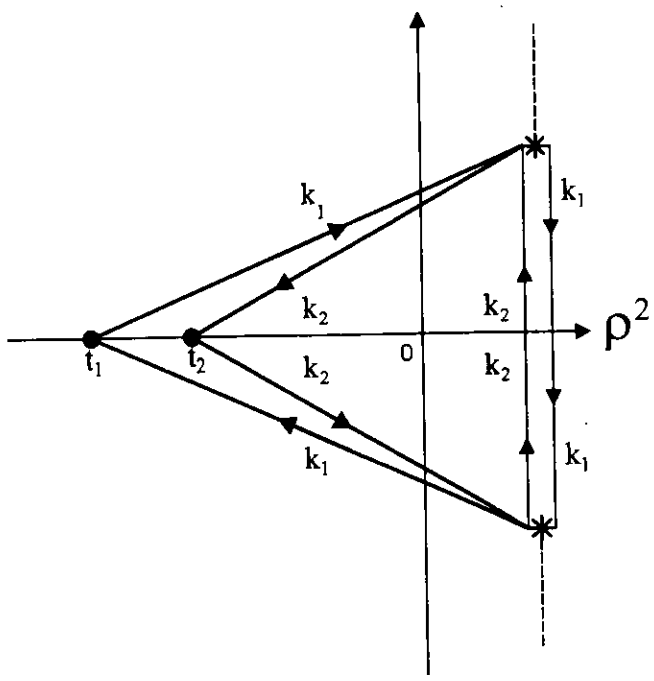

Figure 3 Contours in the complex ρ^2-plane (attractive case).

The two closed contours correspond to L_1^- and L_2^- of Fig. 2 when transformed to the ρ^2 plane. The bold line is the contour for δ_1 while the contour for δ_2 (thin line) winds around the complex crossing points denoted by stars. The adiabatic momenta, integrated on the respective parts of the contours, are denoted as k_1 and k_2, and t_i $(i = 1, 2)$ stands for the corresponding turning points $-\nu^2/c_i$. Branch cuts of adiabatic potentials are plotted as a dashed line. The overall integration result, $\delta = \delta_1 + \delta_2$, is the sum of integrals of k_1 and k_2 on two contours that encircle $\rho^2 = 0$ $(x = \infty)$ in opposite directions.

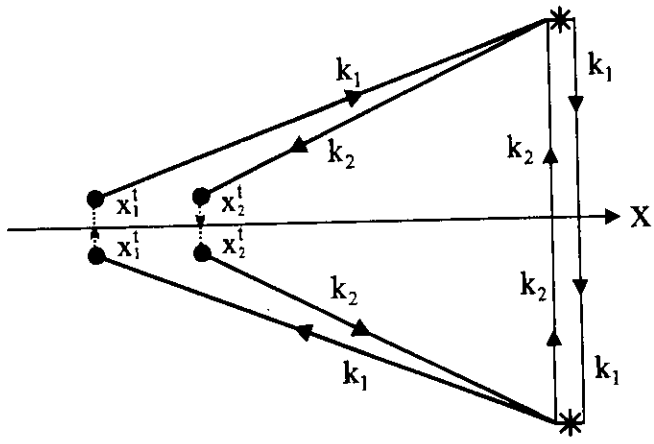

Figure 4 Contours in the complex coordinate plane (attractive case).

The contours for δ_i in the x-plane. Turning points x_i^t are located out of the real axis. As a result the integral for δ_1 (bold line) can be reduced to the integration on the dotted contours. In the repulsive case $\Im x_i^t = 0$, the complex conjugate turning points merge together, and the sum of the two contour integrals equals zero.

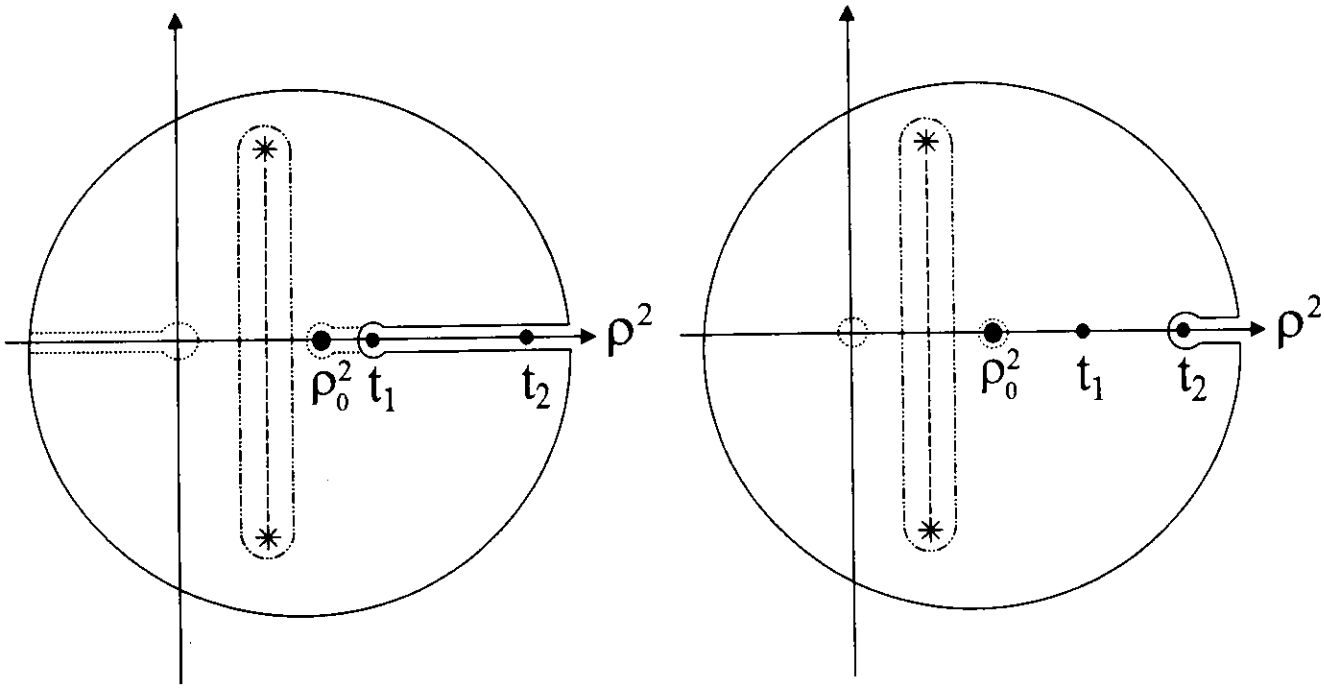

Figure 5 Contours in the complex ρ^2-plane (repulsive case).

a) Integral for δ_1. The full line corresponds to the contour L_1^+ (cf. Eq. (II.H.2) with i=1). The dotted line shows how the contour can be distorted without changing the integration result (see Eq. (II.H.10)). The point ρ_0^2 corresponds to $p_2^\dagger = 0$ which does not contribute to δ_1 (see Eq. (II.H.4)). Stars denote the adiabatic crossing points which are connected by a branch cut (dashed line), t_1 and t_2 are the turning points. The contour for δ_1 can be finally reduced to the double-dot-dashed line.
b) Integral for δ_2. Not only the same contour (double-dot-dashed) as in a) except that $i = 2$ in Eq. (II.H.2) but also the closed dotted contours arising from Eqs. (II.H.11) and (II.H.4) contribute to δ_2.

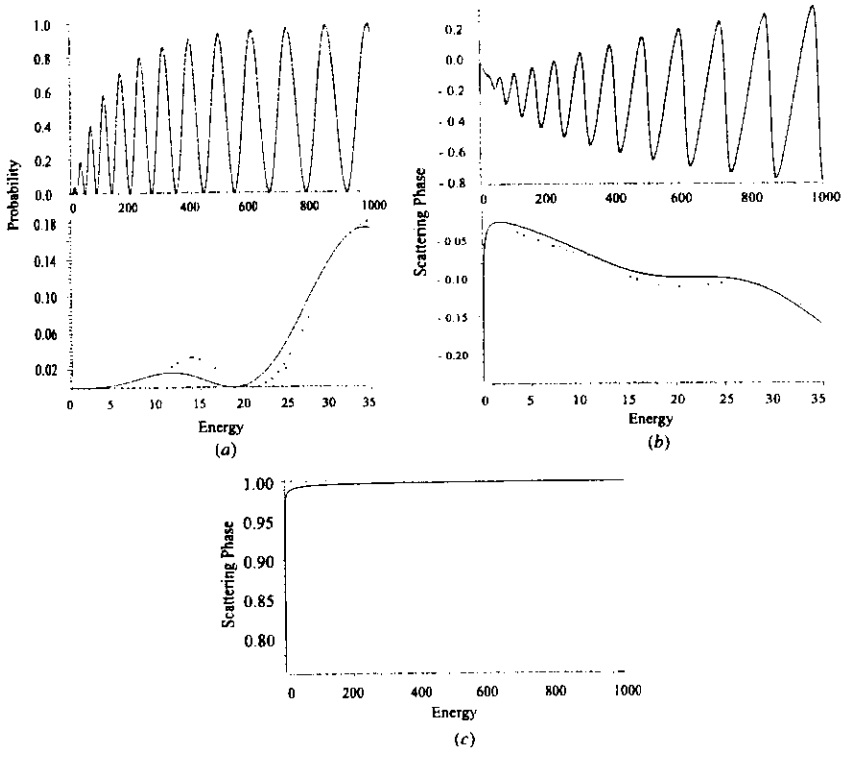

Figure 6 Accuracy of the semiclassical S^R matrix.

a) The transition probability $P(E)$ (see Eq. (II.74))
b) The scattering phase $\Phi(E)$ (see Eq. (II.75))
c) The scattering phase $\Psi(E)$ (see Eq. (II.76))
In the Figs. a)-c) the lower plot is a detail of the upper one.
The potential parameters are $V_1 = -30$, $V_2 = -40$, $V = 20$, $U_1 = 0$ and $U_2 = -15$ which represent a system with big asymptotic energy level separation. That is why the condition in Eq. (II.73) is fulfilled for the energy which is above the scale in this Figure. The total transition probability (Eq. (II.74)) and the rescaled S^R-matrix phases (Eqs. (II.75) and (II.76)) are ploted against the dimensionless energy. The full line is the exact quantum solution and the circles show the analytical result from Eq. (II.62). Energy of the diabatic crossing point is 45, while the energy at the reference point (the average of adiabatic potentials) is ~ 5.2.

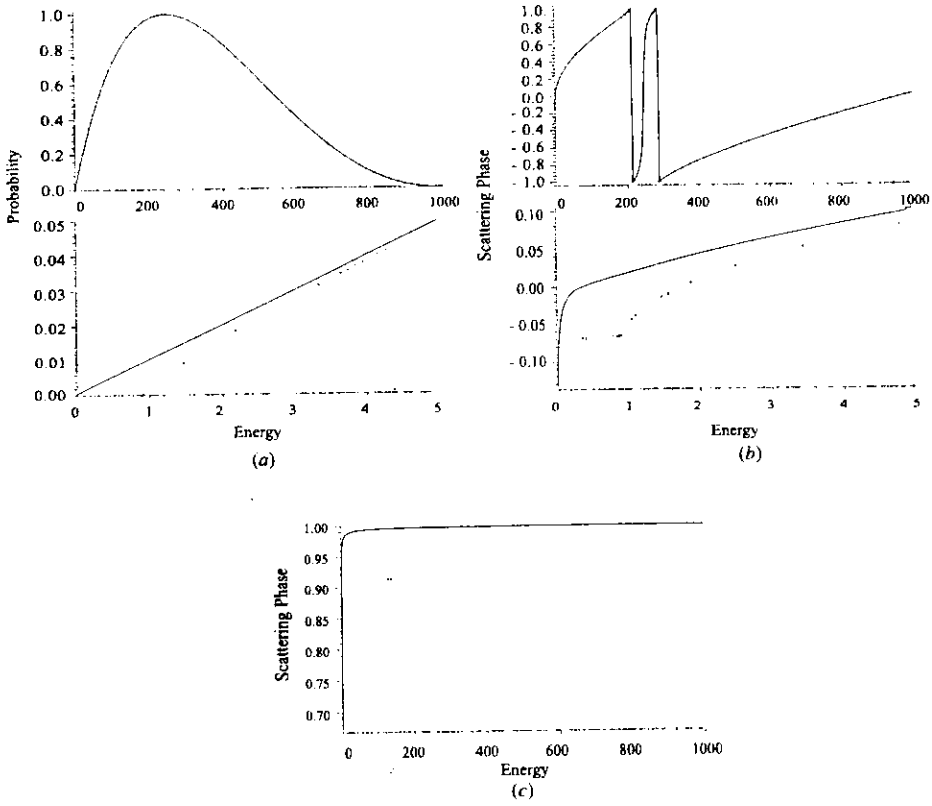

Figure 7 Accuracy of the semiclassical S^R matrix.

The same as in Fig. 6 except that we chose $V_1 = -0.1$, $V_2 = -0.1002$, $V = 0.005$, $U_1 = 0$ and $U_2 = -0.1$. This is an example of almost parallel potentials with small asymptotic energy level separation. Energy of the diabatic crossing point is 50, while the energy at the reference point is ~ 0.95.

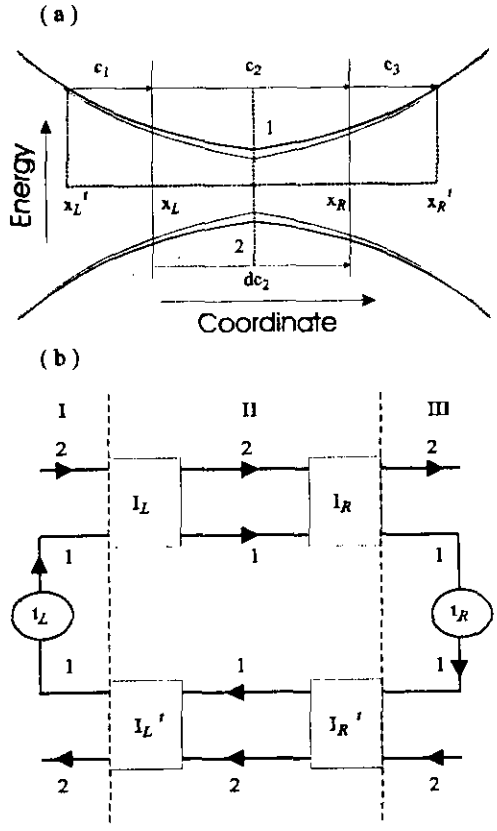

Figure 8 Diabatically avoided crossing model.

(a) The potential curves: the two diabatic potentials (thin lines, arabic numbers) do not intersect and have a constant nonadiabatic coupling. Adiabatic potentials are shown in bold. The sharp potential curves are obtained by cutting and rotating the Rozen-Zener-Demkov model by the angle of $\pi/4$. Arrows and letters indicate the important adiabatic phases. (b) The semiclassical diagram: arrows denote the direction of adiabatic wave (arabic number) propagation. The rectangles represent the two nonadiabatic transition regions with the transition matrix I (from left to right) or its transpose, I^t (from right to left).

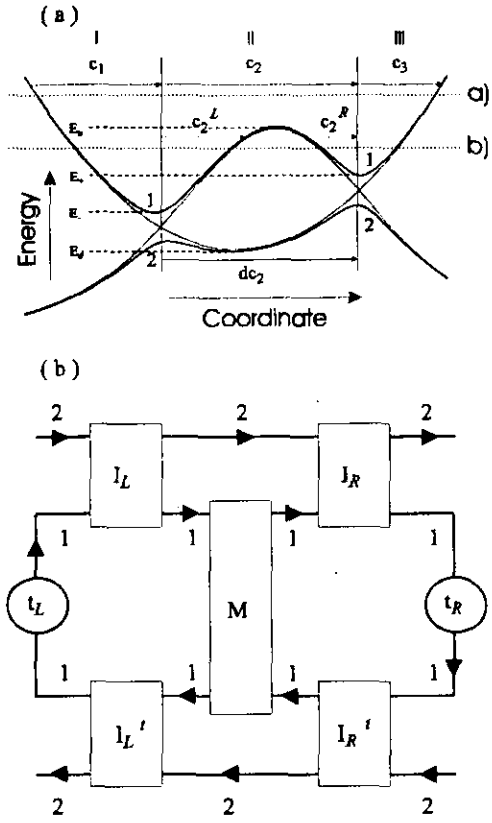

Figure 9 Double crossing NT-type model.

(a) The potential curves: the notation is the same as in Fig. 8a. We distinguish energy above the top of the barrier, a) (for the semiclassical diagram see Fig. 8), and energy below the barrier top, b). The roman numbers denote the three important coordinate regions; arabic numbers index the adiabatic potentials. (b) The semiclassical diagram (energy below the top of the barrier): same as in Fig. 8b. The matrix M stands for the tunneling through the central potential barrier (see Fig. 9a).

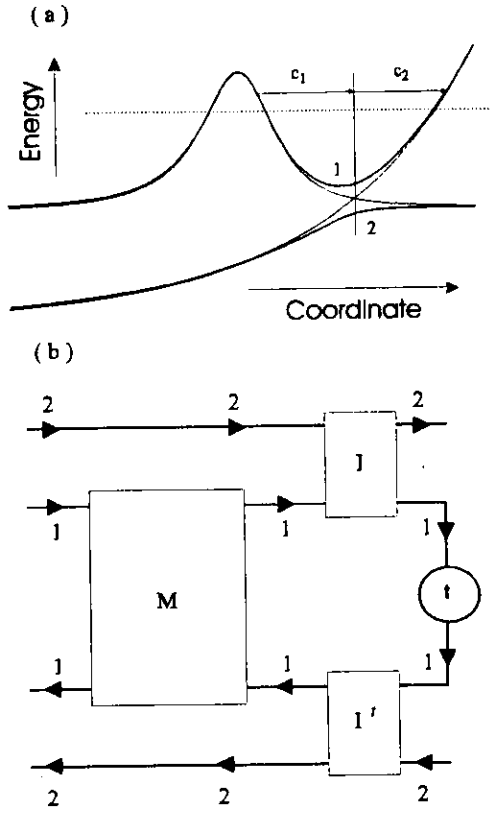

Figure 10 Three channel tunneling model.

(a) The potential curves: the notation is the same as in Fig. 9a. (b) The semiclassical diagram: the notation is the same as in Fig. 9b.

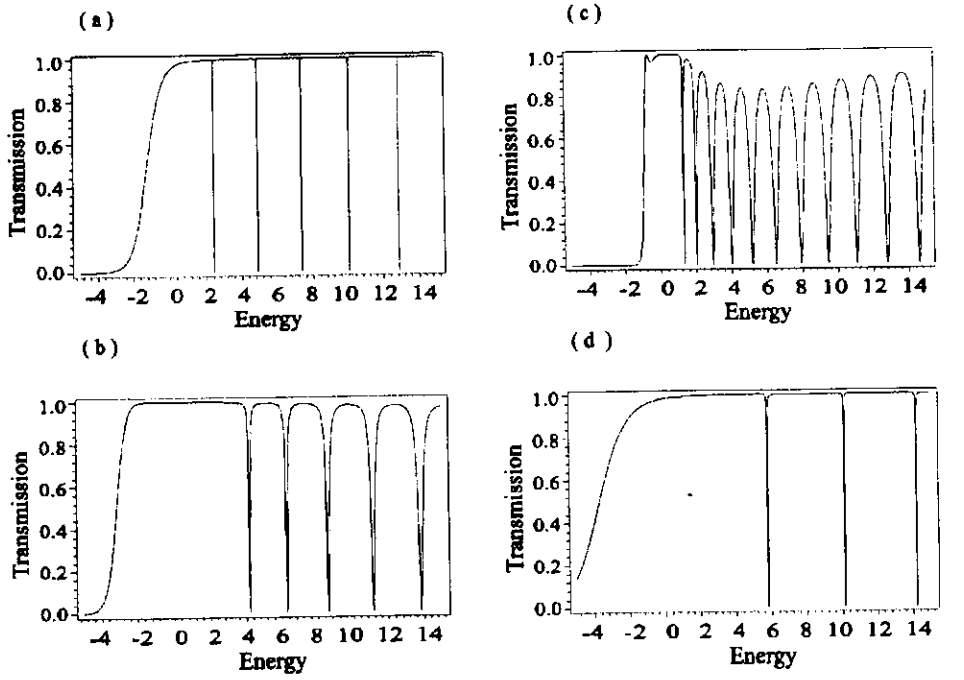

Figure 11 Transmission in DAC model.

Transmission coefficient as a function of energy. In the dimensionless units of Eq. (III.55) the model parameters are ($U = 0$): (a) $C = 0.2$ and $V = 1$ (b) $C = 6$ and $V = 1$ (c) $C = 2$ and $V = 0.1$ (d) $C = 2$ and $V = 3$. The bottom E_b (top $-E_b$) of the upper (lower) adiabatic potential is given by $\sqrt{V^2 + C^2}$, i.e. $E_b \sim$ 1.02 (a), 6.08 (b), 2.00 (c), and 3.61 (d).

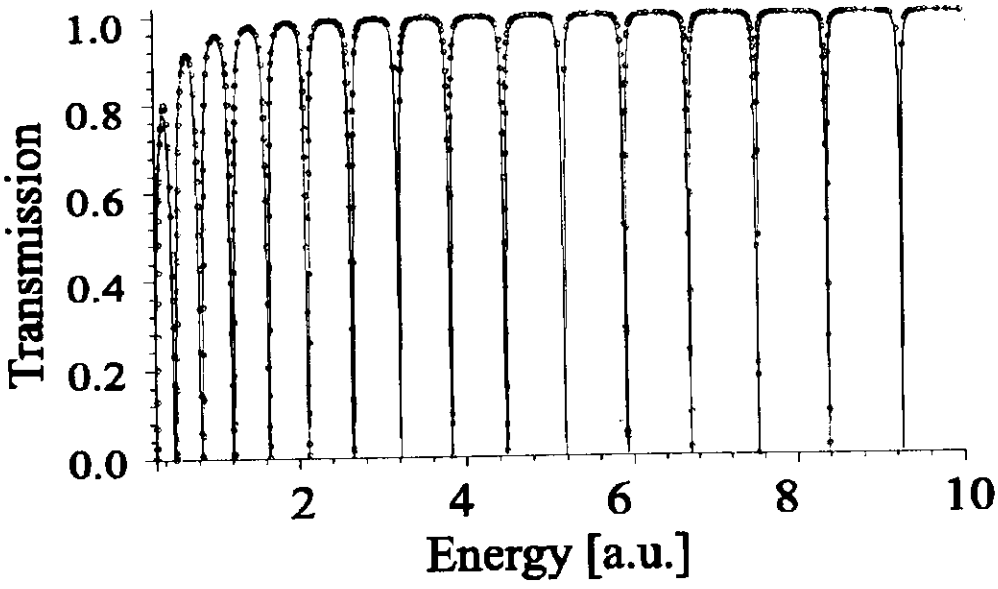

Figure 12 Semiclassical analysis of DAC model.

Semiclassical (circles) and exact (full line) transmission coefficient as a function of enegy. The potential constants, $C = 2$ and $V = 10^{-3}$ in the units of Fig. 11, are chosen so that the potential is flat around $x = 0$ and a sequence of two RZ transitions takes a place. Confer with Eqs. (III.49) and (III.B.1).

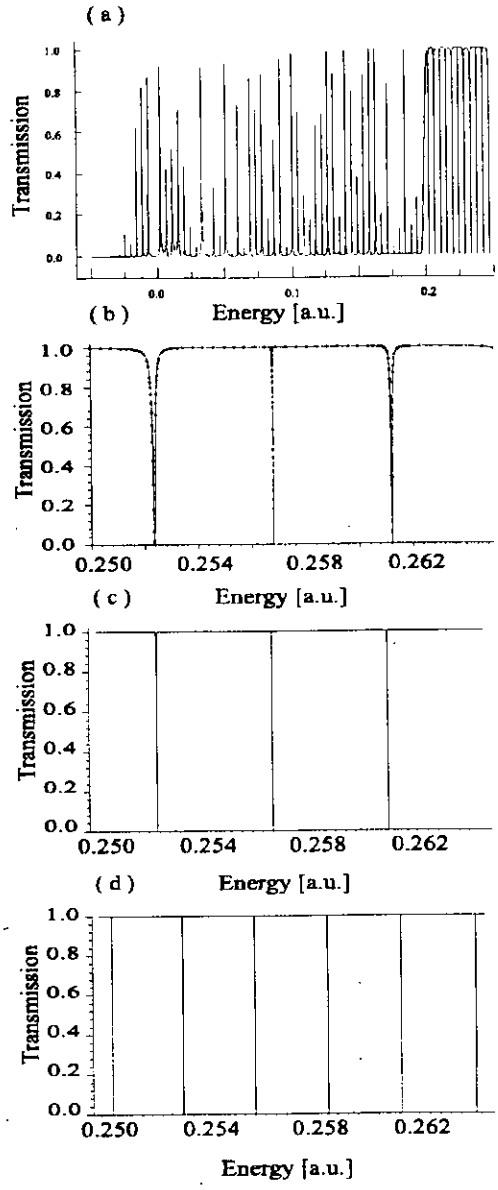

Figure 13 Transmission in double crossing NT case.

The asymmetric model potential is defined by Eq. (III.17). (a) Transmission coefficient as a function of energy (overall feature). (b) Magnification of Fig. 13a ($V_{12} = 5 \times 10^{-3}$). Solid circles represent the semiclassical results from Eqs. (III.49) and (IV.A.1). (c) The same as Fig. 13b except for $V_{12} = 1 \times 10^{-3}$. (d) The same as Fig. 13b except for $V_{12} = 8 \times 10^{-2}$.

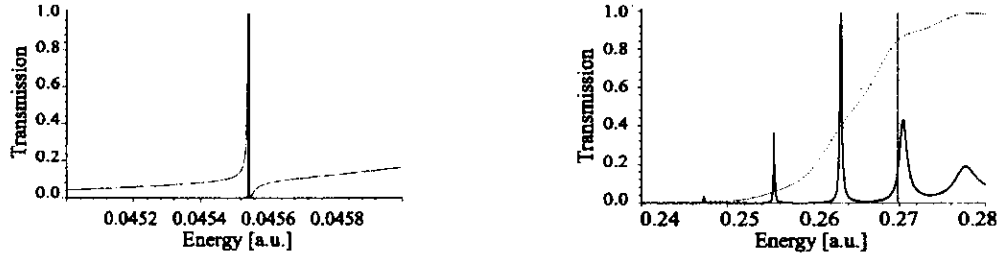

Figure 14 Fano type resonance in the Vardi-Shapiro case [46].

The model potentials are given by Eqs.(III.18)-(IV.A.22). There appear complete reflection and transmission below the top of the central barrier (maximum of $V_{11} \simeq 4.71 \times 10^{-2}$). The thin line corresponds to the potential given in the text; while the bold line is the transmission coefficient for an artificially magnified central barrier to such an extent that the tunneling can be neglected.

Figure 15 Transmission in 3-channel tunneling case.

The transmission coefficient as a function of energy for the model potentials given by Eq. (III.22) with (1) $V_{12} = 4.59 \times 10^{-2}$ (full line) and (2) $V_{12} = 5.0 \times 10^{-3}$ (dotted line). The vertical dashed line indicates the energy of the barrier top.

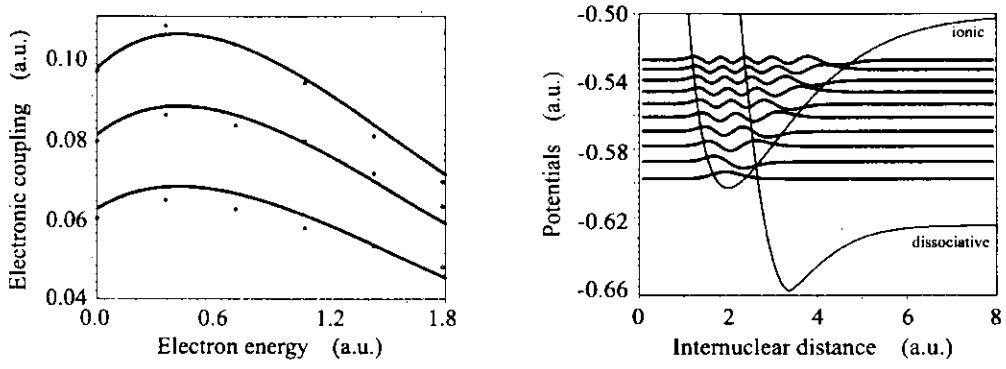

Figure 16 Separable approximation of the electronic coupling of H_2 ($^1\Sigma_g(2p\sigma_u)^2$).

The abscissa ϵ is the energy of the continuous electron, the ordinate measures the electronic coupling $V_l(\underline{R})$. The three curves correspond to $R = 1.4, 2.0, 2.6$ in the increasing order of magnitude. Circles show the data by Hara and Sato [70] and the full lines indicate the separable approximation.

Figure 17 Ionic and dissociative potential curves of H_2.

The dissociative and ionic potentials are plotted as a function of internuclear distance R. H_2^+ vibrational levels and corresponding wave functions are also drawn for convenience.

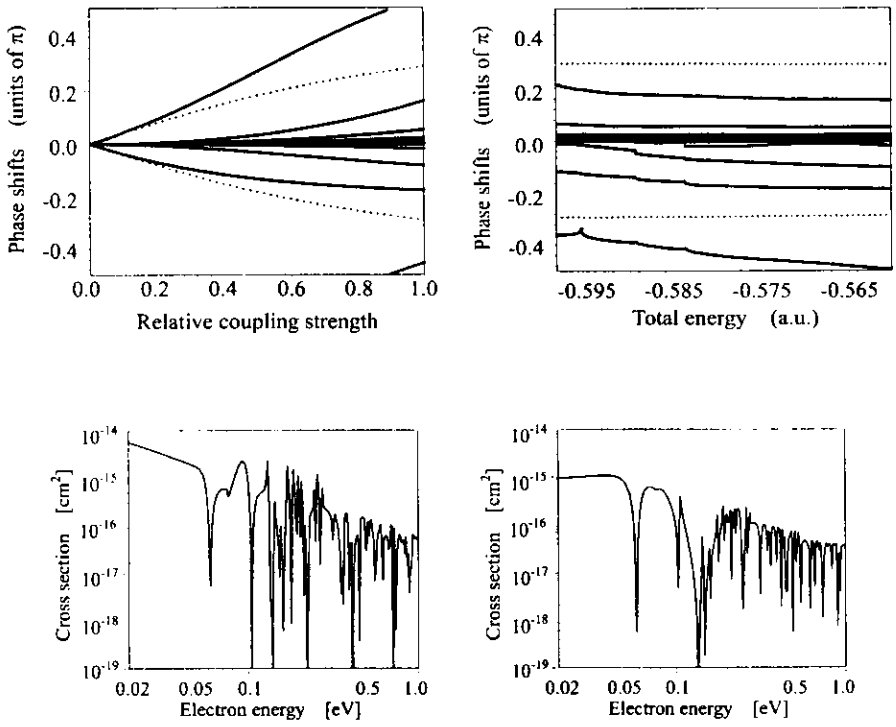

Figure 18 Coupling strength dependence of the eigen-phase shifts.

The coupling has been redefined as $\lambda V_l(\epsilon, R)$ and the K-matrix eigen-phase shifts $\delta_i(\underline{E}; \lambda)/\pi$, $i = 1 \sim 11$ are plotted against λ for the fixed total energy $\underline{E} = -0.575$. The exact numerical results for the general non-separable case appear in full lines. The OSQS (on-shell quasi-separable analytical solution) results coincide with the exact ones, and crosses denote the two symmetric FOPT (first order perturbation theory) phase shifts (other $N_{vib} - 1$ phase shifts degenerate to zero in this case).

Figure 19 Energy dependence of the eigen-phase shifts.

The notation is the same as in Fig. 18 except for the horizontal abscissa, which now denotes the total energy E ($\lambda = 1$).

Figure 20 The DR cross section for $H_2^+(v = 0) + e \rightarrow H + H$ as a function of electron energy (in eV).

The incident electron energy is measured in a logarithmic scale, $-(\log \epsilon - \log(0.02))/\log(0.02)$, and the cross section (in cm^2) is also meased in logarithmic scale, $\log_{10}(\sigma_{v=0\rightarrow d})$.
(a) The general non-separable case and the separable approximation (indistinguishable). (b) The result of the first order perturbation theory.

Tables

Table 1: Principal Value Integrals by Chebyshev and Grid Methods. $E = \epsilon_n + 0.05$ is the total energy in Eq. (IV.A.59), N is the highest Chebyshev polynomial index in the expansion (IV.A.40) as well as the number of mesh-points in Eq. (V.A.4). $PvI_{Chebyshev}$ denotes the principal value integral evaluated by the means of Chebyshev polynomial expansion and $PvI_{Equi-grid}$ stands for the result obtained from the grid method.

N	$PvI_{Chebyshev}$	$PvI_{Equi-grid}$	N	$PvI_{Equi-grid}$
1	-0.13721765$\times 10^1$	-0.08059284	40	-0.98221158
2	-0.11716273$\times 10^1$	-0.08059284	50	-0.10336974$\times 10^1$
3	-0.10172041$\times 10^1$	-0.16427398	60	-0.10646586$\times 10^1$
4	-0.12895849$\times 10^1$	-0.23024873	70	-0.10833267$\times 10^1$
5	-0.12194187$\times 10^1$	-0.28652549	80	-0.10946005$\times 10^1$
6	-0.11288302$\times 10^1$	-0.33635902	90	-0.11014157$\times 10^1$
7	-0.11689960$\times 10^1$	-0.38141667	100	-0.11055386$\times 10^1$
8	-0.11803151$\times 10^1$	-0.42268321	200	-0.11118244$\times 10^1$
9	-0.11685195$\times 10^1$	-0.46080023	300	-0.11118664$\times 10^1$
10	-0.11701910$\times 10^1$	-0.49621710	400	-0.11395432$\times 10^1$
11	-0.11711006$\times 10^1$	-0.52926658	500	-0.11395825$\times 10^1$
12	-0.11709391$\times 10^1$	-0.56020603	600	-0.11495396$\times 10^1$
13	-0.11710051$\times 10^1$	-0.58924165	700	-0.11495745$\times 10^1$
14	-0.11706390$\times 10^1$	-0.61654334	800	-0.11546952$\times 10^1$
15	-0.11709514$\times 10^1$	-0.64225435	900	-0.11547260$\times 10^1$
16	-0.11709120$\times 10^1$	-0.66649777	1000	-0.11578406$\times 10^1$
17	-0.11707939$\times 10^1$	-0.68938100	2000	-0.11642504$\times 10^1$
18	-0.11708963$\times 10^1$	-0.71099895	3000	-0.11664228$\times 10^1$
19	-0.11708665$\times 10^1$	-0.73143638	4000	-0.11675156$\times 10^1$
20	-0.11708547$\times 10^1$	-0.75076966	5000	-0.11681735$\times 10^1$
21	-0.11708699$\times 10^1$	-0.76906809	6000	-0.11686130$\times 10^1$
22	-0.11708638$\times 10^1$	-0.78639496	7000	-0.11689274$\times 10^1$
23	-0.11708645$\times 10^1$	-0.80280836	8000	-0.11691634$\times 10^1$
24	-0.11708642$\times 10^1$	-0.81836183	9000	-0.11693471$\times 10^1$
25	-0.11708652$\times 10^1$	-0.83310492	10000	-0.11694942$\times 10^1$
26	-0.11708645$\times 10^1$	-0.84708363	20000	-0.11701569$\times 10^1$
27	-0.11708644$\times 10^1$	-0.86034076	30000	-0.11703782$\times 10^1$
28	-0.11708650$\times 10^1$	-0.87291626	40000	-0.11704883$\times 10^1$
29	-0.11708645$\times 10^1$	-0.88484746	50000	-0.11705546$\times 10^1$
30	-0.11708646$\times 10^1$	-0.89616934	100000	-0.11706870$\times 10^1$

Table 2: Regular Integrals by Chebyshev and Grid Methods. The notation is the same as in Table 1, except for $E = \epsilon_n - 0.05$, which corresponds to a regular integral. The singular point of the integrand is outside of the integration interval. $I_{Chebyshev}$ denotes the integral evaluated by the means of Chebyshev polynomial expansion and $I_{Equi-grid}$ stands for the result obtained from the grid method.

N	$I_{Chebyshev}$	$I_{Equi-grid}$	N	$I_{Equi-grid}$
1	-1.42395680	-0.10452720×10^{2}	40	-0.11053738×10^{1}
2	-1.29288040	-0.10452720×10^{2}	50	-0.10741976×10^{1}
3	-0.94351396	-0.52589808×10^{1}	60	-0.10539170×10^{1}
4	-0.96417443	-0.36025258×10^{1}	70	-0.10396865×10^{1}
5	-0.96732836	-0.28270204×10^{1}	80	-0.10291588×10^{1}
6	-0.95413852	-0.23894798×10^{1}	90	-0.10210596×10^{1}
7	-0.95949466	-0.21123854×10^{1}	100	-0.10146384×10^{1}
8	-0.96090360	-0.19225837×10^{1}	200	-0.98643418
9	-0.95918080	-0.17850365×10^{1}	300	-0.97731111
10	-0.95943212	-0.16810552×10^{1}	400	-0.97280793
11	-0.95974924	-0.15998326×10^{1}	500	-0.97012557
12	-0.95956551	-0.15347130×10^{1}	600	-0.96834567
13	-0.95957362	-0.14813857×10^{1}	700	-0.96707844
14	-0.95961237	-0.14369424×10^{1}	800	-0.96613029
15	-0.95958881	-0.13993522×10^{1}	900	-0.96539420
16	-0.95959192	-0.13671560×10^{1}	1000	-0.96480619
17	-0.95959667	-0.13392791×10^{1}	2000	-0.96216962
18	-0.95959311	-0.13149133×10^{1}	3000	-0.96129422
19	-0.95959407	-0.12934391×10^{1}	4000	-0.96085718
20	-0.95959443	-0.12743740×10^{1}	5000	-0.96059516
21	-0.95959387	-0.12573367×10^{1}	6000	-0.96042056
22	-0.95959413	-0.12420222×10^{1}	7000	-0.96029589
23	-0.95959412	-0.12281833×10^{1}	8000	-0.96020242
24	-0.95959405	-0.12156178×10^{1}	9000	-0.96012973
25	-0.95959411	-0.12041588×10^{1}	10000	-0.96007158
26	-0.95959409	-0.11936672×10^{1}	20000	-0.95981003
27	-0.95959409	-0.11840261×10^{1}	30000	-0.95972288
28	-0.95959410	-0.11751368×10^{1}	40000	-0.95967931
29	-0.95959409	-0.11669151×10^{1}	50000	-0.95965317
30	-0.95959406	-0.11592890×10^{1}	100000	-0.95960090

Glossary

PHYSICS Natural science about the physical world *noun*
MATHEMATICS Self enclosed science *noun*
SYSTEM Subject of our interest and investigation *noun*
MODEL Way of our description of the system *noun*
STATE Set of conditions determining the system uniquely *noun*
MEASUREMENT Set of actions performed on the system *noun*
QUANTITY Property of the system which can be mathematically formalized *noun*
1. QUANTUM Unit of the quantity[2] *noun*
2. QUANTUM Having the quantum *adjective*
1. VARIABLE Changeable *adjective*
2. VARIABLE Variable quantity *noun*
SCALAR A quantity fully described by one number *noun*
TIME AND CLOCK Time is a scalar quantity measured by the clock *nouns*
ISOLATED Self contained *adjective*
ENERGY Scalar quantity conserved in the isolated system *noun*
EIGEN Proper *adjective*
1. POTENTIAL Possible *adjective*
2. POTENTIAL Potential energy *noun*
ADIABATIC Defined with respect to a fixed quantity *adjective*
ADIABATIC POTENTIAL Adiabatic eigen potential *shortcut*
ADIABATIC STATE Adiabatic eigen state *shortcut*
NONADIABATIC Not adiabatic *adjective*
DIABATIC Not necessarily adiabatic *adjective*
TRANSITION Change of the state *noun*
COORDINATE Way of ordering by numbers *noun*
PLANE Mathematical entity with two independent coordinates *noun*
COMPLEX Composed *adjective*
CROSSING Intersection *noun*
VELOCITY Time change of coordinate *noun*
MASS Scalar quanity measuring inertia *noun*
MOMENTUM Scalar product of mass and velocity *noun*
DISSOCIATION Decomposition *noun*
DISSOCIATIVE Of dissociation *adjective*
CHARGE Scalar quantity measuring electricity *noun*
ATOM AND MOLECULE Atoms are units of which molecules are composed *nouns*
RECOMBINATION Repeated combination *noun*

The important compound words in the thesis are:

[2]which eventually can not be further decomposed

NONADIABATIC TRANSITION Transition in which the adiabatic state is changed
AVOIDED CROSSING Crossing of adiabatic potentials which does not occur
DIABATICALLY AVOIDED CROSSING
Crossing of diabatic potentials which does not occur
DISSOCIATIVE RECOMBINATION Recombination of charge and dissociation of molecule [3].

[3]the list of terms is not comprehensive

List of Papers

1. *Analytical treatment of singular equations in dissociative recombination*, Lukáš Pichl, Hiroki Nakamura and Jiří Horáček, Computer Physics Communications **124** (2000) 1-18.

2. *Non-adiabatic transitions in a two-state exponential potential model*, Lukáš Pichl, Vladimir I. Osherov and Hiroki Nakamura, J. Phys. A: Math. Gen. **33** (2000) 3361-3384.

3. *Complete reflection in two-state crossing and noncrossing potential systems*, Lukáš Pichl, Hiroki Nakamura and Jiří Horáček, Journal of Chemical Physics, scheduled for **111** (2000) 1-13.

4. *Accurate formula for the double-passage transition probability in an exponential potential model*, Lukáš Pichl, Vladimir I. Osherov and Hiroki Nakamura, New Journal of Physics, submitted, Ref: NJP/114175/PAP.

5. *The uncertainty factor and its quantification* Lukáš Pichl, Hiroshi Deguchi and Hiroki Nakamura, in JCIS 2000 Proceedings (AIM, Atlantic City, 2000) vol. 2, 998-1001.

6. *Nonadiabatic transitions in economic systems* Lukáš Pichl, Hiroki Nakamura and Hiroshi Deguchi, in in JCIS 2000 Proceedings (AIM, Atlantic City, 2000) vol. 2, 1002-1004.

[4]these articles were written during my Monbusho fellowship period at the Graduate University of Advanced Studies in Japan

Appendix

Application of the Concept and Theory of Nonadiabatic Transition to Economics

Here we review our achievements in application of physical formalism to economics. The full account is given in the Papers 5 and 6.

The time evolution of trade-off like (TOL) problems is investigated. It is shoum that the efforts of an authority to eliminate an initial fluctuation can cause a quasi-periodic oscillations (on adiabatic states). We can also treat the case of more than two groups of TOL problems. In a real system the choice of such groups is ambiguous to a certain extent, because the quantities usually influence each other (due to nonadiabatic coupling). That is why the initial fluctuation can be transmitted between different adiabatic states as time evolves (i.e. nonadiabatic transition). A partial account of a formalism developed for this purpose in the field of quantum physics is given.

I. INTRODUCTION

Two state dynamical problems which can be described by a set of linear differential equations are well known from different fields [7] and such a linear approximation can be viewed as a first order expansion of a more general (unknown) functional. Here we show that the general formalism developed to treat such problems in quantum physics widely applies in economics, too. We expect that the semiclassical Zhu-Nakamura theory for linear curve crossing [5] could be used.

II. FORMALISM

Let us define a pair of dimensionless quantities q_i

$$q_i = (Q_i - \bar{Q}_i)/\bar{Q}_i \quad i = 1, 2, \tag{V.A.13}$$

as a relative variation of a quantity Q from the equilibrium value, $\bar{Q}$. As an example from the *monetary policy*, be $-q_1$ the money market rate and q_2 the money supply. If $q_2 > 0$ then q_1 increases, the proportionality factor $\alpha(t)$ being in general time dependent. At the same time if $q_1 > 0$, the central bank attempts to respond by a proportional ($\sim k$) decrease of q_2. In such a regime the reason and consequence are difficult to distinguish. The corresponding differential equations read

$$\frac{d}{dt}q_1(t) = \alpha(t)q_2(t), \quad \frac{d}{dt}q_2(t) = -k\alpha(t)q_1(t). \tag{V.A.14}$$

It is natural to rescale the quantities,

$$q_1(t) \to q_1(t)/\sqrt{k}, \quad \alpha(t) \to \alpha(t)\sqrt{k}, \tag{V.A.15}$$

and to introduce a complex quantity,

$$z = q_1 + iq_2, \tag{V.A.16}$$

which better describes the periodic processes. Then Eq. (V.A.14) and the corresponding solution have the form

$$i\frac{d}{dt}z(t) = \alpha(t)z(t) \Rightarrow z(t) = C_z e^{-i\int_{t_0}^{t}\alpha(t')dt'}, \tag{V.A.17}$$

and the quantities $q_i(t)$ periodically develop with a shifted phase and the common frequency

$$\omega(t) = \frac{1}{t}\int^{t}\alpha(t')dt'. \tag{V.A.18}$$

Let's take one more pair of quantities from the *fiscal policy*, the economic growth x_1 and the net government spending, x_2. Using the same analysis,

$$\frac{d}{dt}x_1(t) = \beta(t)x_2(t), \quad \frac{d}{dt}x_2(t) = -\beta(t)x_1(t), \tag{V.A.19}$$

we again define a complex quantity,

$$y = x_1 + ix_2 \tag{V.A.20}$$

and solve the differential equations,

$$i\frac{d}{dt}y(t) = \beta(t)y(t) \Rightarrow y(t) = C_y e^{-i\int_{t_0}^{t}\beta(t')dt'}. \tag{V.A.21}$$

The monetary and fiscal policy can not exist free from each other. The real economy couples them together, say with a proportionality function $V(t)$. Then Eqs. (V.A.17)) and (V.A.21) are transformed into

$$i\frac{d}{dt}z(t) = \alpha(t)z(t) + V(t)y(t) \tag{V.A.22}$$

$$i\frac{d}{dt}y(t) = \beta(t)y(t) + V(t)z(t). \tag{V.A.23}$$

In order to eliminate the diagonal terms the following representation is made,

$$z(t) \equiv Z(t)e^{-i\int^{t}\alpha(t')dt'}, \tag{V.A.24}$$

and

$$y(t) \equiv Y(t)e^{-i\int^{t}\beta(t')dt'}. \tag{V.A.25}$$

This results in

$$i\frac{d}{dt}Z(t) = V(t)e^{i\int^t(\alpha(t')-\beta(t'))dt'}Y(t) \tag{V.A.26}$$

and

$$i\frac{d}{dt}Y(t) = V(t)e^{i\int^t(\beta(t')-\alpha(t'))dt'}Z(t), \tag{V.A.27}$$

which represents a system of equations well treated in quantum physics.

The qualitative explanation of phenomena described by Eqs. (V.A.26) and (V.A.27) is as follows. The initial periodic fluctuation or population is, as time passes, distributed to the other states due to the coupling with certain probabilities. The transition is well described as a local phenomenon in time, if we use the adiabatic representation in which the basic states are the instantaneous eigenstates obtained by diagonalizing the matrix

$$\begin{pmatrix} \alpha(t) & V(t) \\ V(t) & \beta(t) \end{pmatrix} \tag{V.A.28}$$

at each moment t. The transition is induced by the coupling among them called nonadiabatic coupling, and occurs most effectively where $\alpha(t)$ and $\beta(t)$ cross or come close together.

The final distribution can be analytically predicted from the shape of the three quantities, $\alpha(t)$, $\beta(t)$ and $V(t)$. This can be done without solving the differential equations above, just by using the particular characteristics such as an elasticity.

Let us examine Eqs. (V.A.26) and (V.A.27) more in detail. If the coupling $V(t)$ vanishes, $Z(t) = C_z$ and $Y(t) = C_y$. From Eqs. (V.A.24) and (V.A.25) the conservation rule follows,

$$q_1(t)\frac{d}{dt}q_1(t) + q_2(t)\frac{d}{dt}q_2(t) = 0, \text{ dtto } x_i(t). \tag{V.A.29}$$

The magnitude of q_i (x_i) oscillation is limited by $|C_z|$ ($|C_y|$). When the coupling is nonzero, there is a transition mechanism between the cycles. Due to the properties of Eqs. (V.A.26) and (V.A.27) the conservation of the total flux can be written as

$$\sum_{i=1,2}\left(q_i(t)\frac{d}{dt}q_i(t) + x_i(t)\frac{d}{dt}x_i(t)\right) = 0. \tag{V.A.30}$$

Suppose that we start with the initial conditions

$$Z(t_-) = C_z\exp(i\phi), \quad t_- \to -\infty \tag{V.A.31}$$

and

$$Y(t_-) = 0. \tag{V.A.32}$$

If the coupling is localized in time, say around $t = 0$, then there exists a limit

$$|Z(t_+)| = \sqrt{1-p}C_z, \quad 0 \le \sqrt{p} \le 1. \tag{V.A.33}$$

and

$$|Y(t_+)| = \sqrt{p}C_z \equiv C_y, \quad t_+ \to \infty. \tag{V.A.34}$$

Here $\sqrt{p}$ is a converged transmission ratio between the two cyclic processes. The above time limit can be taken for any initial condition unlike from that of Eqs. (V.A.31) and (V.A.32) and also the phases of each separated cycle at t_+ can be obtained. For our purpose here it suffices to consider only the rate $\sqrt{p}$. This quantity controls the efficiency of different policies on treating TOL problems as it formally follows from Eq. (V.A.34). In general it is a functional,

$$p(\alpha[\ ], \beta[\ ], V[\ ]), \tag{V.A.35}$$

that has to be optimized. Numerous models and analytical techniques [1,75] have been developed in order to get the functional in Eq. (V.A.35). Here we just mention the most important linear mode, [76] which is exactly solvable. Taking Taylor expansions of general functions α, β and V to the lowest orders, the model reads

$$\alpha(t) = U - F_\alpha t, \tag{V.A.36}$$

$$\beta(t) = U - F_\beta t, \tag{V.A.37}$$

and

$$V(t) = V. \tag{V.A.38}$$

The ratio p was obtained as

$$p = \exp\left(-2\pi \frac{V^2}{|F_\alpha - F_\beta|}\right). \tag{V.A.39}$$

The main advantage of the above approach is that qualitative understanding of the dynamical processes can be nicely made in terms of the nonadiabatic transitions that are localized in time and the yield of which is given analytically. It is also important to note that the linear approximation to economic processes does not necessarily hold globally, but can give a good interpretation of the local phenomena.

III. CONCLUDING REMARKS

We have introduced the so called two-state problem (Eqs. (V.A.26) and (V.A.27)). However, the above theory covers also many-state problems, higher order differential equations, and can be generalized for different couplings of $Y(t)$ and $Z(t)$. In general, if there is a time dependent problem, which can be described by the *linear equations* such as

$$i\frac{d}{dt}\begin{pmatrix} u_1(t) \\ u_2(t) \\ . \\ . \end{pmatrix} = \begin{pmatrix} V_{11}(t) & V_{12}(t) & . & . \\ V_{21}(t) & V_{22}(t) & & \\ . & & . & \\ . & & & . \end{pmatrix} \begin{pmatrix} u_1(t) \\ u_2(t) \\ . \\ . \end{pmatrix}, \tag{V.A.40}$$

then we have a formalism that enables analytical analysis and understanding of the dynamical processes and thus their efficient control. We would like to stress here that the linearity of equations in quantum physics does not mean linearity in the phenomena. Similar approaches have been discussed in JCIS 2000 also in the case of (continuous) neural networks, a system which can not be regarded as either quantum or linear.

In physics, using the idea of an external field, the multi-channel processes can be controlled with 100% yield [38]. This can be done by using the above formalism. The results of such an approach in the context of economics (finance) are planned to be reported in future. We appreciate any comments, suggestions and cooperation.

References

[1] E. E. Nikitin and S. Ya. Umanskii, *Theory of Slow Atomic Collisions* (Springer, Berlin, 1984)

[2] E. S. Medvedev and V. I. Osherov, Radiationless Transitions in Polyatomic Molecules, Springer Series in Chemical Physics, Vol. 57 (Springer, Berlin, 1994).

[3] H. Nakamura, Int. Rev. Phys. Chem. **10**, 123 (1991).

[4] A. Joye and C. E. Pfister, "Exponential Estimates in Adiabatic Quantum Evolution" in XIIth International Congress of Mathematical Physics: ICMP '97, eds. D. D. Wit, A. J. Bracken, M. D. Gould and P. A. Pearce (International Press, Cambridge, 1999).

[5] C. Zhu and H. Nakamura, J. Math. Phys. **33**, 2697 (1992).

[6] A. Joye, G. Milleti and C. E. Pfister, Phys. Rev. A **44**, 4280 (1991).

[7] H. Nakamura, "Nonadiabatic Transitions: Beyond Born-Oppenheimer" in Dynamics of Molecules and Chemical Reactions, eds. R. E. Wyatt and J. Z. H. Zhang (Marcel Dekker, New York, 1996). Chap. 12.

[8] H. Nakamura and C. Zhu, Comm. Atomic and Molec. Physics **32**, 249 (1996).

[9] C. Zhu and H. Nakamura, J. Chem. Phys. **109**, 4689 (1998).

[10] C. Zhu and H. Nakamura, Chem. Phys. Lett. **258**, 342 (1996); ibid **274**, 205 (1997).

[11] C. Zhu and H. Nakamura, J. Chem. Phys. **106**, 2599 (1997); ibid **107**, 7839 (1997); Erratum, J. Chem. Phys. **108**, 7501 (1998).

[12] V. I. Osherov and A. I. Voronin, Phys. Rev. A **49**, 265 (1994).

[13] V. I. Osherov and H. Nakamura, J. Chem. Phys. **105**, 2770 (1996).

[14] V. I. Osherov and H. Nakamura, Phys. Rev. A **59**, 2486 (1999).

[15] V. I. Osherov, V. G. Ushakov and H. Nakamura, Phys. Rev. A **57**, 2672 (1998).

[16] M. Abramowitz and I Stegun, *Handbook of Mathematical Functions* (Dower, New York, 1972).

[17] M. S. Child, *Semiclassical Mechanics with Molecular Applications* (Clarendon Press, Oxford, 1991).

[18] H. Nakamura, Int. Rev. Phys. Chem. **10**, 123 (1991).

[19] H. Nakamura, in *Dynamics of Molecules and Chemical Reactions*, ed. by R. E. Wyatt and J. Z. H. Zhang (Marcel Dekker Inc., New York, 1996) Chpt. 12.

[20] L. Pichl, H. Nakamura, and H. Deguchi, in *JCIS 2000 Proceedings* (AIM, Atlantic City, 2000) vol. 2, 1002.

[21] H. Nakamura, J. Chem. Phys. **97**, 256 (1992).

[22] S. Nanbu, H. Nakamura and F. O. Goodman, J. Chem. Phys. **107**, 5445 (1997).

[23] H. Nakamura, J. Chem. Phys. **110**, 10253 (1999).

[24] R. J. Gordon and S. A. Rice, Annu. Rev. Phys. Chem. **48**, 601 (1997).

[25] *Molecules in Laser Fields*, edited by A. D. Bandrauk (Marcel Dekker Inc., New York, 1994)

[26] P. Brumer and M. Shapiro, Annu. Rev. Phys. **43**, 257 (1992).

[27] D. J. Tannor and A. Rice, J. Chem. Phys. **83**, 5013 (1985).

[28] S. Chelkovskii and A. D. Bandrauk, J. Chem. Phys. **99**, 4279 (1993).

[29] R. Kosloff, S. A. Rice, P. Gaspard, S. Tersigni, and D. J. Tannor, Chem. Phys. **139** 201 (1989).

[30] D. Neuhauser and H. Rabitz, Acc. Chem. Res. **26**, 496 (1993).

[31] J. C. Wells, I. Simbotin and M. Gavrila, Phys. Rev. A **56**, 3961 (1997).

[32] F. O. Goodman and H. Nakamura, Prog. Surf. Sci. **50**, 389 (1995).

[33] Y. Teranishi and H. Nakamura, Phys. Rev. Let. **81**, 2032 (1998).

[34] I. Levy, M. Shapiro and P. Brumer, J. Chem. Phys. **93**, 2493 (1990).

[35] K. Nagaya, Y. Teranishi and H. Nakamura, to be published.

[36] R. Buffa and S. Cavalieri, Phys. Rev. A **42**, 5481 (1990).

[37] Z. Ficek and T. Rudolph, Phys. Rev. A **60** R4245 (1999).

[38] Y. Teranishi and H. Nakamura, J. Chem. Phys. **111**, 1415 (1999).

[39] S. I. Chu, *Adv. Multiphoton Processes and Spectroscopy*, vol. 2 (World Scientific, Singapore, 1986).

[40] Y. Teranishi and H. Nakamura, J. Chem. Phys. **107**, 1904 (1997).

[41] H. Nakamura and C. Zhu, Comm. Atom. Molec. Phys. **32**, 249 (1996).

[42] H. Nakamura, *XXI-ICPEAC Invited Talks* (Sendai, Japan, 1999) Amer. Inst. Phys., 2000.

[43] C. Zhu, Y. Teranishi, and H. Nakamura, Adv. Chem. Phys. (to be published, 2000).

[44] Yu. N. Demkov and V. I. Osherov, Zh. Eksp. Teor. Fiz. **53**, 1589 (1967).

[45] U. Fano, Phys. Rev. **124**, 1866 (1961)

[46] A. Vardi and M. Shapiro, Phys. Rev. A **58**, 1352 (1998).

[47] Y. Luke, *Mathematical Functions and Their Approximations* (Academic, New York, 1975).

[48] *Dissociative Recombination: Theory, Experiment and Applications* (Ed. J. B. A. Mitchell and S. L. Guberman, World Scientific Publishing, Singapore, 1989).

[49] *Dissociative Recombination: Theory, Experiment and Applications* (Ed. B. R. Rowe, J. B. A. Mitchell and A. Canosa, NATO ASI Series, Series B: Physics Vol. 313, Plenum, New York, 1993)

[50] *Dissociative Recombination: Theory, Experiment and Applications III* (Ed. D. Zaifman, J. B. A. Mitchell, D. Schwalm and B. R. Rowe, World Scientific Publishing, Israel, 1996).

[51] O. Belly, D. L. Moores and M. J. Seaton, *Atomic Collision Processes* (Ed. M. R. C. McDowell, North-Holland, Amsterdam, 1963).

[52] J. M. Seaton, Rep. Prog. Phys. **46** 167 (1983).

[53] U. Fano, Phys. Rev. A **2** 353 (1975).

[54] Ch. Jungen and O. Atabek, J. Chem. Phys. **66** 5584 (1977).

[55] H. Nakamura, International Reviews in Physical Chemistry **10** 123 (1991); J. Chinese Chem. Soc. **42** 359 (1995); Annu. Rev. Phys. Chem. **48** 299 (1997).

[56] A. Giusti, J. Phys. B **13** 3867 (1980).

[57] M. Hiyama and H. Nakamura, in *Structure and Dynamics of Electronic Excited States* (Ed. J. Laane, H. Takahashi and A. Bandrauk, Springer-Verlag, 1998).

[58] M. Hiyama, N. Kosugi and H. Nakamura, J.Chem.Phys. **107** 1 (1997).

[59] S. L. Guberman and A. Giusti-Suzor, J. Chem. Phys. **95** 2602 (1991).

[60] A. L. Sobolewski and W. Domcke, J. Chem. Phys. **86** 176 (1987).

[61] C. Jungen and S. C. Ross, Phys. Rev. A **55** R2503 (1997).

[62] R. K. Nesbet, Phys. Rev. A **54** 2899 (1996).

[63] L. Pichl and J. Horáček, J. Phys. A **29** L405 (1996).

[64] K. Diethelm, J. Comput. Appl. Math. **56** 321 (1994).

[65] D. E. Atems and J. M. Wadehra, Phys. Rev. A **42** 5201 (1990).

[66] A. Peet Hickman, Phys. Rev. A **43** 3495 (1991).

[67] P. L. Gertitschke and W. Domcke, Phys. Rev. A **47** 1031 (1993).

[68] M. Čížek, J. Horáček and W. Domcke, J. Phys. B **31** 2571 (1998)

[69] J. Horáček, J. Phys. B **28** 1585 (1995)

[70] S. Hara and H. Sato, J. Phys. B **17** 4301 (1984).

[71] H. Takagi, p. 75 of ref. [49].

[72] K. Nakashima, H. Takagi and H. Nakamura, J. Chem. Phys. **86** 726 (1987). *(In Eq. (6) therein -0.005215 should read -0.05215)*

[73] H. Takagi, p. 174 of ref. [50].

[74] W. Domcke, J. Phys. B. **18** 4491 (1985).

[75] *An Introduction to Phase Integral Methods* (Methuen, London, 1962)

[76] Proc. Roy. Soc. London A **137**, 696 (1932).